OPTICAL CHARACTERISTICS OF GAS-DISCHARGE PLASMA IN MIXTURES OF MERCURY DIBROMIDE VAPOR WITH GASES

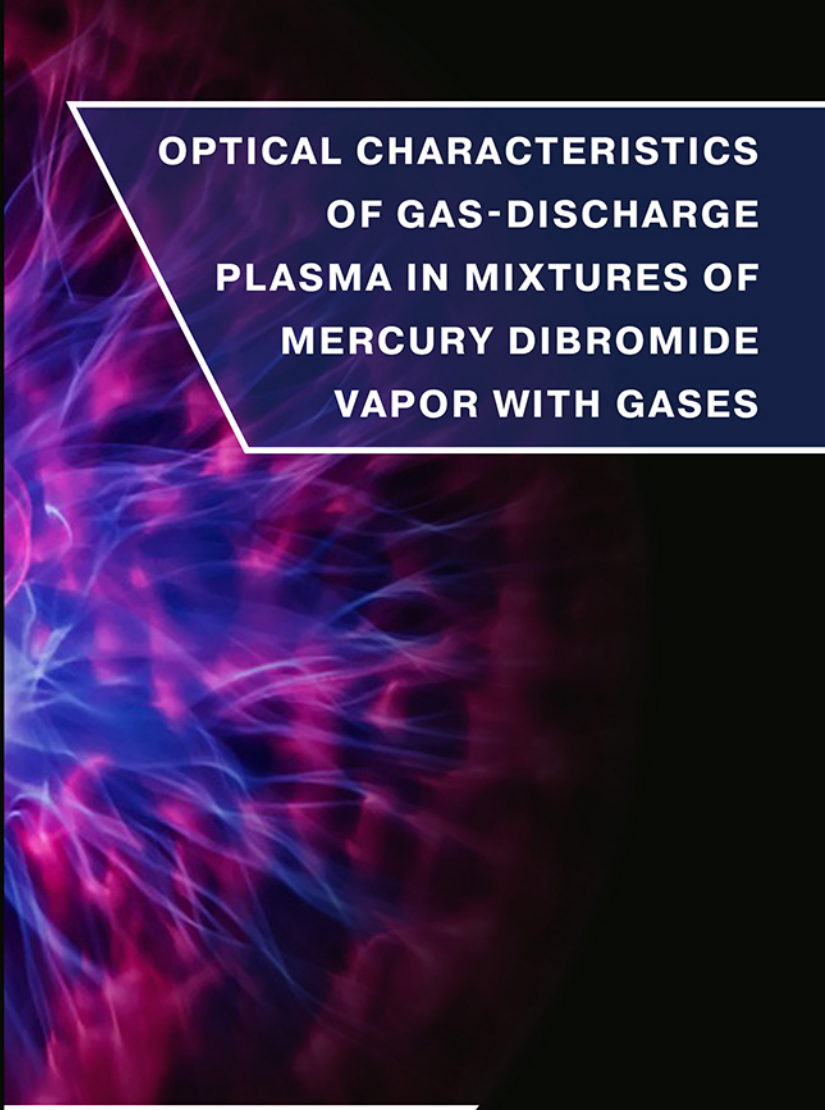

Antonina Malinina

Optical Characteristics of Gas-Discharge Plasma in Mixtures of Mercury Dibromide Vapor with Gases

Optical Characteristics of Gas-Discharge Plasma in Mixtures of Mercury Dibromide Vapor with Gases

By

Antonina Malinina

Cambridge
Scholars
Publishing

Optical Characteristics of Gas-Discharge Plasma in Mixtures of Mercury Dibromide Vapor with Gases

By Antonina Malinina

This book first published 2020

Cambridge Scholars Publishing

Lady Stephenson Library, Newcastle upon Tyne, NE6 2PA, UK

British Library Cataloguing in Publication Data
A catalogue record for this book is available from the British Library

ISBN (10): 1-5275-4481-8
ISBN (13): 978-1-5275-4481-9

TABLE OF CONTENTS

INTRODUCTION

The optical characteristics of gas-discharge plasma in mixtures of different compositions are its most important characteristics. They carry information about the physicochemical processes occurring in plasma and its parameters and characteristics, including: the concentrations of electrons, atoms and molecules; and the energy distribution, temperature and drift velocities of electrons. These optical characteristics also characterize the efficiency of elastic and inelastic collisions of electrons with working gases, quenching the energy states of excited molecules, as well as the discharge power losses in electronic processes [1].

Intensive study into the optical characteristics of gas-discharge plasma began with the discovery of the effect of lasers on mixtures of metal vapors, salts and gases. This led to a need to increase their energy parameters and search for new active media [2–4]. Studies of the characteristic effects of gas-discharge plasma in mixtures of mercury dibromide vapor with gases are particularly prominent. Such plasma is used as a working medium for exciplex sources of pulse-periodic coherent (lasers) and spontaneous radiation (excilamps) in the blue-green region of the spectrum and with a wavelength at maximum intensity of ($\lambda_{max.}$) = 502 nm [5–14]. These sources of radiation have attracted the attention of researchers in connection with the high specific power of radiation, which is recorded in the visible spectral range, by tuning the wavelength of radiation across a wide range of the spectrum, and also with the possibility of operating in a pulse-periodic mode. The average power of laser radiators reaches ~200 W at an efficiency

of 2.1 % with energy in a single pulse of 9.8 Joules (2.4 % efficiency) [8–11]. Such sources of radiation are needed for a number of important applications: the monitoring of air and water basins; range finding of marine objects; underwater communications; the technology of electronic equipment materials; increasing the efficiency of photosynthesis in plants (in greenhouses, space vehicles, submarines, etc.); and pumping solid-state and liquid lasers [15–19].

The data on optical characteristics of the working medium of radiation sources (gas-discharge plasma in mercury dibomide vapor and gas mixtures) make it possible: to diagnose the spectral composition of the discharge plasma radiation; to reveal the optimal component composition of the working mixtures, at which the maximum radiation intensity in the investigated spectral range is reached; and to determine the pulsed radiation characteristics. In addition, such characteristics allow us to establish the physicochemical regularities in the processes that occur in the plasma of a gas discharge in working mixtures, to find ways to increase their energetic and spectral characteristics [3].

During the first studies on optical characteristics, i.e., the emission spectra of gas discharge plasma in a mixture of mercury dibromide with small additions of inert gases (<10 kPa), the emission of spectral bands in the electron-vibrational transitions $B^2\Sigma^+_{1/2} \rightarrow X^2\Sigma^+_{1/2}$ of mercury monobromide molecules was revealed—later, these were called exciplex (HgBr*) molecules [3]. By nature these spectral radiation bands broaden from the side of short wavelengths [20, 21]. When the total pressure of the mixture increases, they become narrower due to the relaxation process of the population of the vibrational levels of the $B^2\Sigma^+_{1/2}$ state [22–24]. The radiation pulses were delayed relative to the discharge current pulses by several tens of nanoseconds and their duration (generation) was 30–70 ns

[5–7, 25, 26]. In the dependencies of the radiation intensity of the exciplex HgBr* molecule on the partial pressures of mercury dibromide and inert gases, the following regularities can be observed: an increase in intensity with an increase in the partial pressures of the mixture components, until a maximum is reached; and a decrease in the radiation intensity with a subsequent increase in the partial pressures of the components of the mixture. The radiation intensity with increasing partial pressures after reaching the maximum decreases with a lower rate for inert gases than for mercury dibromide vapor. The partial pressures at which the maximum radiation power is reached are 0.27–1.06 kPa for mercury dibromide vapor and 90–120 kPa for inert gases [26–28]. The most intense emission of mercury monobromide occurs in a mixture of mercury dibromide and helium. The authors of these studies explained their results by changing the reduced electric field strength E/N (where E is the electric field applied to the plasma and N is the total concentration of the particles in the working mixture), and also by quenching the $B^2\Sigma^+_{1/2}$ state of mercury monobromide molecules with the components of the plasma working mixture. A change in the reduced electric field strength leads to a redistribution of the discharge power into various processes that affect the intensity of the radiation, and also to either an increase or decrease in the efficiency of the processes of populating and depopulating the energy states of the components of the working mixtures. The rate constants of elastic and inelastic processes in the collision of electrons with atoms and molecules, which are a quantitative measure of process efficiency, are mainly determined by the theoretical method, which is associated with methodical difficulties and poor knowledge about the efficiency of plasma-chemical processes occurring in plasma in working mixtures [29–32]. In turn, the quenching rate constants of the $B^2\Sigma^+_{1/2}$ states of mercury monobromide molecules by the components

of the mixture can be determined by optical methods for mercury dibromide vapor with helium and neon mixtures. These are in the range (1.7–2.7) 10^{-10} cm^3/s and (1.5–5.5) 10^{-14} cm^3/s for quenching by mercury dibromide and helium (neon) molecules, respectively [33–36]. The rate constant of the main population process of the $B^2\Sigma^+_{1/2}$ state of mercury monobromide molecules (dissociative excitation of $B^2\Sigma^+_{1/2}$ states of mercury monobromide molecules in the collision of plasma electrons with mercury dibromide molecules) in mixtures of mercury dibromide vapor with helium and neon varies in the limits of the values $1 \cdot 10^{-10}$–$9 \cdot 10^{-9}$ cm^3/s with a change in the reduced electric field strength from 3 to 100 Td [32].

Previous investigations into the optical characteristics of gas-discharge plasma in mixtures of mercury dibromide vapor and gases saw the following experimental conditions: the amplitude of the voltage and current pulses reached 50 kV and several kA, respectively; the repetition rate of the pump pulses was in the range 1–2,000 Hz; and total pressures of the mixtures reached 200 kPa. The studies were carried out with mixtures of mercury dibromide vapor and the following gases: helium, neon, argon, nitrogen, xenon, and krypton. Operating devices with a volume of more than 200 cm^3 were used. The highest radiation powers of mercury monobromide exciplexes were obtained for mixtures of mercury dibromide vapor with helium and small nitrogen additions. This is explained by the addition of a channel for the population of $B^2\Sigma^+_{1/2}$ states of mercury monobromide in collisions of mercury dibromide molecules with metastable nitrogen molecules [37].

The study of the parameters and characteristics of plasma discharge in working mixtures is of paramount importance in the study of their optical characteristics, since the optical characteristics of the plasma discharge constitute their functions [1–3]. The parameters and characteristics of the

plasma discharge in the working mixtures were determined using data on the efficiency of electron collisions with the components of the working mixtures. On the basis of these data, the optimum reduced electric field strength (E/N) was established for which the efficiency of the sources on the mixtures increased. To establish this data, a theoretical method was used [29–32]. In the mixture of mercury dibromide vapor with helium, or neon (argon), and also with the addition of nitrogen (a small amount in the mixture), the transport and energy characteristics; the specific power losses of the discharge during the elastic and inelastic processes of collisions of the discharge electrons with the atoms and molecules of a particular mixture; and the rate constants of these processes were calculated [32].

An analysis of the results available in the scientific literature on the investigation into the optical characteristics of gas-discharge plasma in mixtures of mercury dibromide vapor and gases gave us new research problems. These problems included the establishment of the physicochemical regularities that occur in new working mixtures based on mixtures of mercury dibromide vapor with gases, to reveal ways to increase the energy characteristics of radiation from lasers and excilamps in the blue-green spectral range. In addition, there was a need to carry out investigations into the optical characteristics of gas-discharge plasma in the region of large pump repetition rates (above 2,000 Hz), and the duration of the pump pulses close to the lifetime of the $B^2\Sigma^+_{1/2}$ state of mercury monobromide (≤30 ns), to reveal new and more effective mixtures of mercury dibromide vapor with gases. Finally, we sought to determine the characteristics and parameters of the plasma discharge under the experimental conditions at which the maximum specific energy characteristics of the radiation of mercury monobromide exciplex molecules were observed.

CHAPTER 1

THE RESULTS OF PRELIMINARY INVESTIGATIONS INTO GAS-DISCHARGE PLASMA IN MIXTURES OF MERCURY DIBROMIDE VAPOR WITH GASES

1.1. Optical characteristics of radiation

Investigations into the optical characteristics of the radiation of gas-discharge plasma in mixtures of mercury dibromide vapor with gases have developed apace since the late 1980s with the creation of a laser that could generate radiation in the spectral range of 502 to 506 nm [5]. To obtain an inversion, gas-discharge plasma was used, which created an atmospheric pressure volume discharge in a mixture of mercury dibromide vapor with helium. The active element of the laser was made of a sealed pyrex tube with an inner diameter of 4 cm and a length of 35 cm. The electrodes of the laser were two tungsten rods 6 mm in diameter and 25 cm in length; the distance between them was 1 cm. Near the cathode (parallel to it) an electrode was located, which was placed inside the glass tube and was used to pre-ionize the working mixture in the inter-electrode gap. The laser was pumped by a generator that provided a pulse voltage to the laser electrodes with an amplitude above 8 kV, a duration of 70 ns, and a pulsed voltage on the pre-ionization electrode. Crystals of mercury dibromide were placed in the active element of the laser and filled with a buffer gas—helium—at a pressure of 1,000 mm Hg. The partial pressure of the mercury dibromide

vapor was created by heating the powder with an external electric heater. The laser-generated energy of several tens of millijoules had a pulse duration of 50 ns. The efficiency of the laser did not exceed 1 %. The authors of [5] have established that the radiation in this spectral region appears in the electron-vibrational transition $B^2\Sigma^+_{1/2} \rightarrow X^2\Sigma^+_{1/2}$ from v' = 0–3 v'' = 22–23 diatomic molecules of mercury monobromide. In subsequent work on the optical characteristics, the design of the active element and the parameters of the pump pulses, as well as the component compositions of the working mixtures, were changed, making it possible to increase the energetic characteristics of the laser. When the working mixtures were pumped by a discharge controlled by an electron beam, the radiation energy and efficiency reached 9.8 J and 2.4 %, respectively. In the pulse-periodic mode with electric-discharge pumping and X-ray pre-ionization, the average radiation power was soon brought to 200 W, and the efficiency to 2.1 % [8–11].

These experiments were preceded by studies into the emission spectra of a high-frequency discharge in mixtures of mercury dihalides with small additions of inert gases (several kPa) [20, 21]. The emission of electron-vibrational spectral bands for the transition $B^2\Sigma^+_{1/2} \rightarrow X^2\Sigma^+_{1/2}$ of the mercury monohalide molecule was observed. At the atmospheric pressure of working mixtures necessary for more efficient laser generation of radiation, the emission spectra were almost the same as for mixtures with the addition of buffer gases of several kPa. However, the emission bands were narrower due to the rapid relaxation of the population of vibrational levels of $B^2\Sigma^+_{1/2}$-state mercury monobromide [22–24].

A weak dependency of the intensity of radiation on the partial pressure of an inert gas for two-component mixtures was noted in [26–28], as well as the presence of an interval of the partial pressure of dihalides and inert

gases (for multicomponent mixtures) at which the radiation intensity was high.

The temporal characteristics of plasma radiation in mixtures of mercury dihalides and inert gases were investigated in [5–7, 25, 26]. The half-widths of the current pulses through the gas-discharge gap and its generation were 30–70 ns. Current pulses outran radiation pulses by several tens of nanoseconds.

The necessity of explaining the optical characteristics of plasma radiation dischage in mercury dibromide vapor mixtures has stimulated interest in the molecular terms of mercury monobromide and mercury dibromide [20, 21, 38, 39].

Figure 1.1 shows a simplified diagram illustrating the formation of HgBr molecules ($B^2\Sigma^+_{1/2}$) under conditions of gas-discharge excitation of a mercury dibromide with gas mixture. According to the data of [38], the $B^2\Sigma^+_{1/2}$ state of mercury monobromide has a strongly bound ionic character, while the ground $X^2\Sigma^+_{1/2}$ state is weakly bound and has a covalent character. The minimum of the potential curve of the B-state of mercury monobromide shifts by 0.6 A relative to the X-state, which causes a preferential transition from lower vibrational levels of the $B^2\Sigma^+_{1/2}$ state to the upper $X^2\Sigma^+_{1/2}$ states. Such molecules are usually called exciplex-like and are denoted by an asterisk (HgBr*) [2, 3].

It has been established that dissociative excitation in the collision of mercury dibromide molecules with electrons is the main mechanism for the population of the upper energy level ($B^2\Sigma^+_{1/2}$ state) of mercury monobromide in gas-discharge plasma in a mercury dibromide vapor and helium (neon) mixture [3, 13, 40–43]. Immediately after the formation of this excited state of mercury monobromide in the plasma of a gas discharge,

its radiative decay begins. In addition, the $B^2\Sigma^+_{1/2}$ state of HgBr* is quenched by heavy particles and electrons [3]:

(1.1) $HgBr_2+e \rightarrow HgBr^*+ \begin{cases} Br+e \\ Br^- \end{cases}$ (1.2)

(1.3) $HgBr^* \rightarrow HgBr+h\nu$

(1.4) $HgBr^*+M \rightarrow HgBr+M+\Delta E$

where M represents the particles that quench the $B^2\Sigma^+_{1/2}$ state of mercury monobromide and ΔE is the energy difference in the reaction.

These processes (1.1–1.4) primarily explain the dependency of the intensity of emission of mercury monobromide exciplex molecules on the partial pressures of mercury dibromide. The contribution of processes (1.1–1.4) to radiation intensity depends on the rate constants of excitation and quenching of the $B^2\Sigma^+_{1/2}$ state and particle concentrations [1, 3].

For the same mixtures with the addition of molecular nitrogen or xenon, the excitation of the HgBr $B^2\Sigma^+_{1/2}$ state can occur via an additional channel due to the transfer of energy from nitrogen molecules that are in the metastable state $A^3\Sigma^+_u$ and xenon atoms in the metastable state $^3P_2$. The rate constants of this process are rather high: $1 \cdot 10^{-10}$ cm^3/s and $5.3 \cdot 10^{-10}$ cm^3/s, respectively [37].

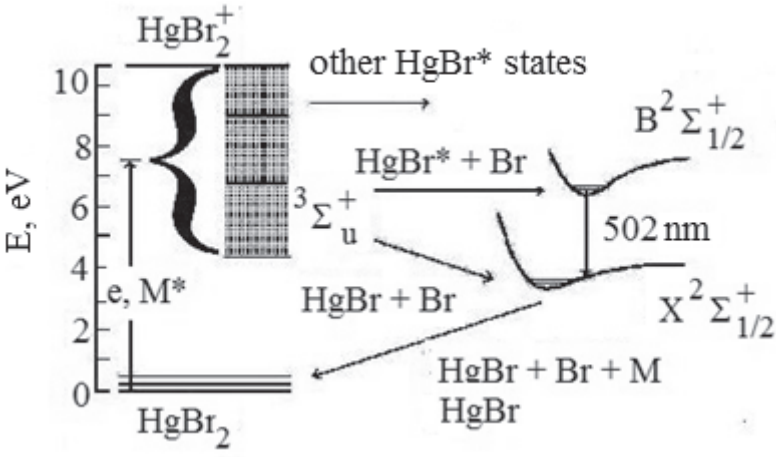

Figure 1.1. A simplified diagram illustrating the formation of HgBr ($B^2\Sigma^+_{1/2}$) molecules under gas discharge excitation of mercury dibromide with gas mixtures; M*—metastable atoms and molecules [30, 39].

The addition of neon, along with nitrogen and sulfur hexafluoride, to the mixture leads to an increase in the population of metastable state $A^3\Sigma^+_u$ nitrogen molecules due to the relaxation of the population from higher-lying nitrogen levels in collisions with sulfur hexafluoride molecules and the fragments thereof. This leads to a 50 % increase in the energy of HgBr laser radiation [4]. In addition to the above processes, the HgBr $B^2\Sigma^+_{1/2}$ state can also be excited through collision reactions with the ions of inert gases and nitrogen, as the rate constants of these processes reach high values $(3–7)\times 10^{-10}$ cm^3/s [44]. However, the energy deposition of such processes to the excitation of mercury monobromide $B^2\Sigma^+_{1/2}$ state in gas-discharge plasma in mixtures of mercury dibromide vapor with gases has not yet been determined.

In most studies of the characteristics of gas-discharge plasma in mixtures of mercury dibromide vapor with gases, excitation of the working mixtures was done by discharge through barrier-dielectric quartz glass, which provided a uniform burning of the discharge without the use of preliminary ionization at typical atmospheric pressures of the working mixtures and simplification of the design of the gas-discharge device [12, 14, 26–28, 45–47]. The first report on the studies of the spectral, integral, and temporal characteristics of gas-discharge plasma in mixtures of mercury dibromide vapor with gases for excitation, using a single-barrier discharge, dates from April 1980 [12]. The excitation of $HgBr_2$ vapor in a mixture with helium, as an inert gas, was carried out in a gas discharge cuvette and used a thin-walled quartz tube. Two tungsten electrodes were located inside the gas discharge cuvette, one of which was fitted with a quartz tube. To fill the gases in the side of the cuvette, a quartz glass tube was welded in place. Inside the tube there was a capillary, which reduced the removal of mercury dibromide vapor to the pumping and gas inlet system. To create the desired partial pressure of mercury dibromide vapor, the gas discharge cuvette was heated using an electric heater, which was located on an additional external quartz tube. A high-voltage pulse-periodic voltage of 30–40 kV, with a pulse duration of 50 ns and a repetition rate of 10–100 Hz, was applied to the electrodes. In these studies, only one spectral band with a maximum intensity of $\lambda = 502$ nm was detected in the spectral range 300–700 nm. A weak dependency of the radiation intensity on the partial pressure of helium was observed in the temperature range 100–2,000 °C in the heating of the gas-discharge cuvette. Experiments on the temporal characteristics of gas-discharge plasma in a mixture of mercury dibromide vapor with gases used a mixture of mercury dibromide vapor with helium [12]. Current pulses were twofold. Each individual current pulse had a duration of 50 ns with a

leading rise-front of ~10 ns. The time between pulses was 150 ns. The radiation pulses were also twofold. The amplitude of the second pulse in the radiation was higher than in the first one. As the pressure of helium increased, the amplitude of both pulses decreased. However, for the first pulse, this decrease was faster. The authors suggested that the first pump pulse generated excited and non-excited molecules of mercury monobromide. The radiation of the excited molecules was determined by the amplitude of the first optical pulse. Under the action of the second pump pulse, molecules of mercury monobromide from the $X^2\Sigma^+_{1/2}$ state were excited. As a result of this, there was an additional increase in the population of the $B^2\Sigma^+_{1/2}$ state, leading to an increase in the amplitude of the second radiation pulse. The decrease in the amplitude of the radiation pulses with an increase in the partial pressure of helium was caused by a decrease in mean electron energy, leading to a decrease in the efficiency of the process of excitation of the $B^2\Sigma^+_{1/2}$ state and, accordingly, its population decreased.

Figure 1.2 shows the results of the author's investigations into the optical characteristics of gas-discharge plasma in mixtures of mercury dibromide vapor with inert gases, [26]. It shows the characteristic emission spectrum of a mixture of $HgBr_2$ vapor with helium (neon, xenon) and the dependency of the emission intensity of the spectral band of λ = 502 nm HgBr* on the partial pressures of mercury dibromide vapor with helium, neon and xenon [26]. The spectra differed in the rate of the decrease in the intensity of the spectral band of λ = 502 nm HgBr* molecules in the ultraviolet part, as well as in width, depending on the partial pressure of the inert gases. The emission spectra of a mixture of $HgBr_2$ vapor with helium (neon, xenon) for low pressures (less than atmospheric) continued further into the region of shorter wavelengths. The dependency of the emission intensity of the spectral band in the short-wave region can be explained by

the relaxation processes of the population of the upper (v'>1) vibrational levels of the $B^2\Sigma^+_{1/2}$ states, which occur more rapidly than the electron-vibrational transition to the ground $X^2\Sigma^+_{1/2}$ state [22–24]. The dependency of the radiation intensity on the partial pressure of mercury dibromide shows an increasing trend, and the region of maximum radiation is found at HgBr* 0.27–1.06 kPa. The results of the studies presented in Figure 1.2 show that the most intense emission of mercury monobromide molecules takes place in a mixture of mercury dibromide vapor with a light helium gas. The behavior of the radiation intensity of gas-discharge plasma in the partial pressures of mercury dibromide vapor and inert gases can be explained by the rate of the processes of population and depopulation of the mercury monobromide $B^2\Sigma^+_{1/2}$ state, which, in turn, depends on the parameter E/p (where E is the electric field strength, which is applied to the plasma gap, and p is the total pressure of the mixture). For a mixture with helium, the excitation efficiency of the mercury monobromide $B^2\Sigma^+_{1/2}$ state is higher, and the quenching process by helium is lower [30–36]. With increasing voltage of up to 40 kV and a repetition rate of the generator pulses from 10 Hz to 100 Hz, a proportional increase in the radiation intensity can be observed. Over a period of time (>50 hours), the decrease in the radiation intensity in the spectral band is negligible [26].

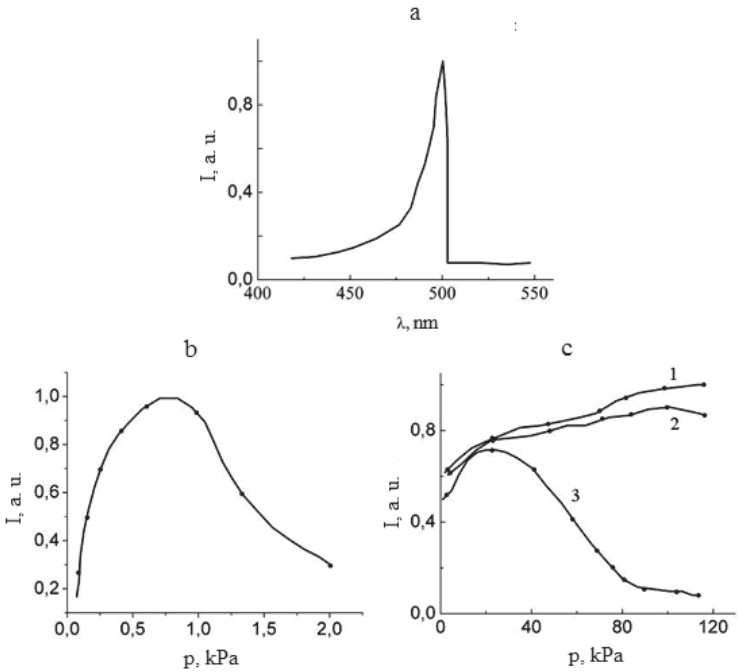

Figure 1.2. a) The radiation spectrum of a pulsed discharge in a He:$HgBr_2$ = 119.7:0.27 kPa mixture; b) the dependency of the emission intensity of the spectral band λ = 502 nm HgBr* on the saturated vapor pressure $HgBr_2$ for the He:$HgBr_2$ mixture where the partial pressure of helium is 106.4 kPa; c) the dependency of the emission intensity of the λ = 502 nm HgBr* band on the buffer gas pressure for the mixture: (1) He:$HgBr_2$, (2) Ne:$HgBr_2$; (3) Xe:$HgBr_2$—the saturated vapor pressure of $HgBr_2$ was 0.27 kPa [26].

A number of articles [14, 27, 28, 45, 46] present data on the optical characteristics of gas-discharge plasma at high pumping frequencies of working mixtures (up to 2,000 Hz). When pumping a mixture of mercury dibromide and neon with a microwave discharge for a discharge volume of 14.13 cm^3, an average radiation power of 42.8 W and an emission efficiency

of 9.4 % [47] can be achieved. [14, 27, 28, 45, 46] have all reported on the optimization of the energy and resource characteristics of working mixtures of HgBr laser and an excilamp in a pulse-periodic discharge plasma at pump repetition rates of 400—1,900 Hz. The gas-discharge plasma was created by combined surface and barrier discharge. Investigations were carried out on two, three and four-component mixtures of the following compositions: $HgBr_2$:He; $HgBr_2$:N_2:He; $HgBr_2$:Xe:He; $HgBr_2$:Xe:N_2:He. The partial vapor pressure of $HgBr_2$ in the working mixtures was created by dissipation of the discharge energy. The dependency of the radiation intensity on the composition of the mixture was measured at a pump pulse repetition rate of 1,000 Hz and pulse voltage of 18 kV. For a double $HgBr_2$:He mixture, the increase in helium pressure from 141 kPa to 200 kPa resulted in an increase in the average radiation power of 1.7 times. For the three-component mixtures (curves 1 and 2, Figure 1.3a), maximum radiation powers were achieved with xenon partial pressures of 2.03–4.05 kPa; for nitrogen the range was 12.13–47.96 kPa. The average radiation power for four-component mixtures was greater than for a ternary mixture with xenon, but smaller than with nitrogen. The optimal ratio of the average power for the component composition mixtures was: 1:1.9:4.2:21.5 = mixture 1:mixture 2:mixture 3:mixture 4, where: 1 - $HgBr_2$:He (helium pressure 121.6 kPa); 2 - $HgBr_2$:Xe: He (Xe: He = 1:39); 3 - $HgBr_2$:Xe:N_2:He (the ratio of Xe:N_2:He = 1:10:29); and 4 - $HgBr_2$:N_2:He (the ratio of N_2:He = 1:3). Fig. 1.3b shows the dependency of the average radiation power on the number of pump pulses on one portion of the working mixture. The growth rate of the average radiation power was larger for the $HgBr_2$:N_2:He mixture than for the $HgBr_2$:Xe:He mixture. At the same time, when the maximum value of the average radiation power was reached, mixtures with added nitrogen showed more steady behaviour than mixtures with added xenon. Thus, for

the mixture $HgBr_2$:N_2:He at a ratio of the gas components N_2:He = 1:4, after reaching the maximum value, the radiation power during $8 \cdot 10^5$ pulses decreased by no more than 10 %. In addition to studying the radiative characteristics of the component composition of the working mixture, measurements were made of the dependency of the average radiation power on the pumping voltage and the repetition rate of the pulses. With an increase in the energy stored on the capacitance of 0.06 nF dielectric (quartz glass) from 0.13 mJ/cm^3 to 0.34 mJ/ cm^3, the average radiation power increased proportionally. This also occurs when the repetition rate of pulses varies from 400 to 1,900 Hz. Saturation of power in the frequency of the investigated range was not observed. For the mixture $HgBr_2$:N_2:He at a ratio N_2:He = 1: 3, a total pressure of

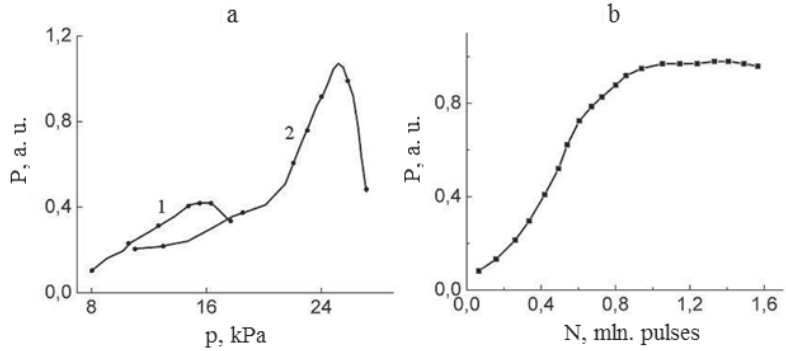

Figure 1.3. a) The dependency of the average radiation power on the partial pressure: 1 - xenon and 2 - nitrogen in the mixtures $HgBr_2$:Xe:He and $HgBr_2$:N_2:He, respectively; b) the dependency of the average radiation power on the total number of pulses in the $HgBr_2$:N_2:He (ratio N_2:He = 1:4). The total pressure of the gas components was 121.6 kPa, the repetition rate of the pump pulses was 1,000 Hz [27].

121.6 kPa and a repetition rate of 1,900 Hz, an average radiation power of 6.8 mW was achieved. When pumping a gas-discharge tube with only a barrier discharge, the average radiation power was less than 1.5 times the value achieved when pumping with a combined (barrier and surface) discharge.

1.2. Parameters and characteristics of plasma

Data on the characteristics and parameters of gas-discharge plasma in some mixtures of mercury dibromide vapor and gases were established in [29–32]. As experimental physics does not yet have satisfactory diagnostic methods for dense gas-discharge plasma, studies in this direction rely heavily on theoretical methods. The kinetic Boltzmann equation for electrons was used to find the electron energy distribution function (EEDF) [1, 48]. In determining the EEDF, it was assumed that under the experimental conditions, the duration of the pump pulses was longer than the time required to set the electron energy distribution function in the plasma. The plasma medium was spatially homogeneous and characterized by the constancy of the composition of all its components. Taking into account these features, which in most experiments are justified, allowed us to use the quasi-stationary Boltzmann equation for electrons in numerical calculation of the EEDF.

Figure 1.4a shows the results of numerical calculation of the EEDF for a mixture of mercury dibromide vapor with helium [32]. In this paper, it is noted that the maximum value of Boltzmann's EEDF shifted to a region of high electron energies in comparison to Maxwell's maximum of EEDF. The energy distribution function of electrons occupies a narrow energy range for small values of the parameter E/p, and when it increases, it expands.

According to the calculated EEDF, the following were determined for gas-discharge plasma in helium (neon) and mercury dibromide vapor mixtures: transport and energy characteristics; electron drift velocity; mean electron energy; specific powers in the elastic and inelastic electron scattering channels for helium (neon) atoms; and dissociative excitation and ionization of mercury dibromide molecules. The drift velocity of the electrons in the mixtures studied increased linearly from 10^6 to 10^8 cm/s with an increase in the parameter E/p in the range 1–30 $V \cdot cm^{-1} \cdot mm\ Hg^{-1}$. In the parameter region E/p = 1-15 $V \cdot cm^{-1} \cdot mm\ Hg^{-1}$, the electron drift velocity for the plasma in a $HgBr_2$:Ne mixture was greater than for the $HgBr_2$:He mixture; in the parameter range E/p = 15-30 $V \cdot cm^{-1} \cdot mm\ Hg^{-1}$, their values practically coincided [32]. The average electron energies in the same range of changes in the parameter E/p also increased from 4 eV to 12.5 eV. In the range of the parameter E/p = 5-30 $V \cdot cm^{-1} \cdot mm\ Hg^{-1}$, mean electron energies for a mixture of mercury dibromide vapor with helium were higher than those in mixtures of mercury dibromide vapor with neon [32]. Fig. 4b presents the dependencies of the specific power losses in the process of electron collision in gas-discharge plasma in mixtures of mercury dibromide vapor with helium at a different ratio of the partial pressures of the components in the value of the parameter E/p [30, 32].

In the discharge in the first mixture at E/p = 1 $V \cdot cm^{-1} \cdot mm\ Hg^{-1}$, 90 % of the power was lost to elastic collision (heating of the gas). In a mixture of mercury dibromide vapor with neon, this value was 15 % [32]. The dissociative excitation and ionization of mercury dibromide molecules consumes 20–35 % of the discharge power in the parameter range E/p ~1÷4 $V \cdot cm^{-1} \cdot mm\ Hg^{-1}$. With an increase in the parameter E/p, losses entail in the processes of excitation and ionization of inert gas atoms from the ground

state, while part of the power that is transferred to the mercury dibromide molecules and to the helium and neon atoms in elastic and stepwise processes is reduced. The inelastic processes in the plasma mixtures with neon lose several times more power in the range of the changes in the values of the parameter E/p in comparison to mixtures of mercury dibromide vapor with helium [32]. For the mixture $HgBr_2$:Ne = 0.35 %:99.65 %, which was used as a working mixture in the active element of an HgBr laser [30], discharge power losses in the dissociative excitation of HgBr (B) at the maximum of its value were ~8%. With an increase in the parameter E/N (≥4 Td), this power gradually decreased. The power that is deposited in other processes also decreased with the increase of the parameter E/N, with the exception of the power for ionization processes and general electronic excitation. This regularity is related to the dependency of the effective cross section of the processes acting on the electron energy. The difference in the dependency of the specific power losses of discharge power on these processes can be explained by the introduction into the numerical calculation of more effective processes of inelastic cross-sections, namely, the vibrational excitation of mercury dibromide molecules and their attachment. Fig. 1.4c presents data on the dependencies of the rate constants of the elastic and inelastic processes of electron collisions with molecules and atoms in mixtures of mercury dibromide vapor with helium and neon in the parameter E/p, which were determined in [31, 32]. They are a quantitative measure of the efficiency of these processes [1, 3]. The rate constants of processes for both mercury dibromide molecules and for helium and neon atoms increase with an increase in the parameter E/p. In the dissociative excitation and ionization of $HgBr_2$ molecules, they increase by one to two orders of magnitude when the parameter E/p changes from 1 to 30 $V \cdot cm^{-1} \cdot mm\ Hg^{-1}$. In the parameter region E/p ~2–3 $V \cdot cm^{-1} \cdot mm\ Hg^{-1}$,

where a greater contribution of the discharge power to these processes can be observed, the constants depend weakly on the kind of inert gas. The highest value of the constant (10^{-7} cm^3/s) was obtained for excitation of the D-state of $HgBr_2$ molecules (sums of states above the excitation threshold of 7.9 eV) [31]. For E/p <2 $V \cdot cm^{-1} \cdot mm\ Hg^{-1}$ in a mixture with neon, the rate

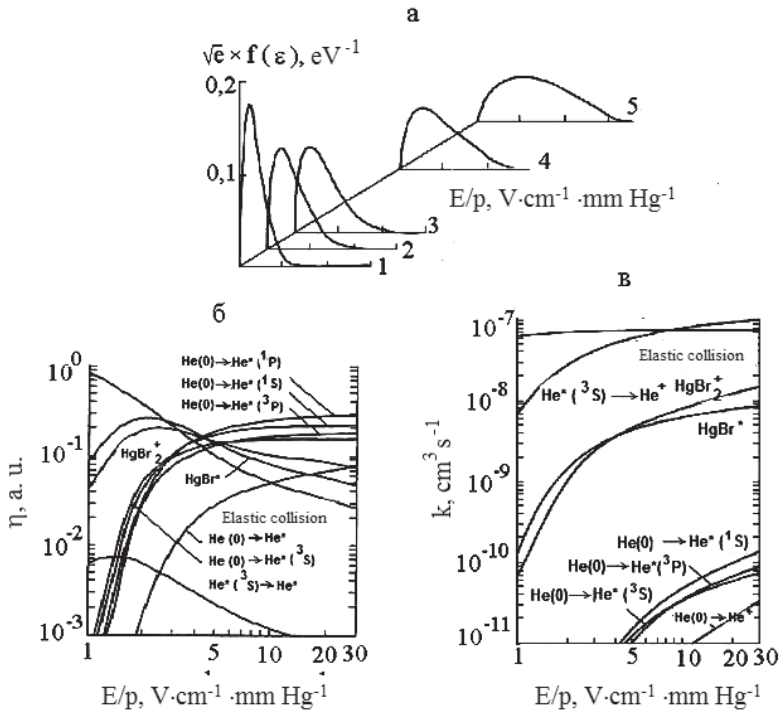

Figure 1.4. a). The electron energy distribution functions for a mixture of $HgBr_2$:He = 0.5:99.5; b). Specific power losses from the processes of electron collision with mercury dibromide molecules and helium in the mixture: a) $HgBr_2$:He = 0.5:99.5; c). The rate constants of the excitation and ionization processes in the mixture: a) $HgBr_2$:He = 0.5:99.5 [32].

constants are of great importance. The rate constants of the processes of elastic scattering of electrons with inert gas atoms and ionization are characterized by high values of ~10^{-8}–10^{-7} cm^3/s, which are associated with higher effective cross-sections of these processes [32].

The numerical calculation of the electron distribution functions in gas-discharge plasma in three component mixtures of mercury dibromide vapor and neon with 10 % additions of either nitrogen or xenon are presented in [3]. The value of the E/N parameter was chosen to provide approximately equal mean electron energies for these mixtures. In a mixture with nitrogen, the electron energy distribution was depleted in the energy range 2–5 eV. This is due to the fact that in this range the vibrational excitation cross-sections have high values (above 10^{-16} cm^2). In plasma mixed with Xe in this electron energy range, there is an excess of electrons, and for energies exceeding the 8.3 eV excitation threshold of the Xe ($^3P_2$) state a depletion in the distribution is observed. These features have a strong influence on the electron energy distribution function by changing the E/N parameter and, accordingly, on the excitation efficiency of mercury dibromide molecules in the plasma in these mixtures [3].

1.3. Conclusions to Chapter 1

An analysis of the literature on the processes in gas-discharge plasma of mercury dibromide vapor shows the following. The optical characteristics and parameters of plasma in mixtures of mercury dibromide vapor with gases were investigated for a limited set of compositions of working mixtures. There is no data on these characteristics for the pulse-periodic and sinusoidal modes of pumping working mixtures for pulse repetition rates above 2,000 Hz and for short pump pulse durations (at the level of exciplex molecule lifetimes). The possibility of the radiation of

several exciplex molecules simultaneously, which can be formed in gas-discharge plasma in the mixtures studied, has not yet been elucidated. The parameters and characteristics of the plasma for most working mixtures has not yet been clarified. There is no data on the optical characteristics in devices of small dimension (with a radiation area of <10 cm^2), which are necessary for exciplex sources in a number of practical applications.

These circumstances determined the direction of our work.

CHAPTER 2

TECHNIQUE AND EXPERIMENTAL METHODS

The optical characteristics of plasma in mixtures of mercury dibromide vapor and gases were investigated through barrier discharge (dielectric-quartz glass) [16]. The most important characteristic of this discharge is that the conditions for obtaining a non-equilibrium plasma can be provided at increased (atmospheric) pressures. In a barrier discharge, this can be achieved more simply than in other alternative methods, such as low-pressure discharges, high-pressure pulse discharges, or through the injection of an electron beam into a gas. It provides flexibility in relation to geometry, working media and plasma parameters. Ozone was first produced with the help of a barrier discharge, as well as powerful coherent infrared radiation from a CO_2 laser; and incoherent UV, VUV, and visible radiation from excimer and exciplex molecules [16, 49].

2.1. Experimental installations

Investigation into barrier discharge characteristics was carried out using three experimental installations, the block diagrams of which are shown in figures 2.1–2.3.

The structural elements of the installations are designed to take into account the peculiarities of the experimental conditions with a discharge that is formed in mixtures of mercury dibromide vapor and gases when a high-voltage pulse-periodic voltage or a sinusoidal voltage is applied to the

working electrodes with frequencies of 5 Hz, 3–9 kHz and 120 kHz, respectively; interference in the range (5 Hz–150 MHz); and salt vapor and gases of working mixtures at pressures of 70–200 kPa.

The main units of the first experimental installation (Figure 2.1) are: a gas discharge cuvette (GDC); a vacuum pumping and gas filling system (VPGFS); a high voltage (HVG) generator (pulse-periodic voltage); and a system for recording the optical and electrical discharge characteristics. The generator allows the reception of pulses with an adjustable voltage amplitude in the range 3–10 kV, a duration of 400–600 ns, and a pulse repetition rate of f = 3,000–9,000 Hz. The registration system consists of: a diffraction monochromator SD 7 (with a grating of 600 lines/mm and spectral resolution of the recording system at 2.4 nm); photodetectors (FD); photoelectronic multipliers FEU-106 and 14 ELU-FS; an electrical signal amplifier (A)—U5-9; spectra recorder (SP)—KSP-4; a digital voltmeter (V)—S-4300; an oscilloscope (O)—C1-72 (or C7-10A); a Rogovsky coil (RC); a radiation power meter (PM)—Quartz-01; and a light filter (F)—SZS-16.

The second experimental setup (Figure 2.2) was designed to study sinusoidal optical and electrical signals at high frequency. Its main units are: a high voltage generator with a sinusoidal form of the output voltage; a monochromator—Jobin Yvon FHR 1000 (grating 2,400 lines/mm and spectral resolution of the recording system at 0.08 nm); a photodetector—a high-speed CCD solid-state matrix; a personal computer; a digital oscilloscope—LeCroy WaveRuner 6100A; and a power meter—Newport 1918-C. The generator made it possible to change the amplitude and frequency of the sinusoidal voltage up to 7 kV and 130 kHz, respectively.

The third experimental setup (Figure 2.3) consisted of: a high-voltage generator (FID FPG 10-1MKS20); a coaxial cable (RG213, R = 50 Ω);

current shunts (R = 0.157 Ω); attenuators (A1 = 20, A2 = 30 Db); generators for starting a high-voltage generator; a Shamrock sr-303i spectrograph (diffraction grating 2,400 lines/mm and spectral resolution of the recording system of 0.04 nm); a photodetector—ICCD camera (temporal resolution 2 ns); a personal computer; and a digital oscilloscope—LeCroy WR44Xi. The generator provided a voltage of 10 kV and pulse repetition rate of 10 Hz for a duration of 30 ns.

2.2. System for recording optical and electrical characteristics

The system for detecting the radiation of discharges made it possible to carry out spectral studies; to study the dependency of the emission intensity of spectral bands and lines on the component composition of the working mixtures; and to study the temporal characteristics of the radiation of barrier discharges and their pump parameters to determine the radiation power in absolute units.

When investigating the optical characteristics of a pulse-periodic barrier discharge (Figure 2.1), the plasma radiation was directed using lens A through the diaphragm D1 to the input slit of the SD-7 spectral monochromator, analyzed in the spectral range 250–800 nm and recorded by a photoelectric multiplier FEU-106. The electrical signal from the photomultiplier arrived at the input of the amplifier V5-9 and was recorded by a KSP-4 spectra recorder or a digital voltmeter SCH-4300. Calibration of the sensitivity of the recording system in relative units in this spectral range was carried out with the help of a standard hydrogen lamp DVS-25 and a tungsten lamp SI 8-200 at filament temperature T = 2,173 K.

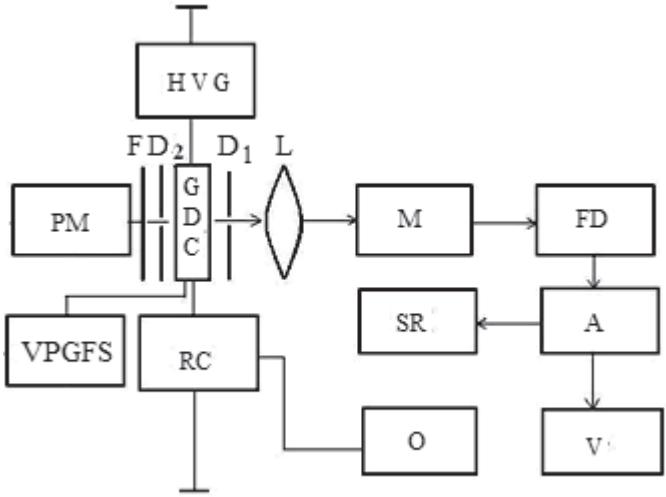

Figure 2.1. Block diagram of the experimental setup: GDC—gas-discharge cuvette; HVG—high voltage generator with pulse periodic form; M—monochromator; FD—photodetector; A—amplifier; SR—spectra recorder; V—voltmeter; O—oscilloscope; RC—Rogowski coil; VPGFS —vacuum pumping and gas filling system; PM—power meter; L, D1, D2, F—lens, diaphragm and filter, respectively [54].

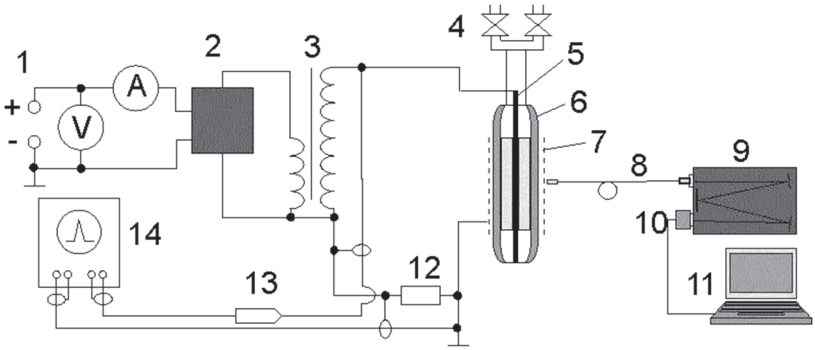

Figure 2.2. The system for recording optical and electrical characteristics in the mode of pumping working mixtures with sinusoidal voltage: 1 - constant current source; 2 - generator; 3 - high-voltage transformer; 4 - gas pumping and filling

system; 5 - electrode; 6 - quartz tube; 7 - mesh (external electrode); 8 - optical fiber; 9 - monochromator; 10 - CCD detector; 11 - personal computer; 12 - shunt; 13 - voltage divider; 14 - digital oscilloscope [58].

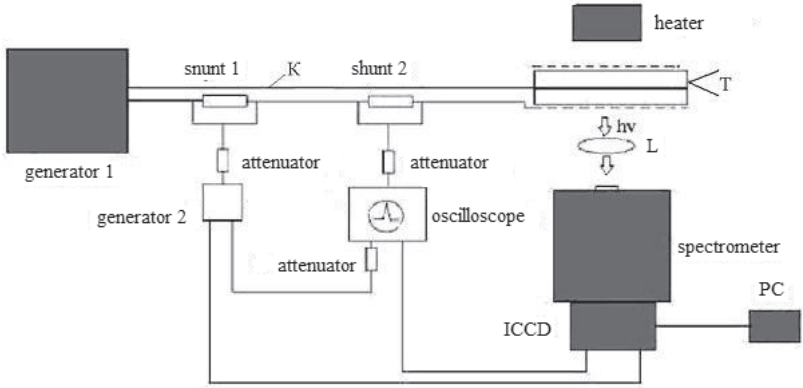

Figure 2.3. Block diagram of the system for recording optical and electrical characteristics in the pumping mode of working mixtures with pulse-periodic voltage of nanosecond duration: 1—high-voltage pulse generator of nanosecond duration; K—coaxial cable (R = 50 Ω); shunts: 1, 2 current shunts; GDC—gas discharge cuvette; L—quartz lens; generator 2—ICCD camera trigger generator; oscilloscope; PC—personal computer [70].

The relative error in measuring the optical characteristics of a pulse-periodic barrier discharge did not exceed the reduced error of the measuring instrument—the digital voltmeter SCH-4300. The error was 1 %.

To investigate the temporal characteristics of radiation, an electronic linear multiplier 14 ELU-FS was used, instead of the photoelectric multiplier FEU-106, which provided a time resolution of 2.5 ns. The electrical signal from it was fed into a wideband oscilloscope C7-10A or C1-72, using a cable with a wave resistance of 50 Ω. Using this oscilloscope, we also investigated the amplitude and temporal characteristics of the pump pulses (the amplitude of the voltage pulses applied to the gas discharge cell

and the amplitude of the discharge current). The calibrated capacitive voltage divider and Rogowski coil were used as the primary signal converters.

The relative error in the study of the temporal characteristics of the radiation was 10 %.

The average radiation power was measured with the help of the Quartz-01 instrument. The optical signal after passing through the diaphragm D2 of 0.25 cm^2 area was incident to the SZS-16 light filter with a maximum transmission of $\lambda = 500$ nm. After this it was directed to the measuring head of the instrument, which was 10 cm from the diaphragm. The power emitted by the entire surface of the cell was determined from the expression [50]:

$$P_{rad.} = \Omega_0 \cdot P_{p.}/\Omega_{p.}$$

where $P_{p.}$ is the power detected by the photodetector; Ω_0 is the equivalent solid angle (for a cylindrical surface, its value is π^2 [50]); $\Omega_{p.} = S_{p.}/l_0^2$ is the solid angle of the photodetector; $S_{p.}$ is the area of the photodetector window; and l_0 is the distance at which the photodetector is located from the radiation source.

The relative error in measuring the radiation power was 6 %, which included: the relative error of the Quartz-01 instrument; the relative error in determining the area of the photodetector; and the distance at which the photodetector was located from the radiation source.

When studying the characteristics of a sinusoidal barrier discharge, which was ignited by a sinusoidal voltage (Figure 2.2), the radiation was analyzed in the spectral range 200–740 nm. Radiation from the cuvette was directed onto the input slit of the Jobin Yvon FHR 1000 monochromator after passing through the optical quartz fiber and recorded with a high-speed

CCD detector, Spectrum ONE, which was cooled with liquid nitrogen. The signal from the CCD detector was sent to the personal computer. The spectra were processed using the Spectrum Analyzer 1.5. The temporal characteristics were recorded with a digital oscilloscope, LeCroy Wave Runer 6100A, the sensors were a high-voltage divider, Tetronix P6015A, and a low-inductance 50 Ω resistor TVO for measuring the amplitude of the voltage and current. The average power was recorded by the Newport 1918-C power meter. The sensor head of the 918D-UV power meter was located at a distance of 40 cm from the gas discharge cuvette.

In studying the characteristics of a pulse-periodic barrier discharge (Figure 2.3) of nanosecond duration, plasma radiation was recorded and analyzed in the spectral range 200–600 nm. The amplitudes of the voltage and current pulses, as well as their temporal characteristics, were measured with a current shunt (R = 0.157 Ω) and an oscilloscope, LeCroy WR44Xi. The temporal characteristics of the radiation were recorded using a photoelectric multiplier, R5320 Hamamatsu, with a temporal resolution of 0.7 ns and an Istar-7260 ICCD camera (with a temporal resolution of 2 ns). To study the temporal characteristics of the emission of exciplex molecules of mercury monobromide HgBr*, a filter with a transmission maximum of 480 nm $\pm$ 10 nm was used. In order to study the temporal characteristics of the emission of exciplex molecules KrBr* a filter with a transmission maximum at a wavelength of 210 nm $\pm$ 10 nm was used.

The relative measurement error was 2 %.

2.3. Gas-discharge cuvettes

The gas-discharge cuvettes were made of quartz tubes (quartz glass of mark KU-2). The tubes had a wall thickness of 1 mm and an outer diameter

of 8.8 mm or 6 mm. They were used to study the optical characteristics of radiation when the working mixtures were pumped with pulse-periodic voltage, with a pulse duration of 400–600 ns, as well as sinusoidal voltage. Along the axis inside them was a molybdenum electrode with a diameter of 1–2 mm. The spacing gap was 2.4 mm or 1.5 mm. The outer electrode was made of metal mesh (stainless steel) and had a transmittance of ~0.7 or 0.9. It had a length of 3 cm. The working volume was ~(0.35–1) cm^3.

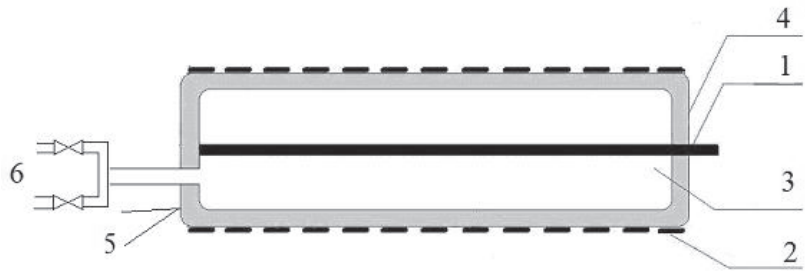

Figure 2.4. Gas-discharge cuvette: 1 - internal electrode; 2 - external (mesh) electrode; 3 - discharge zone; 4 - quartz glass; 5 - thermocouple; 6 - valves of the pumping and gas filling system [68].

At the end of the quartz tube there was a capillary with a diameter of 1.5 mm, which served to reduce the removal of mercury dibromide vapor from the cuvette into the vacuum gas mixing system.

To study the optical characteristics of radiation when the working mixtures were pumped with a pulse-periodic voltage with nanosecond pulse duration, ~30 ns, the same design of gas-discharge cuvette was used. The difference was in its size. The tube was 210 mm long and the external diameter was 10 mm. A tungsten electrode with a diameter of 2 mm was located in the tube along the axis. The interelectrode distance was ~3 mm.

On the outer surface of the quartz tube an electrode made of a metal mesh with a transmittance of 0.7 was placed. A tap was welded on one of the end surfaces of the tube to connect to the gas filling system.

2.4. Vacuum pumping and gas filling system

The vacuum pumping and gas filling system (VPGFS) was designed for pumping a gas-discharge cuvette (GDC), as well as filling it with gas mixtures. The block diagrams of the VPGFS show its separate elements. Figure 2.5 shows a typical block diagram of the VPGFS. It includes: a vacuum pump, type 2NVR-5DM or Edwards XDS-5; valves; reducers; a membrane sample manometer; and a vacuum gauge or a capacitive pressure sensor TPR-280; gas cylinders; and a buffer volume that is used to fill gases of small partial pressures (<133 Pa). The gas is introduced into the GDC after evacuation of the entire system to a pressure of $1.3 \cdot 10^{-1}$ Pa.

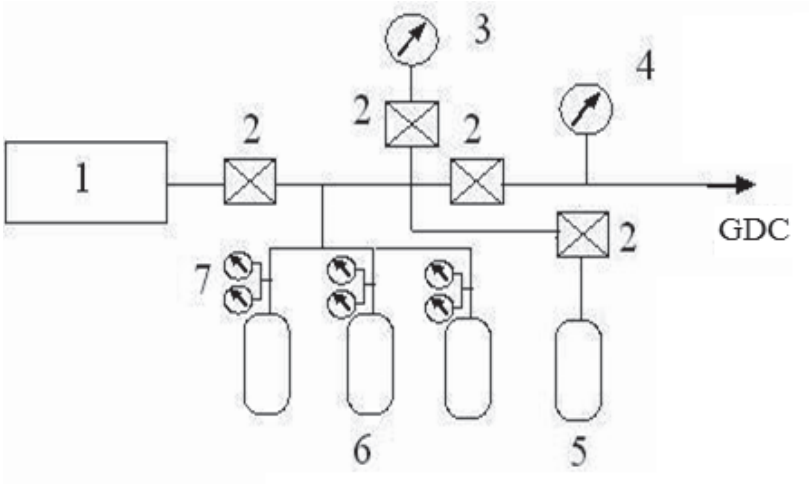

Figure 2.5. Block diagram of the vacuum pumping and gas filling system: 1 - pump; 2 - valves; 3 - vacuum gauge; 4 - manometer; 5 - buffer volume; 6 - cylinders with gases, or gas mixtures; 7 - reducers; GDC—gas discharge cuvette.

2.5. Control experiments

Control experiments were carried out to determine the operability of the experimental setup for measurements, as well as the optical, electrical and temporal characteristics of the recording system. At the beginning of the control experiments, the range of voltage amplitudes at which the discharge was to be ignited were determined. This consisted of the following procedure. The gas discharge cuvette was degassed to a vacuum of $1.3 \cdot 10^{-3}$ Pa by heating it up to 200 °C for 1 hour. It was then filled with "high" purity helium (GOST 1021) to a pressure of 121.6 kPa. A pulse-periodic voltage with an amplitude of 6–10 kV and a pulse repetition rate of 6,000 Hz was applied to the electrodes of the cuvette. When the discharge was ignited, a uniform, transverse discharge of pink color could be visually observed.

To investigate the operability of the recording system for pulsed optical and electrical signals, radiation pulses and the discharge current of a nitrogen laser, LGI-21, whose passport data are known, were used. To this end, the pulses from this laser (λ = 337 nm), after attenuation by a neutral filter, were applied to the input slit of the spectral monochromator SD-7, which was previously tuned to this wavelength. The current pulses of the active element of the laser were recorded using a Rogowski coil. Figure 2.6 a) and b) show the measurements. They coincided with the passport data within an error of 10 %.

To determine the range of the linear change in the photodetector current (PMT, ELU) with the change of the optical signal, we carried out an experiment in which the radiation from the nitrogen laser LGI-21 was directed to the input slit of the monochromator and its power changed

linearly. The experiment revealed a linear change in the output signal within a tenfold change in the laser radiation power.

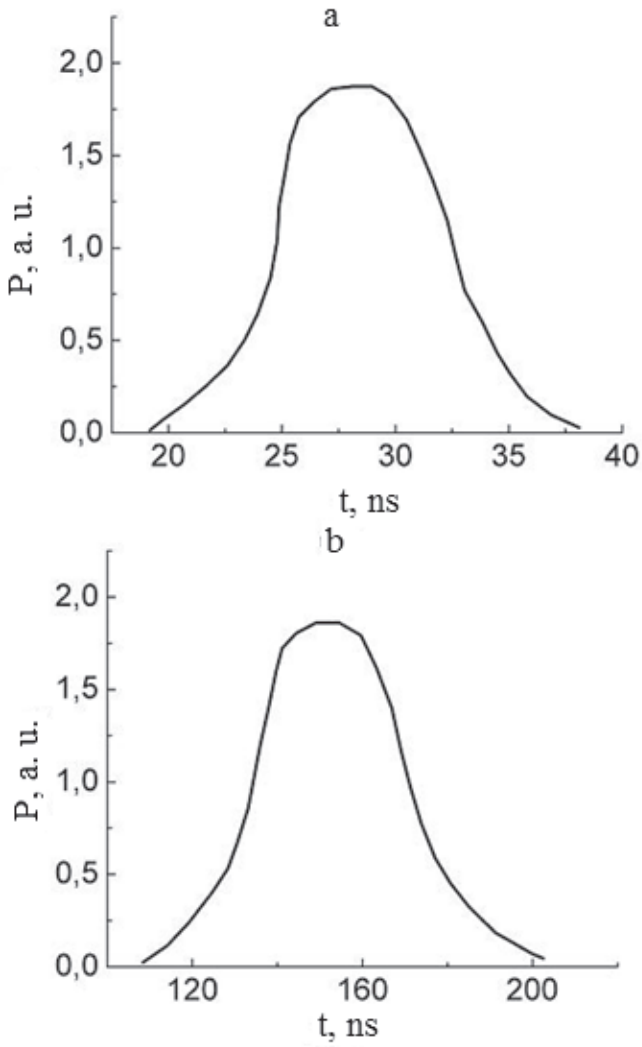

Figure 2.6. a) Oscillogram of laser LGI-21 radiation pulse; b) Oscillogram of laser LGI-21current pulse.

Due to the fact that the spectral sensitivity of the FEU-106 photomultiplier varies with the wavelength of the optical signal, a calibration of the optical signal recording system in the spectral range 200–900 nm was carried out.

The results of calibration of the optical signal recording system in the spectral range 200–900 nm are shown in Figure 2.7.

Calibration of the Rogowski coil was carried out as follows. A low-inductance 50 Ω resistor of the TVO brand was connected to the load circuit of the generator G5-15. The braid of the generator cable passed through the free space of the Rogowski coil.

A voltage pulse from the Rogowski coil was fed to an oscilloscope C1-72 or C7-10A. The known resistance of the resistor and the amplitude of the voltage applied to it, along with the amplitude of the oscillogram, determined the amplitude of the current in the electrical circuit. The sensitivity of the Rogowski coil was eventually equal to $5.35 \cdot 10^{-2}$ V/A.

Calibration of the recording system for the study of high frequency sinusoidal signals was also carried out. This involved the use of standard deuterium and tungsten lamps with relative intensities in the region of 200–400 nm and 400–900 nm, respectively.

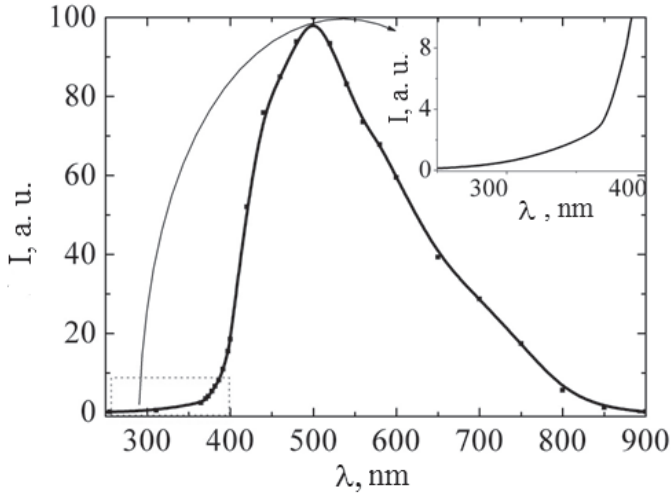

Figure 2.7. Calibration graph for the optical radiation detection system.

Calibration of the recording system for pulse-periodic signals of nanosecond duration (30 ns) and low frequency (10 Hz) was carried out in the spectral range 200–600 nm (figures 2.8–2.10). A reference lamp (EQ-99FC) was used for this purpose. Its emission spectrum according to the passport data is shown in Figure 2.8.

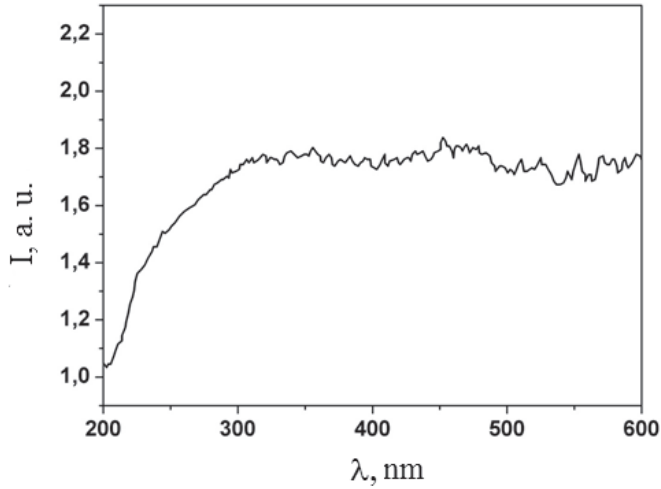

Figure 2.8. The emission spectrum of the standard lamp (EQ-99FC).

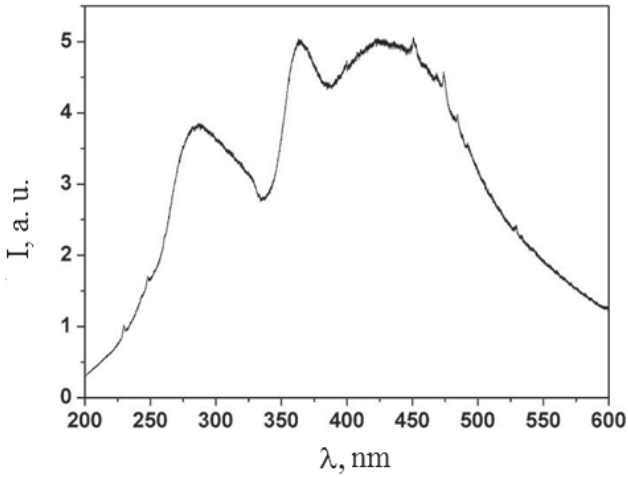

Figure 2.9. Calibration graph for the optical emission detection system for the standard lamp (EQ-99FC).

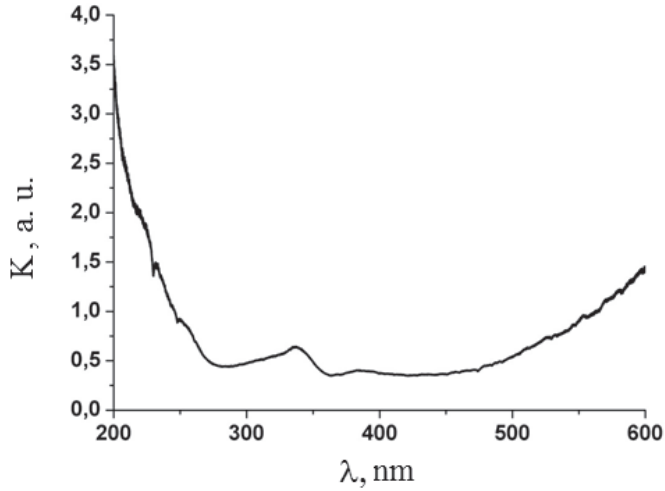

Figure 2.10. The correction factor of the optical system for recording radiation of wavelengths 200–600 nm.

2.6. Conclusions to Chapter 2

The experimental setup allows for systematic study of the optical and electrical characteristics of the barrier discharge plasma, namely, to study the emission spectra; the dependency of the radiation intensity on the partial pressures of the mixture components; the impulse voltage, current and plasma emission characteristics of the gas discharge; and the operating mixture life and pumping conditions. The creation of plasma in the investigated mixtures of vapor and gases was achieved by discharge through the dielectric quartz glass. Control experiments, as well as calibration of the optical signal recording system and Rogowski coil, allowed us to ensure that the optical, temporal and electrical discharge characteristics were reliably recorded by the optical and electric signal recording system.

CHAPTER 3

OPTICAL CHARACTERISTICS OF GAS-DISCHARGE PLASMA IN MIXTURES OF MERCURY DIBROMIDE VAPOR WITH ATOMIC AND MOLECULAR GASES

The optical characteristics of the plasma were studied in a barrier discharge using mixtures of mercury dibromide vapor with gases, including: helium, argon, neon, nitrogen, sulfur hexafluoride, xenon and krypton. The main components of the working mixtures were mercury dibromide vapor and a buffer gas such as helium, argon, neon or krypton. Nitrogen, sulfur hexafluoride, xenon and krypton were used as additives to the main components, and their partial pressures did not exceed 10 kPa. The plasma was formed in a barrier discharge with a pulse-periodic and sinusoidal waveform of the voltage pulse at a frequency f = 1–10 kHz (with the mixtures $HgBr_2$:He; $HgBr_2$:Ar; $HgBr_2$:Ne; $HgBr_2$:N_2:He; $HgBr_2$:SF_6:He; $HgBr_2$:SF_6:N_2:He); 10 Hz (with the mixture $HgBr_2$:Kr:He); and 120 kHz (with the mixtures $HgBr_2$:He and $HgBr_2$:Xe:Kr).

Working mixtures were prepared directly in the volume of the radiator. Mercury dibromide powder in the amount of 60 mg was uniformly loaded into the discharge cuvette. The partial pressure of the saturated vapors of mercury dibromide was created by self-heating the working mixture through the dissipation of discharge energy, as well as by applying an electric heater as an external heat source. After loading the salt, the radiation

source was degassed by heating with the external electric heater at a temperature of 70 °C and pumping out for 2 hours. The value of the partial pressure of saturated mercury dibromide vapor was determined from the temperature of the coldest point of the radiator, based on the reference data [51]. Under the conditions of our experiment, it varied within the limits 0.1–2,000 Pa. The partial pressures of the gases were measured using an exemplary membrane manometer and a vacuum gauge, as well as through the use of a buffer volume for measurement of low partial pressures (<133 Pa) of gases (see Figure 2.5, Chapter 2). In experiments with pumping by pulse-periodic voltage of nanosecond duration, a capacitive pressure sensor, TPR-280, was used to measure the pressure of the gas mixture (Kr:He). The error in measuring the partial pressures of the gases was not more than 1 %, and the partial pressure of mercury dibromide was 5 %.

The results of these studies were published in [52-60, 62-74].

3.1. Optical characteristics of gas-discharge plasma in a mixture of mercury dibromide vapor with helium

Immediately after ignition of the atmospheric pressure barrier discharge, a filamentary burning of the BR was observed in the form of a set of cone-shaped microdischarges with a vertex on the metal electrode and a base on the inner surface of the quartz tube of the radiator. The color of the discharge in the initial stage (for the first 30 s) was determined by the buffer gas helium—it therefore had a pink color. In the next time interval of 30–60 s, the discharge had a blue-green color. During the self-heating of the mixture, the color of the discharge became green. At the same time, a diffuse (homogeneous) character of the discharge glow was observed, and the contrast in brightness in the volume discharge and filaments appreciably smoothed out.

3.1.1. Oscillograms of the pump pulses

In Figure 3.1, typical oscillograms of the pump pulses (voltage and current of the barrier discharge) are presented. The amplitudes of voltage and current pulses were 8 kV and 9A, respectively. The oscillatory structure of the current pulse (Figure 3. 1) is caused by multiple discharges of the dielectric capacitance during a voltage pulse with an amplitude sufficient for the breakdown of the discharge gap [75]. The difference in the oscillatory structure of the current pulses at the leading and trailing edges of the pump pulse (voltage) was due to opposite directions of current passing through the gas-discharge gap (2.4 mm). As a result, unequal conditions of charge dissipation on the dielectric inner surface created single-barrier discharge conditions, which were used in our experiments.

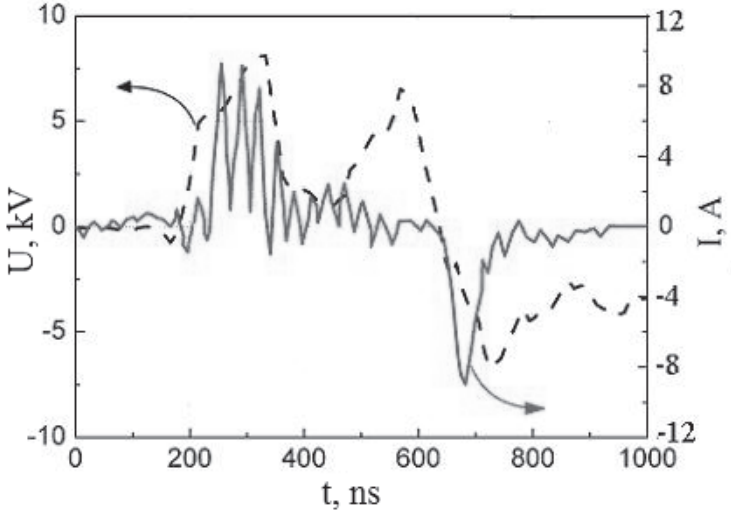

Figure 3.1. Oscillograms of the current and voltage pulses at the emitter electrodes for the mixture $HgBr_2$:He = 0.1:117; the total pressure of the mixture was P = 117.1 kPa; the repetition rate was f = 6 kHz [52].

3.1.2. Spectrum of plasma radiation

In Figure 3.2, a survey spectrum of the radiation of BR plasma in a mixture of mercury dibromide vapor with helium is shown. In the emission spectrum, a spectral band with a maximum intensity at a wavelength of λ = 502 HgBr (B→X) nm was significant. It had a poorly-structured vibrational structure and corresponded to the $B^2\Sigma^+_{1/2} \rightarrow X^2\Sigma^+_{1/2}$ electron-vibrational transition of the exciplex HgBr* molecule [76]. The main part of the radiation intensity was concentrated in the wavelength range 475–512 nm. The shape of the band and its width at half-height (15–16 nm) were similar to bands corresponding to the transition of B→X mercury monohalides, as given in those studies where the ignition of the barrier discharge was carried out in quartz tubes of large dimensions [12, 13, 26–28, 43, 45, 46]. There was a sharp increase in the intensity in the spectrum from the side of the region with large wavelengths and a slow decline in the region of smaller wavelengths.

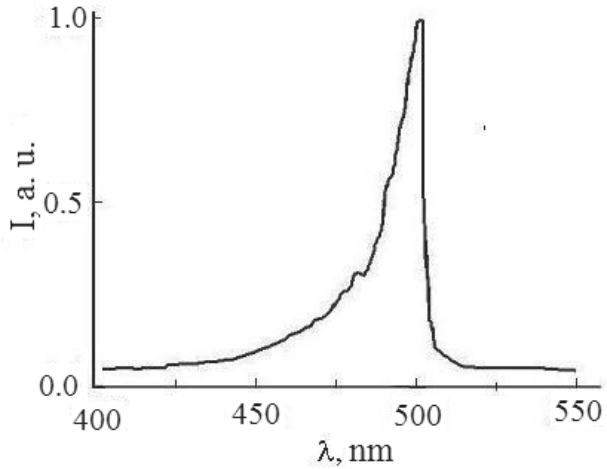

Figure 3.2. The radiation spectrum of the barrier discharge in the mixture $HgBr_2$:He = 0.1:117 kPa. The total pressure of the mixture was P = 117.1 kPa. The repetition rate of the pump pulses was f = 6 kHz; the amplitude was U_a = 9 kV [52].

3.1.3. The dependency of the average radiation power of exciplex HgBr* molecules on the partial pressures of helium and mercury dibromide vapor

Figures 3.3a and 3.3b present the results of studies on the dependency of the radiation power of the exciplex HgBr* molecule on the partial pressure of helium and mercury dibromide vapor, respectively. (In experiments on the dependency of the radiation power of the HgBr* molecule, the partial pressures of mercury dibromide vapor in mixtures with helium were created by heating the radiator with an electric heater, Figure 3.3b.) An increase in the radiation power of the HgBr* molecule was observed with an increase in the partial pressure, both for helium and mercury dibromide vapor, from 80 kPa to 117–120 kPa and 0.1 kPa to 0.8 kPa, respectively.

A further increase in the partial pressure, both for helium and mercury dibromide vapor, led to a decrease in the radiation power of the exciplex of mercury monobromide.

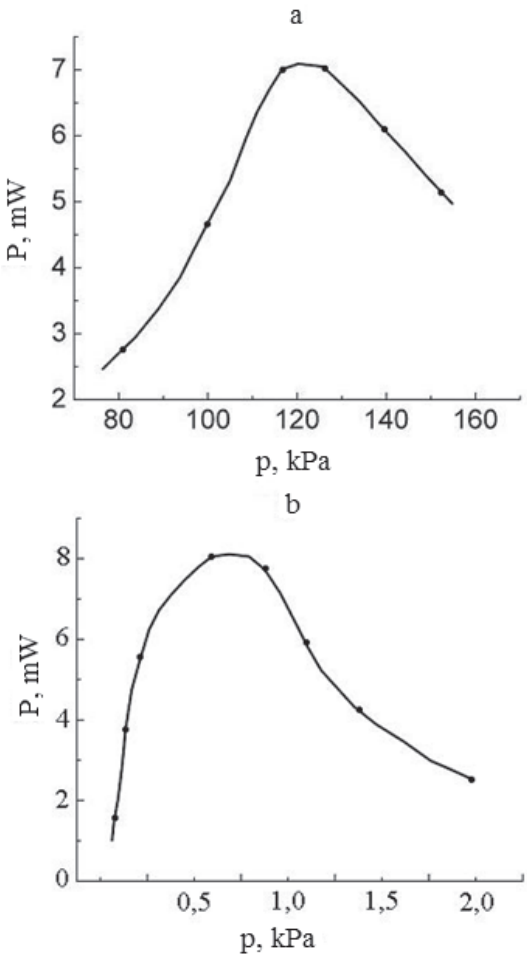

Figure. 3.3. a) The dependency of the radiation power of HgBr* exciplex molecules on the partial pressure of helium for the mixture $HgBr_2$:He. The partial vapor pressure of $HgBr_2$ was P = 0.1 kPa. The repetition rate was f = 6 kHz; the voltage amplitude was U_a = 9 kV; b) the dependency of the radiation power of the HgBr* exciplex on the partial pressure of mercury dibromide vapor for the $HgBr_2$:He mixture. The partial pressure of helium was P = 117 kPa. The repetition rate was f = 6 kHz; the voltage amplitude was U_a = 9 kV [52].

3.1.4. Pulsed radiation power of exciplex HgBr* molecules

Figure 3.4 shows the pulsed radiation power of HgBr* molecules for plasma in the mixture $HgBr_2$:He, at the maximum values of the average radiation power in the self-heating mode of the mixture. A structure consisting of three pulses was characteristic. The amplitude of the first radiation pulse was larger than the amplitude of the second pulse. The first and third emission maxima coincided (within the measurement error) with the maxima of the pump current amplitudes (Figure 3.1). The amplitude of the third radiation pulse was larger in magnitude than the amplitudes of the first and second pulses. Additionally, there was an additional maximum amplitude in the third pulse.

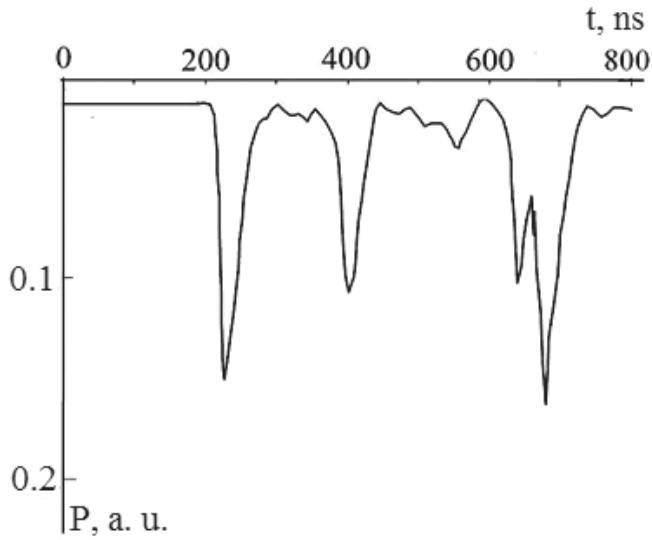

Figure 3.4. The pulsed power of the emission of exciplex HgBr* molecules of a gas-discharge plasma in an $HgBr_2$:He mixture. Partial pressures: $HgBr_2$ = 0.1 kPa; He = 117 kPa [59].

3.1.5. Discussion of research results

The appearance of spectral band emissions with a maximum wavelength of λ = 502 nm with the $B^2\Sigma^+_{1/2} \rightarrow X^2\Sigma^+_{1/2}$ electron-vibrational transition of exciplex HgBr* molecules in gas-discharge plasma in a mercury dibromide vapor with helium mixture, led to the formation and destruction of the $B^2\Sigma^+_{1/2}$ state of mercury monobromide molecules. The main transitions were [13, 26, 40–43]:

$$HgBr_2+e \rightarrow HgBr_2(^{3,1}\Sigma^+_u)+e \rightarrow HgBr(B^2\Sigma^+_{1/2})+Br+e \quad (3.1)$$

$$HgBr_2+e \rightarrow HgBr_2(^{3,1}\Sigma^+_u)+e \rightarrow HgBr(B^2\Sigma^+_{1/2})+Br^- \quad (3.2)$$

$$HgBr(B^2\Sigma^+_{1/2}) \rightarrow HgBr\ (X^2\Sigma^+_{1/2})+h\nu \quad (3.3)$$

$$HgBr(B^2\Sigma^+_{1/2})+M \rightarrow HgBr\ (X^2\Sigma^+_{1/2})+M+\Delta E \quad (3.4)$$

where M is the concentration of quenching molecules and atoms ($HgBr_2$, He), respectively and ΔE is the energy difference in the reaction.

A strong increase in the intensity from the side of the region in the spectrum with large wavelengths and a slow decline in the short wavelength region (Figure 3.2) is due to the type of potential curves and relaxation processes of the population of the upper vibrational levels of the $B^2\Sigma^+_{1/2}$ state of the HgBr* molecule. A shift was seen towards larger internuclear distances in comparison to the $X^2\Sigma^+_{1/2}$ state (see Figure 1.1, Chapter 1). As such, the relaxation processes occur faster than the electron-vibrational transition to the ground $X^2\Sigma^+_{1/2}$ state [22-24, 36].

The dependency of the radiation power of HgBr* molecules on the partial pressure of helium (Figure 3.3a) is due to the following processes: an increase in the electron concentration with an increase in the partial pressure of helium in the mixture; a change in the fraction of the discharge energy that is spent on heating the working mixture; the change in the mean

electron energy and rate constant of HgBr* molecule excitation as a function of the parameter E/N value; and the quenching of the $B^2\Sigma^+_{1/2}$ state of HgBr* molecule upon collision with helium atoms [1, 3]. With an increase in the partial pressure of helium, the value of the parameter E/N decreased. This led to an increase in the specific losses of the discharge power in the elastic scattering of electrons by atoms and molecules (Figure 4.3a, Chapter 4, dependency 2), which increased the heating of the mixture. This in turn increased the partial pressure of the mercury dibromide vapor and, correspondingly, the radiation power of HgBr* molecules. In addition, the increase in the radiation power with increasing partial pressure, in both helium and mercury dibromide vapor, was promoted by an increase in the electron concentration, which increased with the increasing concentration of the components of the working mixture [77]. The presence of a maximum and a further decrease in the radiation power of exciplex HgBr* molecules, with an increase in the partial pressure of helium, is caused by a decrease in the fraction of the discharge energy that is spent on the excitation of the HgBr* molecule $B^2\Sigma^+_{1/2}$ state (Figure 4.3a, Chapter 4, curve 7), as well as the process of quenching a given state of the mercury monobromide molecule upon the collision of molecules with helium atoms (process 3.4) [33].

The dependency of the radiation power of exciplex HgBr* molecules on the partial pressure of mercury dibromide vapor (Figure 3.3b) and the optimal value of the partial pressure of mercury dibromide vapor is determined by the kinetics of the processes leading to the excitation and quenching of the HgBr* molecule $B^2\Sigma^+_{1/2}$ state—the process (3.1) and the efficiency of the process of quenching this state by $HgBr_2$ molecules (process 3.4). Above a certain value of the partial pressure of mercury dibromide vapor, the quenching process (3.4) will have a predominant value

in connection with which the radiation power decreases. The rate constant of this process is $(2.7 \pm 0.2)\ 10^{-10}$ cm^3/s [78].

The first radiation pulse (Figure 3.4) is caused by the process of dissociative excitation of the $B^2\Sigma^+_{1/2}$ state of mercury monobromide molecules in the collision of electrons with mercury dibromide molecules (process 3.1). The presence of a second radiation pulse can cause an additional excitation channel of $B^2\Sigma^+_{1/2}$-state mercury monobromide molecules. Mercury monobromide molecules, which are in the $X^2\Sigma^+_{1/2}$ state (and thus do not have time to unite into the triatomic mercury dibromide molecule), are excited in collisions with plasma electrons in the $B^2\Sigma^+_{1/2}$ state, after which the decay of this state through the optical channel yields an additional (second, Figure 3.4) radiation pulse:

$$HgBr(X^2\Sigma^+_{1/2})+e \rightarrow HgBr(B^2\Sigma^+_{1/2})+e \quad (3.5)$$

$$HgBr(B^2\Sigma^+_{1/2}) \rightarrow HgBr(X^2\Sigma^+_{1/2})+h\nu\ (\lambda_{max.}\ 502\ nm) \quad (3.6)$$

which are similar to the experimental results obtained at low repetition rates of the pump pulses in papers by previous authors [2, 13].

The second pump pulse leads to the excitation of HgBr molecules along the main channel (reaction 3.1) to the $B^2\Sigma^+_{1/2}$ state and gives the corresponding amplitude in the third radiation pulse. The appearance of an additional maximum amplitude in the third radiation pulse is possibly caused by a current of negative ions $HgBr_2^-$ and Br^- [3, 79–83].

3.2. Optical characteristics of gas-discharge plasma in a mixture of mercury dibromide vapor, nitrogen and helium

Studies were carried out in a ternary mixture of $HgBr_2$:N_2:He. The partial vapor pressure of the mercury dibromide and helium was 0.1–0.8

kPa and 120 kPa, respectively; the partial pressure of nitrogen varied within the range 1–10 kPa. The partial pressure of helium was the same across the experiments. It was chosen as optimal for the maximum observed radiation power of the double $HgBr_2$:He mixture (Section 3.1).

3.2.1. Oscillograms of the voltage and current pulses of the barrier discharge plasma

Figure 3.5 shows oscillograms of the voltage and current pulses of the barrier discharge plasma for the ratio of the components of the mixture at which maximum radiation was reached. The oscillatory regime of the energy input of the pump source into the plasma was observed. The maximum amplitude values of the voltage and current pulses were 9 kV and 11 A, respectively. The oscillatory structure of the pulse, as well as its difference in the current pulse at the leading and trailing edges of the pump pulse (voltage), have the same causation in $HgBr_2$:He mixtures.

There were differences in the current pulses for the mixture with N_2 gas (Figure 3.5) and for the mixture without it (3.1). In the mixture with nitrogen, a characteristic pulse appears on the leading front with a larger amplitude and duration than the mixture without nitrogen.

In addition, in the region t = 400 ns, its amplitude was higher than the amplitude of the pulse in the mixture without nitrogen, which may be due to the large charge in the dielectric surface compared to the discharge in the $HgBr_2$:He mixture.

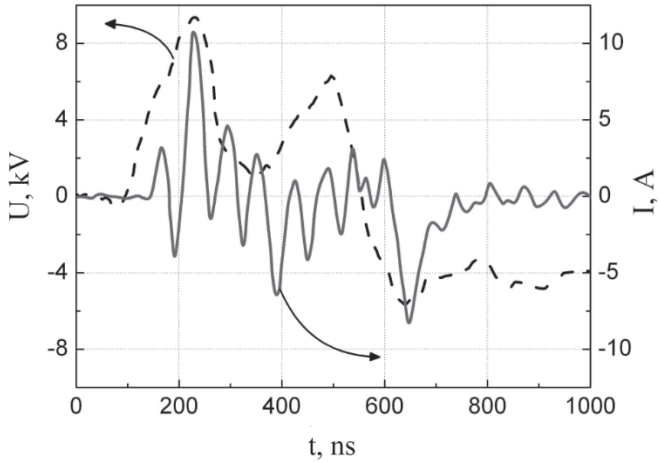

Figure 3.5. Oscillograms of the current and voltage pulses at the emitter electrodes for the mixture $HgBr_2$:N_2:He = (0.1:4:120) kPa. The pulse repetition rate was f = 6 kHz [54].

3.2.2. Spectrum of plasma radiation

The spectral band with a maximum wavelength of λ = 502 nm was significantly allocated. It had a weakly-resolved vibrational structure and corresponded to the $B^2\Sigma^+_{1/2} \rightarrow X^2\Sigma^+_{1/2}$ electron-vibrational transition of the exciplex HgBr* molecule [76]. The main part of the radiation intensity was concentrated in the wavelength range 475–512 nm. The shape of the band and its width at half-height (15–16 nm) was similar to the bands corresponding to the B→X transition in mercury monohalides, as reported in papers in which the creation of a barrier discharge was carried out in quartz tubes for both large and small-sized radiation sources (Chapter 3.1) [12, 13, 26–28, 43, 45, 46, 52]. There was the same strong increase in intensity in the spectrum from the side of the region with large wavelengths and a slow decline in the region of shorter wavelengths, as in the study of

the spectra of the mixture of mercury dibromide vapor and helium (Figure 3.2).

3.2.3. The dependency of the average radiation power of exciplex HgBr* molecules on the partial pressure of nitrogen

Figure 3.6 shows the results of a study on the dependency of the average radiation power of HgBr* exciplex molecules on the partial pressure of nitrogen molecules. An increase in the radiation power of HgBr* molecules was observed with the increase in the partial pressure of nitrogen from 0 kPa to 4 kPa and the value 8.7 mW (the partial pressure of mercury dibromide vapor was 0.1 kPa). A further increase in the partial pressure of the nitrogen led to a drop in the radiation power of the exciplex molecule. A similar dependency of the emission power of the HgBr* molecule on the nitrogen partial pressure was also observed for a mixture in which the partial pressure of the mercury dibromide vapor was higher and which was created by heating the quartz tube of the radiator with an external electric heater. The maximum emission power of the exciplex molecule HgBr* was 87 mW for values of the partial pressures of mercury dibromide vapor, nitrogen and helium of 0.8 kPa, 4 kPa and 120 kPa, respectively.

3.2.4. Pulsed radiation power of exciplex HgBr* molecules

Figure 3.7 shows the pulsed power of exciplex HgBr* molecule emissions for a radiation source acting on a $HgBr_2$:N_2:He mixture. The radiation pulse consisted of three peaks.

The amplitude of the first peak of the radiation pulse was larger than the amplitude of the second, and the first and third radiation maxima coincided (within the measurement error) with current peak maxima (Figure 3.5). The amplitude of the third radiation pulse was larger than the

amplitude of the first and second pulses; its width at half-height of the amplitude exceeded the values for both the first and second peak. These pulse amplitudes exceeded the amplitudes of discharge pulses in the $HgBr_2$:He mixture (Figure 3.4).

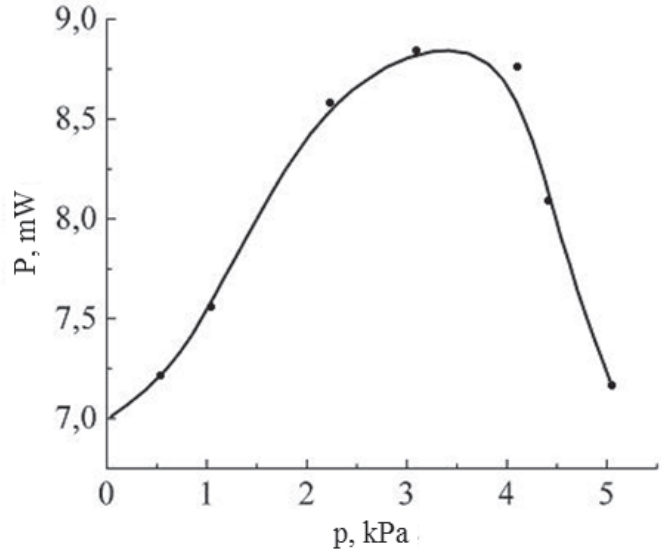

Figure 3.6. The dependency of the radiation power of exciplex HgBr* molecules on the partial pressure of nitrogen molecules for the mixture $HgBr_2$:N_2:He. The partial pressures of mercury dibromide vapor and helium were p = 0.1 and 120 kPa, respectively. The pulse repetition rate was f = 6 kHz [54].

3.2.5. Discussion of research results

The appearance of spectral band emissions at a maximum wavelength of λ = 502 nm of the electronic-vibrational transition $B^2\Sigma^+_{1/2} \rightarrow X^2\Sigma^+_{1/2}$ of exciplex HgBr* molecules in gas-discharge plasma in a mixture of mercury dibromide vapor, nitrogen and helium occurred due to processes leading to

the formation and destruction of $B^2\Sigma^+_{1/2}$-state mercury monobromide—this was the same as with the mixture of mercury dibromide vapor and helium (Chapter 3.1, reactions 3.1–3.4). In addition, the process of dissociative excitation of the $B^2\Sigma^+_{1/2}$ state occurs with the collision of mercury dibromide molecules with nitrogen molecules excited to the metastable state ($A^3\Sigma^+_u$) and the $B^3\Pi_g$ state [29, 37].

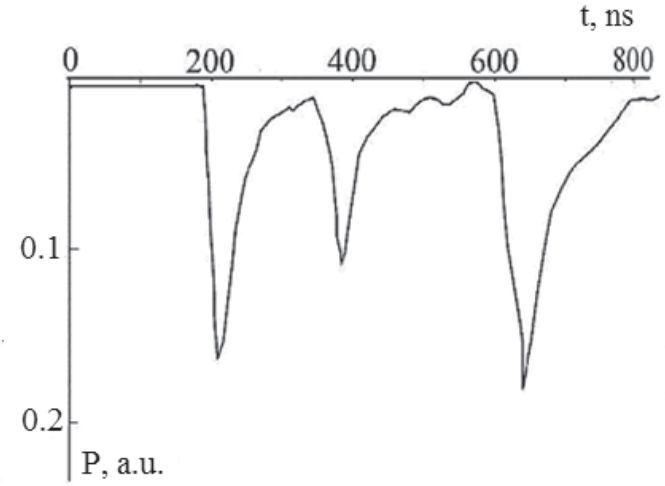

Figure 3.7. The pulsed power of the emission of exciplex HgBr* molecules in gas-discharge plasma in the $HgBr_2$:N_2:He mixture. Partial pressures: $HgBr_2$ = 0.1 kPa; N_2 = 4 kPa; He = 120 kPa [59].

The dependency of the radiation power of exciplex HgBr* molecules on the partial pressure of nitrogen (Figure 3.6) is primarily due to an increase in electron concentration with an increase in the partial pressure of the nitrogen in the mixture and a change in the fraction of the discharge energy that is spent on heating the working mixture (Figure 4.7, Chapter 4). In addition, the following is seen: a change in the mean electron energy; a

constant rate of dissociative excitation of HgBr* molecules by electrons (figures 4.5, 4.8, Chapter 4); the collision of nitrogen molecules excited to the metastable states $A^3\Sigma^+_u$ and $B^3\Pi_g$ with mercury dibromide; and quenching of HgBr* by nitrogen molecules and helium atoms [1, 3, 29, 33, 37, 38]. When the partial pressure of nitrogen increases, the value of the parameter E/N decreases, which leads to an increase in the specific losses of the discharge power on elastic scattering of electrons by atoms and molecules [Figure 4.7b, Chapter 4, dependency 1 (heating of the mixture)]. This in turn leads to an increase in the partial pressure of the mercury dibromide vapor and the radiation power of exciplex HgBr* molecules. An increase in the electron density, which increases with an increase in the nitrogen concentration, also contributes to an increase in the radiation power with an increase in partial nitrogen pressure [3]. The presence of a maximum and a further decrease in the emission power of the HgBr* (B→X) band with an increase in partial nitrogen pressure is associated with a decrease in the fraction of the discharge energy that is spent on excitation of the $B^2\Sigma^+_{1/2}$ state (Figure 4.7a, Chapter 4), as well as the process of quenching the exciplex molecules by the nitrogen molecules [3]. The constant rate of this process is $k = (4.4 \pm 0.5)\ 10^{-12}$ cm^3/s [33].

Above a certain value of nitrogen partial pressure, the quenching process plays an important role, in comparison to the optical channel, in the destruction of exciplex HgBr* molecules in connection with which the radiation power decreases.

The first radiation pulse (Figure 3.7) is caused by the process of dissociative excitation of the $B^2\Sigma^+_{1/2}$ state of the exciplex molecules upon the collision of electrons with mercury dibromide molecules (process 3.1). The presence of a second radiation pulse can be caused by both process 3.1 in the interval t = 400 ns, where a peak was observed on the oscillogram of

the current pulse; and by an additional excitation channel HgBr ($B^2\Sigma^+_{1/2}$) in the collision of electrons with mercury monobromide molecules located in the $X^2\Sigma^+_{1/2}$ state. The third pump pulse (current) led to the excitation of HgBr molecules along the main channel (reaction 3.1) to the $B^2\Sigma^+_{1/2}$ state and gave the corresponding amplitude in the third radiation pulse. The pulse duration at half-height of the amplitude was higher than the value of both the first and second peak due to the longer duration of the third current pulse. The excess of the pulse amplitudes in this medium above the pulse amplitudes for the discharge in the $HgBr_2$:He mixture was caused by an additional process of dissociative excitation of the $B^2\Sigma^+_{1/2}$ state in the collision of mercury dibromide molecules with nitrogen molecules excited to the metastable states ($A^3\Sigma^+_u$) and ($B^3\Pi_g$).

3.3. Optical characteristics of gas-discharge plasma in mixtures of mercury dibromide vapor, sulfur hexafluoride and helium

The studies were carried out in a ternary mixture of $HgBr_2$:SF_6:He. The partial pressures of mercury dibromide vapor and helium were 0.1–0.8 kPa and 117 kPa, respectively. The partial pressure of the sulfur hexafluoride varied from 0 to 200 Pa. The partial pressure of the helium in the experiments was the same, at a value considered optimal, as that at which the maximum radiation power for the double $HgBr_2$:He mixture was observed (Chapter 3.1).

3.3.1. Oscillograms of voltage and current pulses

Figure 3.8 shows the characteristic oscillograms of the voltage and current pulses of barrier discharge plasma in $HgBr_2$:SF_6:He mixtures for the ratio of the partial pressure of the components of the mixture at which maximum

radiation was observed. The amplitude of the voltage pulses reached 9 kV and the current was 10 A. The oscillatory structure of the pulse, as well as the difference in the oscillatory structure of the current pulses at the leading and trailing edges of the pump pulse (voltage) were for the same reasons in the mixtures of $HgBr_2$:He and $HgBr_2$:N_2:He. There were differences in the current pulses for the mixture with the presence of a ligase (Figure 3.8) and without it (3.1). The addition of sulfur hexafluoride to the working mixture resulted in a redistribution of pulses in the structure of the negative half-cycle, in favor of one of them, and in the positive half-period, an increase in the amplitude of the pulses following the first.

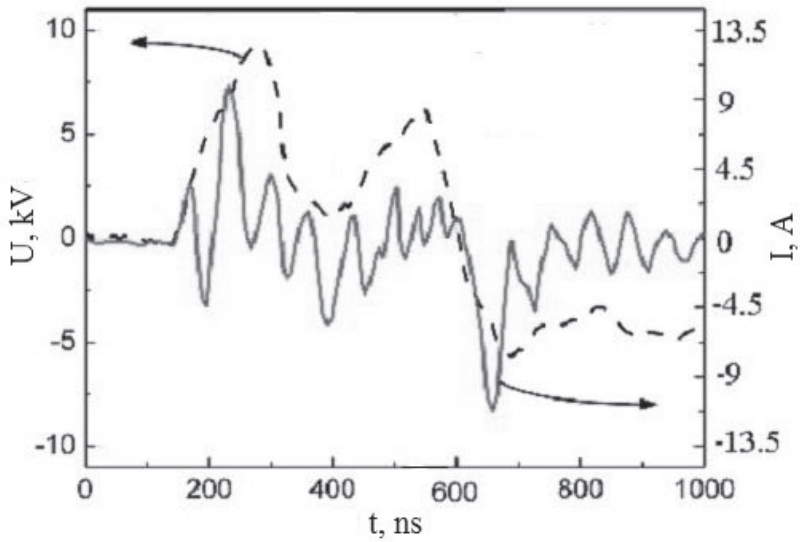

Figure 3.8. Oscillograms of the current and voltage pulses at the emitter electrodes for the mixture: a) $HgBr_2$:SF_6:He = 0.1:0.07:117; total mixture pressure P = 117.17 kPa [59].

3.3.2. Spectrum of plasma radiation

Figure 3.9 shows the characteristic emission spectra of gas-discharge plasma in the visible spectral range for the mixtures $HgBr_2$:SF_6:He and $HgBr_2$:He. The spectral band of the radiation at a maximum of λ = 502 nm, where maximum radiation intensity was observed, had a weakly-resolved vibrational structure and corresponded to the $B^2\Sigma^+_{1/2} \rightarrow X^2\Sigma^+_{1/2}$ electron-vibrational transition of mercury monobromide molecules [76]. The main part of the radiation intensity was concentrated in the wavelength range of 450–512 nm. There was a strong increase in intensity in the spectrum from the side of the region with large wavelengths and a slow decline in the region of shorter wavelengths. The shape of the spectral band and its width at half-height (15–16 nm) were similar to the spectral bands corresponding to the B→X transition in mercury monohalides, which are given in [12, 13, 26–28, 43, 45, 46]. In the same figure, the emission spectrum of gas-discharge plasma for a double $HgBr_2$:He mixture (spectrum 2) is given for comparison. The partial pressures of the mercury dibromide vapor and helium were the same as in the mixture of mercury dibromide vapor and helium (0.1 kPa and 117 kPa, respectively).

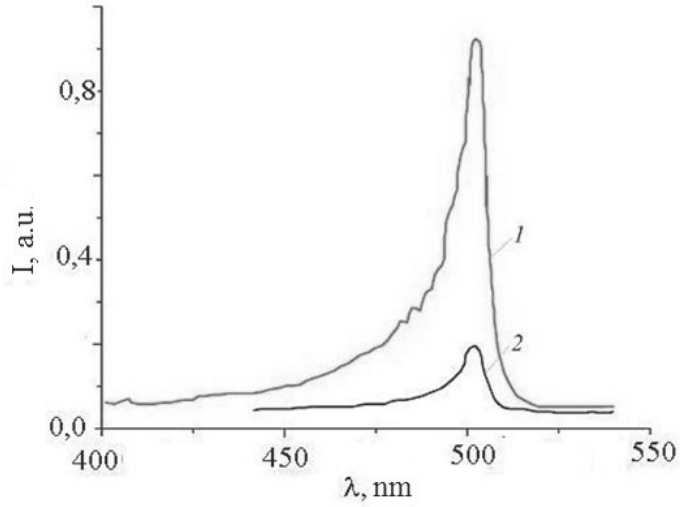

Figure 3.9. The radiation spectra of the barrier discharge plasma in the mixture: 1.) $HgBr_2$:SF_6:He = 0.1:0.07:117 kPa; the total pressure of the mixture P = 117.17 kPa. 2.) $HgBr_2$:He = 0.1–117 kPa. The total pressure of the mixture was P = 117.1 kPa. The repetition rate of the pump pulses was f = 6 kHz; the amplitude was U_a = 9 kV [57].

3.3.3. The dependency of the average radiation power of HgBr* molecules on the partial pressure of sulfur hexafluoride

In Figure 3.10, the results of investigation into the dependency of the average radiation power of exciplex HgBr* molecules on the partial pressure of sulfur hexafluoride are presented. A sharp increase in the emission power of HgBr* molecules was observed in the range of 7.5–42 mW as the partial pressure of SF_6 increased from 0 Pa to 70 Pa. A further increase in the partial pressure of sulfur hexafluoride (p>70 Pa) led to a relatively smooth fall in the radiation power of the mercury monobromide. A similar dependency of the radiation power of HgBr* molecules on the partial pressure of SF_6 gas was observed for a mixture in which the partial

pressure of the mercury dibromide vapor was higher and which was created by heating the quartz tube of the radiator with an external electric heater. The maximum radiation power of mercury monobromide in this experiment was 0.42 W. The partial pressures of the mercury dibromide vapor, sulfur hexafluoride and helium were 0.8 kPa, 70 Pa, and 117 kPa, respectively.

3.3.4. Pulsed radiation power of exciplex HgBr* molecules

Figure 3.11 shows the pulsed output power of HgBr* molecules in the discharge in the mixture $HgBr_2$:SF_6:He. The radiation pulses were threefold.

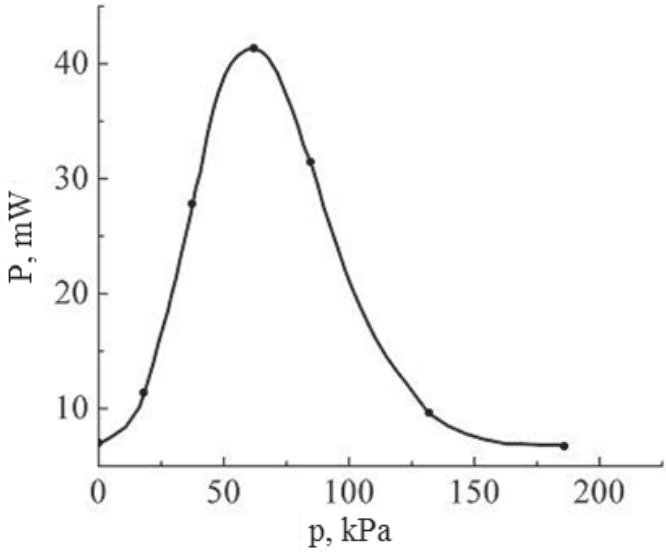

Figure 3.10. The dependency of the radiation power of exciplex HgBr* molecules acting on the partial pressure of sulfur hexafluoride for the mixture $HgBr_2$:SF_6:He. The partial pressures were: $HgBr_2$ vapor P = 0.1 kPa; helium P = 117 kPa. The repetition rate was f = 6 kHz; the amplitude of the pulses was U_a = 9 kV [57].

The amplitude of the first radiation pulse was greater than the amplitude of the second pulse. The time of appearance of the emission maxima coincided (within the limits of the measurement error) with the maxima of the current amplitudes (Figure 3.8). The amplitude of the third pulse was larger in magnitude than the amplitudes of the first and second pulses. In addition, there was an additional maximum in the third radiation pulse. The magnitude of the amplitudes of all three pulses exceeded their values for the mixtures $HgBr_2$:He and $HgBr_2$:N_2:He (figures 3.4 and 3.7).

3.3.5. Discussion of research results

The appearance of spectral band emissions at a maximum wavelength of λ = 502 nm of the electronic-vibrational transition $B^2\Sigma^+_{1/2} \rightarrow X^2\Sigma^+_{1/2}$ of exciplex HgBr* molecules in gas-discharge plasma in the mixture of mercury

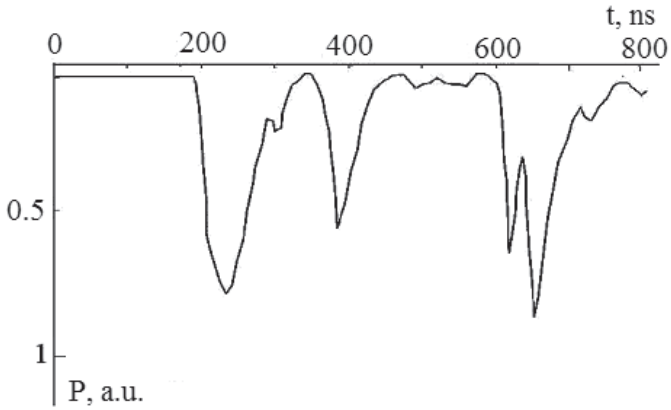

Figure 3.11. The pulsed power of exciplex HgBr* molecule emission from gas-discharge plasma in the mixture $HgBr_2$:SF6:He. Partial pressures: $HgBr_2$=0.1 kPa, SF_6= 70 Pa, He=117 kPa [59].

dibromide vapor, sulfur hexafluoride and helium is due to processes that lead to the formation and destruction of $B^2\Sigma^+_{1/2}$-state mercury monobromide; the same as in the mixture of mercury dibromide vapor and helium (Chapter 3.1, reactions 3.1 to 3.4). (Under [M], in reaction 3.4, concentrations of quenching molecules and atoms ($HgBr_2$, SF_6, He), respectively, were implied.)

The dependency of the emission power of the (B→X) band of HgBr* molecules on the partial pressure of sulfur hexafluoride (Figure 3.10) is primarily due to the following processes: an increase in the electron concentration with increasing partial pressure of sulfur hexafluoride in the mixture; a change in the fraction of the discharge energy that is consumed by heating the working mixture; changes in the mean electron energy and the rates of dissociative excitation of exciplex HgBr* by electrons; and the quenching of exciplex HgBr* molecules by molecules of sulfur hexafluoride, mercury dibromide and helium atoms [1, 3, 13, 33, 34, 36, 78]. In addition, as the partial pressure of sulfur hexafluoride increased, the value of the parameter E/N decreased in the mixture, leading to an increase in the specific losses of the discharge power in the elastic scattering of electrons by atoms and molecules (heating of the mixture) and, accordingly, to an increase in the partial pressure of the mercury dibromide vapor and radiation power of the HgBr* molecules. The presence of a maximum and a further decrease in the radiation power of HgBr* molecules with an increase in the partial pressure of sulfur hexafluoride is due to the quenching of HgBr* by sulfur hexafluoride molecules [3].

$$HgBr(B^2\Sigma^+_{1/2})+SF_6 \rightarrow HgBr(X^2\Sigma^+_{1/2})+SF_6+\Delta E \qquad (3.7)$$

where ΔE is the difference in reaction energy.

Data on the magnitude of the rate constant of this process are not found in the literature. In the course of our studies we determined it to be equal to $71 \cdot 10^{-10}$ $cm^3 \cdot s^{-1}$ (Chapter 3.4.2). At partial pressures of sulfur hexafluoride exceeding 70 Pa, the quenching process plays an important role in the destruction of HgBr* molecules in comparison to the optical channel (3.3) and in connection with which the radiation power of the band ($B \rightarrow X$) decreases.

A significant increase in radiation power in the discharge in the mercury dibromide vapor with sulfur hexafluoride and helium mixture, in comparison to the mixture containing only mercury dibromide vapor and helium (Figure 3.10 and Figure 3.3a), was caused both by an increase in the amplitude of the current pulses in the mixture with sulfur hexafluoride (Figure 3.7), and by the quenching of higher-lying $C^2\Pi_{1/2}$ and $D^2\Pi_{3/2}$ states of mercury monobromide molecules with a transfer of excitation to the $B^2\Sigma^+_{1/2}$ state:

$$HgBr_2 + e \rightarrow HgBr_2(D) \rightarrow HgBr(C^2\Pi_{1/2}, D^2\Pi_{3/2}) + M \rightarrow HgBr(B^2\Sigma^+_{1/2}) + M + \Delta E_{1,2} \quad (3.8)$$

where $\Delta E_{1,2}$ is the difference between the excitation energies of the $C^2\Pi_{1/2}$, $D^2\Pi_{3/2}$ and $B^2\Sigma^+_{1/2}$ states of mercury monobromide molecules. In favor of such a process, the value of the rate constant of the excitation of the sum of the states of mercury dibromide molecules above the threshold of 7.9 eV (D state, Figure 1.2). This is an order of magnitude higher than the value of the excitation constant of the $B^2\Sigma^+_{1/2}$ state (Figure 4.12, Chapter 4), and accordingly, the population of the $C^2\Pi_{1/2}$ and $D^2\Pi_{3/2}$ states of mercury monobromide, to which it decays, is an order of magnitude higher than the

population of the B-state. In the process of quenching, this can lead to a significant increase in the radiation power of exciplex molecules HgBr*. A necessary condition in this case is, first of all, a large value of the constant rate of quenching for the states $C^2\Pi_{1/2}$ and $D^2\Pi_{3/2}$, compared to the $B^2\Sigma^+_{1/2}$ state of mercury monobromide. A similar process (quenching of the overlying state $C^2\Pi^+_{1/2}$) with a population transfer to the underlying $B^2\Sigma^+_{1/2}$ state was observed previously for the exciplex molecule of mercury monoiodide in experiments on the photo-dissociation of mercury di-iodide under the working conditions given in [84–86].

The first and subsequent radiation pulses (Figure 3.11) arise due to the same processes that caused the same pulses in the discharge in the $HgBr_2$:He mixture. The excesses of the pulse amplitudes over the pulse amplitudes for the discharges in the $HgBr_2$:He mixture were caused by the quenching of the $C^2\Pi_{1/2}$ and $D^2\Pi_{3/2}$ states of mercury monobromide by molecules of sulfur hexafluoride, with a transfer of excitation to the $B^2\Sigma^+_{1/2}$ state. The appearance of an additional maximum to the amplitude in the third peak of the radiation pulse may be caused by a current of negative ions: $HgBr_2^-$, Br^-, SF_6^-, SF_5^- [1, 3, 84–88].

3.4. Optical characteristics of gas-discharge plasma in mixtures of mercury dibromide vapor, sulfur hexafluoride, nitrogen and helium

Research was carried out using a four-component mixture $HgBr_2$:SF_6:N_2:He. The partial pressures of mercury dibromide vapor, sulfur hexafluoride and helium were 0.1, 0.07 and 117.2 kPa, respectively. The nitrogen partial pressure varied from 0 to 10.5 kPa. The partial pressures of the helium and sulfur hexafluoride in the experiments were the same. These partial pressure values of He and SF_6 allowed for the observation of the

maximum radiation power for the discharges in the two-component mixture $HgBr_2$:He and the three-component mixture $HgBr_2$:SF_6:He (Chapter 3.1, 3.3).

3.4.1. Oscillograms of voltage and current pulses

Figure 3.12 shows the oscillograms of the voltage pulses and current of the plasma barrier discharge of the radiator for the ratio of the components of the mixture at which maximum radiation power was reached. The oscillatory regime of the energy input of the pump source into the plasma was observed. The maximum amplitude values of the voltage and current pulses were 9 kV and 9.1 A, respectively. The oscillatory structure of the pulse, as well as the difference in the oscillatory structure of the current pulses at the leading and trailing edges of the pump pulse (voltage), have the

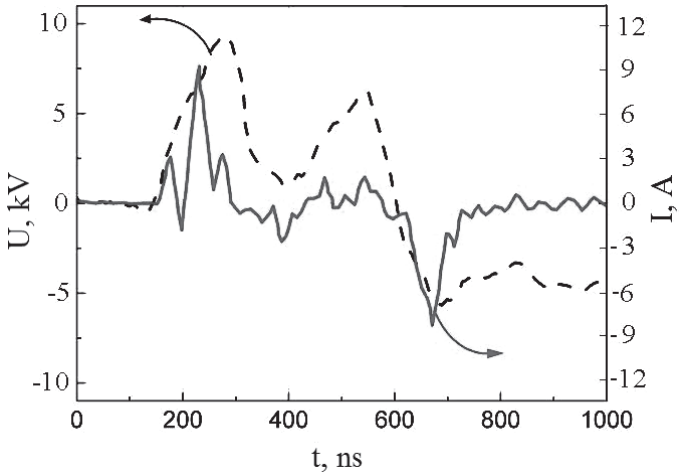

Figure 3.12. Oscillograms of the current and voltage pulses at the emitter electrodes for the mixture $HgBr_2$:SF_6:N_2:He = 0.1:0.07:4:117.2 kPa at a total mixture pressure of 121.37 kPa and a repetition rate of f = 6 kHz [60].

same causation as the mixtures $HgBr_2$:He and $HgBr_2$:N_2:He. The distinctive feature of these oscillograms is the less developed vibrational structure of the current pulse compared to that with mixtures without nitrogen and sulfur hexafluoride.

3.4.2. Radiation spectra

In the emission spectra in the visible wavelength range, a spectral band 10–15 nm wide with a maximum wavelength of λ = 502 nm (Figure 3.13) was significantly allocated. This has a weakly resolved vibrational structure and corresponds to the electronic-vibrational transition $B^2\Sigma^+_{1/2} \rightarrow X^2\Sigma^+_{1/2}$ of the exciplex molecule HgBr* [76]. The main part of the radiation intensity was concentrated in the spectral range 475–512 nm. There was a strong increase in the intensity in the spectrum from the side of the region with large wavelengths and a slow decline in the region of shorter wavelengths.

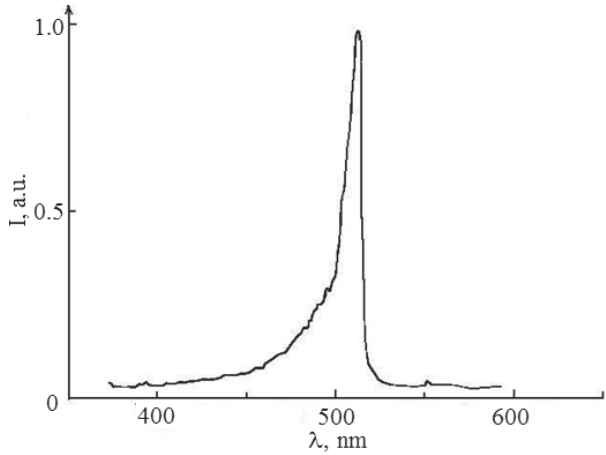

Figure 3.13. The radiation spectrum of a barrier discharge in the mixture $HgBr_2$:SF_6:N_2:He = 0.1:0.07:4:117.2 kPa at a total mixture pressure of 121.37 kPa and a pump pulse repetition frequency of f = 6 kHz at a voltage amplitude U_a = 9.5 kV [60].

3.4.3. The dependency of the average radiation power of exciplex HgBr* molecules on the partial pressure of nitrogen

Figure 3.14 presents the results of studies into the dependency of the average radiation power of exciplex HgBr* molecules on the partial nitrogen pressure.

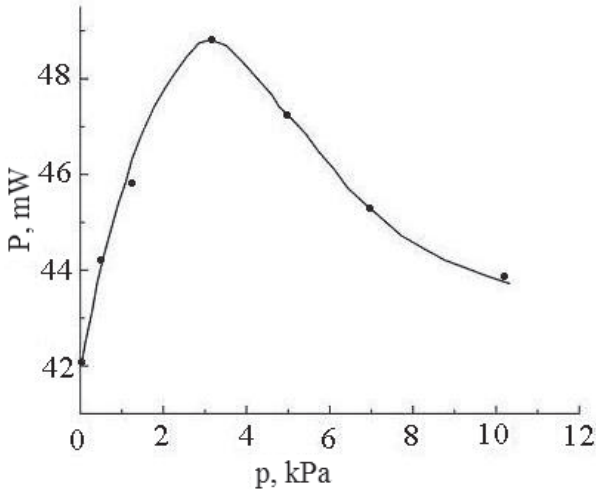

Figure 3.14. The dependency of the radiation power of exciplex HgBr* molecules on the partial pressure of nitrogen for a discharge in the mixture $HgBr_2$:SF_6:N_2:He at a partial mercury dibromide vapor pressure of 0.1 kPa, sulfur hexafluoride of 70 Pa, helium of 117.2 kPa; a pulse repetition rate of f = 6 kHz; and an amplitude of the voltage pulse U_a = 9.5 kV [60].

An increase in the radiation power of the B→X band HgBr* from a value of 42 mW to a value of 48.8 mW was observed with an increase in the nitrogen partial pressure in the range 0–4 kPa. A further increase in the partial pressure of nitrogen leads to a decrease in the radiation power of mercury monobromide. A similar dependency of the emission power of HgBr(B→X) molecules on the partial nitrogen pressure was observed for a

discharge in a mixture in which the partial pressure of the mercury dibromide vapor was higher.

The maximum radiation power of the B→X band of HgBr molecules was 480 mW for values of partial pressure of the mercury dibromide vapor, sulfur hexafluoride, nitrogen and helium of 0.7 kPa, 70 Pa, 4 kPa and 117.2 kPa, respectively (the partial pressure of the mercury dibromide vapor was 0.7 kPa due to heating of the radiator with an external electric heater).

3.4.4. Pulsed radiation power of exciplex HgBr* molecules

Figure 3.15 shows the pulsed radiation power of exciplex HgBr* molecules in plasma in the mixture $HgBr_2$:SF_6:N_2:He. The radiation pulses are threefold. Maxima of radiation by the time of occurrence coincide (within the limits of the measurement error) with the maxima of the current amplitudes (Figure 3.12).

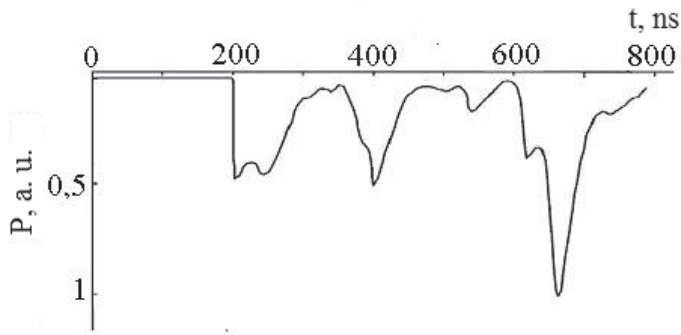

Figure 3.15. The pulsed power of the emission of exciplex HgBr* molecules in gas-discharge plasma in the mixture $HgBr_2$:SF_6:N_2:He. Partial pressures: $HgBr_2$ = 0.1 kPa; SF_6 = 70 Pa; N_2 = 4 kPa; He = 117.2 kPa [59].

The amplitude of the third pulse was larger than the amplitudes of the first and second pulses; an additional maximum amplitude was also observed in the third pulse.

3.4.5. Discussion of research results

The occurrence of a spectral emission band with a maximum wavelength of λ = 502 nm of the electron-vibrational transition $B^2\Sigma^+_{1/2} \rightarrow X^2\Sigma^+_{1/2}$ of HgBr* exciplex molecules with gas discharge plasma in a four component-mixture of mercury dibromide vapor, sulfur hexafluoride, nitrogen, and helium is due to processes leading to the formation and destruction of the $B^2\Sigma^+_{1/2}$ state of mercury monobromide. The main processes are shown in 3.1–3.4, where M represents the particles that quench the $B^2\Sigma^+_{1/2}$ state of mercury monobromide ($HgBr_2$, N_2, SF_6). In addition, the process of dissociative excitation of the $B^2\Sigma^+_{1/2}$ state occurs in the collision of mercury dibromide molecules with nitrogen molecules excited in metastable $A^3\Sigma^+_u$ and $B^3\Pi_g$ states.

The character of the dependency of the radiation power of the B→X band of exciplex HgBr* molecules on the partial pressure of nitrogen (Figure 3.14) is primarily due to an increase in the electron concentration with an increase in the nitrogen partial pressure in the plasma and a change in the fraction of the discharge energy that is consumed in the heating of the working mixture. Other factors that have an effect on this dependency include: changes in the mean electron energy and the rates of dissociative excitation of exciplex HgBr* molecules by electrons and nitrogen molecules excited to metastable $A^3\Sigma^+_u$ and $B^3\Pi_g$ states; an increase in the population of these states due to population relaxation from higher vibrational levels upon collision with molecules of sulfur hexafluoride; and

the process of quenching HgBr* molecules by nitrogen molecules, sulfur hexafluoride and helium atoms [1, 22–24, 29, 33, 37, 78]. As the partial pressure of nitrogen increases, the value of the parameter E/N decreases, which leads to an increase in the specific losses of discharge power in the elastic scattering of electrons by atoms and molecules (heating of the mixture). This, in turn, leads to an increase in the partial pressure of the mercury dibromide vapor and the emission power of HgBr* exciplexes. An increase in the radiation power with an increase in the partial pressure of molecular nitrogen is also facilitated by an increase in the electron concentration, which increases with an increase in the concentration of nitrogen molecules. The presence of a maximum and further decrease in the radiation power of HgBr* molecules with increasing partial nitrogen pressure is associated with a decrease in the fraction of the discharge energy that is spent on the excitation of the $B^2\Sigma^+_{1/2}$ state of HgBr* molecules and also by the quenching of HgBr* molecules by nitrogen molecules [3]. The constant rate of this process in a multicomponent mixture is unknown (for a two-component mixture ($HgBr_2$:He) it is $(4.4 \pm 0.5)\cdot 10^{-12}$ cm^3/s [33]). Above a certain value of nitrogen partial pressure, the quenching process plays an important role, in comparison to the optical channel in the destruction of exciplex HgBr* molecules, in connection with which the radiation power decreases.

The increased value of the radiation power of a discharge in a mixture of mercury dibromide vapor, sulfur hexafluoride, nitrogen and helium, in comparison to a discharge in a mixture of mercury dibromide vapor, sulfur hexafluoride and helium (Figure 3.14 and Figure 3.10), is caused by the quenching of the $C^2\Pi_{1/2}$ and $D^2\Pi_{3/2}$ states of mercury monobromide by nitrogen molecules and a transfer of excitation to the $B^2\Sigma^+_{1/2}$ state:

$$HgBr_2+e\rightarrow HgBr_2(D)\rightarrow HgBr(C^2\Pi_{1/2},D^2\Pi_{3/2})+N_2\rightarrow \quad (3.9)$$
$$HgBr(B^2\Sigma^+_{1/2})+N_2+\Delta E_{1,2}$$

where $\Delta E_{1,2}$ is the difference in excitation energy of the $C^2\Pi_{1/2}$, $D^2\Pi_{3/2}$ and $B^2\Sigma^+_{1/2}$ states of mercury monobromide molecules. Such a mechanism is indicated by the value of the rate constant of excitation of the sum of states of mercury dibromide molecules above the threshold 7.9 eV (D-state, Figure 1.2, Chapter 1), which is an order of magnitude higher than the value of the excitation constant of the $B^2\Sigma^+_{1/2}$ state (Figure 4.15, Chapter 4) and, accordingly, the population of $C^2\Pi_{1/2}$ and $D^2\Pi_{3/2}$ states of mercury monobromide, into which it decays at an order of magnitude higher than the population of the B-state. During the quenching process, this leads to an increase in the radiation power of exciplex HgBr* molecules.

The first and subsequent radiation pulses (Figure 3.15) arise with the same processes that cause the same pulses in the discharge in the $HgBr_2$:He mixture. The excess of the values of the pulse amplitudes over the pulse amplitudes in the discharge in the $HgBr_2$:He mixture is caused by the addition of the process of dissociative excitation of the exciplex molecule HgBr* by nitrogen molecules excited to metastable $A^3\Sigma^+_u$ and $B^3\Pi_g$ states and the process of quenching the $C^2\Pi_{1/2}$ and $D^2\Pi_{3/2}$ states of mercury monobromide by sulfur hexafluoride and nitrogen with a transfer of excitation to the $B^2\Sigma^+_{1/2}$ state. The appearance of an additional maximum in the amplitude of the third radiation pulse may be caused by the current of negative ions: $HgBr_2^-$, Br^-, SF_6^-, SF_5^- [1, 3, 84–88].

As such, the action of plasma in the $HgBr_2$:SF_6:N_2:He mixture in self-heating mode achieves the highest average radiation power in the blue-green spectral range equal to 48.8 mW. The pulsed power reached 40.6 W.

This was determined on the basis of the known average power ($P_{av.}$), duration ($\Delta\tau$) and pulse repetition rate (f) from the expression:

$$P_{av.} = P_{pul.} \cdot \Delta\tau \cdot f$$

The efficiency of the radiation, at the same time, was 7.3 %.

3.5. Optical characteristics of gas-discharge plasma in mixtures of mercury dibromide vapor, xenon, krypton and helium

3.5.1. Oscillograms of voltage and current

Investigations were carried out with a barrier discharge in the mixtures $HgBr_2$:He and $HgBr_2$:Xe:Kr. In the initial stage of the discharge (20–30 s), the discharge color depended on the component composition of the mixture. As the mixture warmed up, the color of the discharge became blue-green. In each half-period of the applied voltage U_0 (Figure 3.16), a series of sharp bursts of different amplitudes, and approximately the same duration, were observed in the current oscillogram. Each current burst was caused by a set of filamentary microdischarges—filaments that occurred in the discharge gap and were statistically distributed in time. The bursts in the current oscillogram reflect the value of the conduction current in the barrier discharge. With increasing voltage U_0, the active component made an increasing contribution to the total current. The current peaks did not exceed 52 mA and their duration was in the range 0.2–0.5 μs.

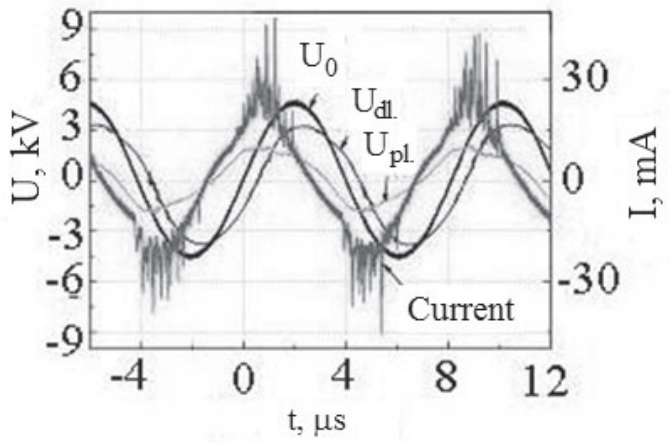

Figure 3.16. The oscillograms of the voltage pulses (U_0—voltage applied to the lamp; U_d—voltage drop at the dielectric surface; U_{pl}—voltage drop on the plasma) and current in a discharge in the mixture $HgBr_2$:Xe:Kr = 300 Pa:8 kPa:92 kPa at frequency f = 120 kHz and U_0 = 4.5 kV [58].

3.5.2. The emission spectrum of plasma in the mixture $HgBr_2$:He. Dynamics of spectrum changes in the mixture $HgBr_2$:Xe:Kr

Figure 3.17 shows the emission spectrum of barrier discharge plasma for a discharge in the $HgBr_2$:He mixture pumped by a sinusoidal voltage of 120 kHz. In addition to the emission of HgBr (B→X) and mercury spectral lines, atomic lines of the buffer gas, helium (at λ = 589 and λ = 706 nm), were observed, as well as the spectral bands $N_2(C^3\Pi_u \rightarrow B^3\Pi_g)$, which appeared due to the presence of nitrogen in the residual gases (P<10 Pa) [53, 67, 69]. The intensity of the spectral lines of helium decreased considerably when the working medium was heated.

Figures 3.18–3.20 show the dynamics of the change in the emission spectrum with a discharge in the mixture $HgBr_2$:Xe:Kr (8 % Xe, 92 % Kr)

at total atmospheric pressure as a function of the temperature of the mixture. The discharge was pumped by a sinusoidal voltage at a frequency 120 kHz. At low temperatures (T ~40 °C), the spectral emission bands of XeBr excimer molecules, (B→X), XeBr (B→A) and HgBr (B→X), with maxima at wavelengths of 281, 320, and 502 nm, were observed, together with the atomic lines of mercury and bands of OH* molecules [2, 53, 89–91].

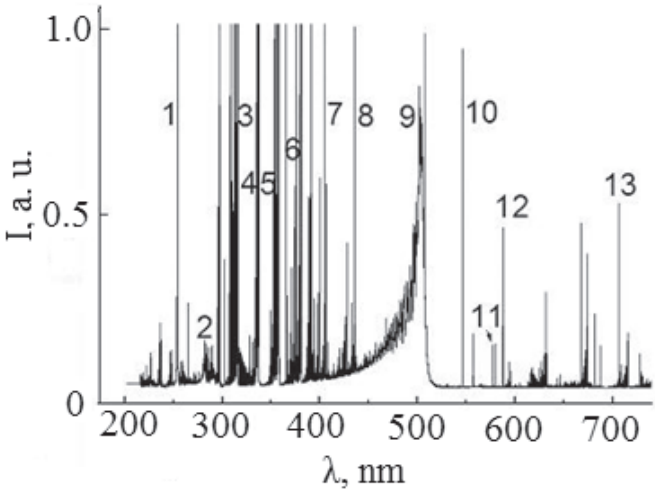

Figure 3.17. The surveyed spectrum of plasma emissions in the mixture $HgBr_2$:He = 0.28–101 kPa: 1 - 254 nm Hg; 2 - 281 nm XeBr*; 3 - 306 nm OH*; 4 - 337 nm N_2*; 5 - 357 nm N_2*; 6–365 nm Hg; 7 - 404 nm Hg; 8 - 436 nm Hg; 9 - 502 nm HgBr*; 10 - 546 nm Hg; 11 - 578 nm Hg; 12 - 589 nm He; 13 - 706 nm He; frequency f = 120 kHz; voltage U_0 = 4.5 kV [55, 56, 58].

In the spectra, a system of spectral bands with a maximum wavelength of λ = 502 nm was allocated, the intensity of which increased with increasing temperature (figures 3.2–3.4). The emission of the HgBr (B→X) band manifested itself starting at λ ~340 nm. In addition, low-intensity

spectral bands of HgBr (C→X) molecules in the range $\Delta\lambda$ = 285–295 nm were observed. At a mixture temperature of ~160 °C, the maximum intensity of HgBr* emission was observed in the electron-vibrational transition (B→X). With an increase in the temperature of the mixture to 180 °C, the emission intensity of exciplex molecules, HgBr* and XeBr*, decreased as a result of the increased role of the quenching process:

$$HgBr, XeBr(B)+HgBr_2 \rightarrow products \quad (3.10)$$

In addition to the emission of HgBr (B→X) and mercury spectral lines, atomic lines of the helium buffer gas were observed at λ = 589 and λ = 706 nm; as well as the spectral bands N_2 ($C^3\Pi_u \rightarrow B^3\Pi_g$) and OH* ($\lambda$ = 306 nm), which appeared due to the presence of nitrogen in the residual gases (P<10 Pa) and adsorbed water on the surface of the electrode.

3.5.3. Discussion of research results

Radiation of spectral bands and lines occur due to the primary reactions in 3.1–3.4, as well as:

$$HgBr_2+Xe(^3P_2) \rightarrow HgBr^*+Br+Xe \quad (3.11)$$

$$Xe^*(Xe_2^*)+Br_2 \rightarrow XeBr^*+(Xe)+Br \quad (3.12)$$

$$Xe^+(Xe_2^+, Xe_3^+)+Br_2^-+M \rightarrow XeBr^*+Br+(Xe, 2Xe)+M \quad (3.13)$$

$$Xe^++Br^-+M \rightarrow XeBr^*+ \quad (3.14)$$

$$XeBr^* \rightarrow XeBr+h\upsilon, \lambda_{max.} = 281, 320 \text{ nm} \quad (3.15)$$

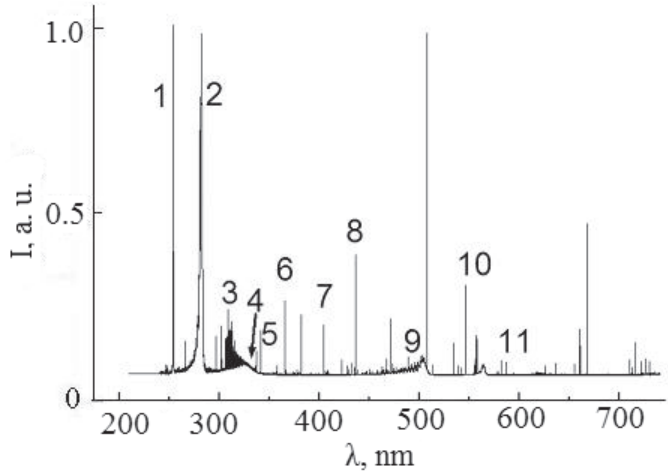

Figure 3.18. The surveyed spectrum of plasma emission in the mixture $HgBr_2$:Xe:Kr, Xe = 8 %, Kr = 92 %: 1 - 254 nm Hg; 2 - 281 nm XeBr*; 3 - 306 nm OH*; 4 - 320 nm XeBr*; 5 - 337 nm N_2*; 6 - 365 nm Hg; 7 - 404 nm Hg; 8 - 436 nm Hg; 9 - 502 nm HgBr*; 10 - 546 nm Hg; 11 - 578 nm Hg. T = 40 °C; total pressure 101 kPa; frequency f = 120 kHz; voltage U_0 = 4.5 kV [55, 56, 58].

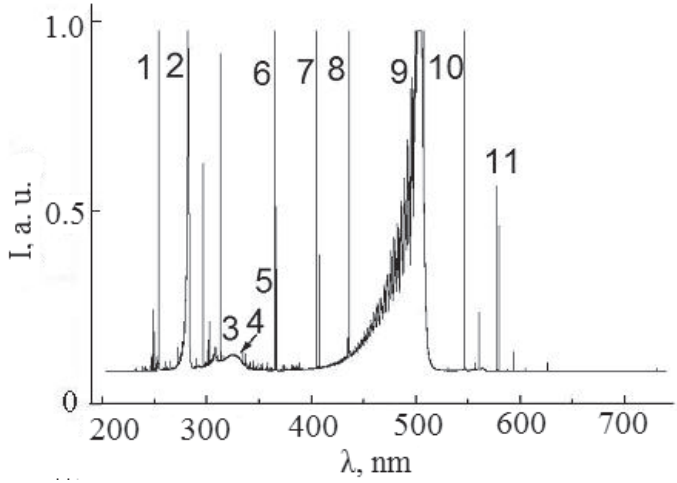

Figure 3.19. The surveyed spectrum of plasma emission in the mixture $HgBr_2$:Xe:Kr, Xe = 8 %; Kr = 92 %; total pressure 101 kPa; 1 - 254 nm Hg; 2 - 281

nm XeBr*; 3 - 306 nm OH*; 4 - 320 nm XeBr*; 5 - 337 nm N_2*; 6 - 365 nm Hg; 7 - 404 nm Hg; 8 - 436 nm Hg; 9 - 502 nm HgBr*; 10 - 546 nm Hg; 11 - 578 nm Hg. T = 160 ºC; frequency f = 120 kHz; voltage U_0 = 4.5 kV [55, 56, 58].

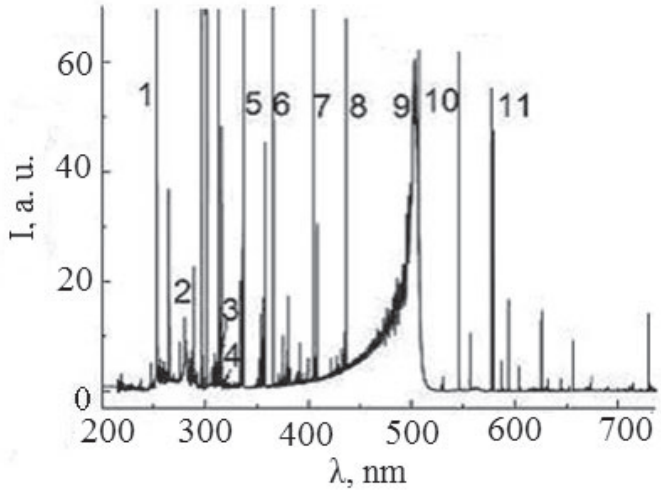

Figure 3.20. The surveyed spectrum of plasma emission in the mixture $HgBr_2$:Xe:Kr, Xe = 8 %; Kr = 9%: 1 - 254 nm Hg; 2 - 281 nm XeBr*; 3 - 306 nm OH*; 4 - 320 nm XeBr*; 5 - 337 nm N_2*; 6 - 365 nm Hg; 7 - 404 nm Hg; 8 - 436 nm Hg; 9 - 502 nm HgBr*; 10 - 546 nm Hg; 11 - 578 nm Hg. T = 180 ºC; total pressure 101 kPa; frequency f = 120 kHz; voltage U_0 = 4.5 kV [55, 56, 58].

$$HgBr_2+e \rightarrow Hg^*+2Br\ (Br_2^*\ Br_2,\ Br_2^-)+(e) \quad (3.16)$$

$$HgBr_2+e \rightarrow Hg^*+Br_2^+ +2e \quad (3.17)$$

$$HgBr_2+e \rightarrow Hg^*+Br^+ +Br+2e \quad (3.18)$$

$$XeBr^*+M \rightarrow XeBr\ (X^2\Sigma^+_{1/2})+M+\Delta E \quad (3.19)$$

where M is the third particle ($HgBr_2$, He, Kr) and ΔE is the difference of the reaction energy [2, 3, 26, 30, 41–43, 49].

The reaction of the xenon atom in the metastable state with molecules of mercury dibromide (3.11) is an important channel in the formation of exciplex HgBr* molecules [2, 3, 49]. Excited mercury atoms arise due to these reactions (3.16–3.18). Exciplex molecules XeBr* at an atmospheric pressure of the mixture arise both as a result of a “harpoon” reaction (3.12) and ion-ion recombination (3.13–3.14).

For discharges in this mixture, an average radiation power of 4.6 mW/cm^3 is achieved (with a discharge volume of 0.35 cm^3). The ratio of the partial pressures of the components, in this case, was as follows: $HgBr_2$:Xe:Kr = 30 Pa:8 kPa:92 kPa.

3.6. Optical characteristics of gas-discharge plasma in mixtures of mercury dibromide vapor with krypton and helium

Figure 3.21 shows images of the glow of gas discharge plasma from a barrier discharge in the mixture $HgBr_2$:Kr:He = 0.1 Pa:10 kPa:110 kPa. The amplitude of the voltage pulse applied to the electrodes of the gas discharge cuvette was 10 kV; the pulse duration was 30 ns; and the repetition frequency was 10 Hz. The first image was obtained at the time of appearance of a glow after 11 ns following the initiation of the barrier discharge; the second was 1.5 ns after the appearance of the discharge glow; and subsequent images were recorded with a time interval of 4 ns.

At the initial instant of the appearance of discharge radiation in the inter-electrode gap, a separate bright channel of cylindrical-shape microdischarge was observed, with bases on the inner metal electrode and the inner dielectric surface. With the passage of time, the number of microdischarges increased and against their background a volumetric glow appeared. At time t = 5.5 ns after the appearance of radiation, the discharge

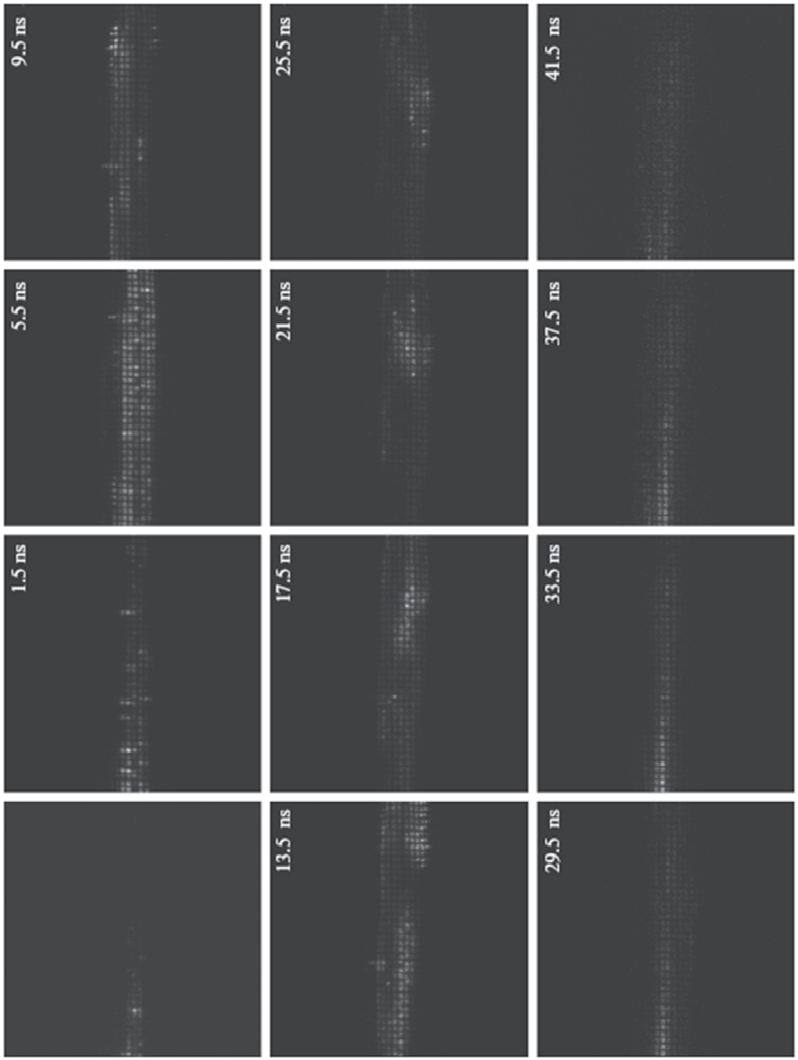

Figure 3.21. Images of the glow of gas-discharge plasma in the mixture $HgBr_2$:Kr:He = 0.1 Pa:10 kPa:110 kPa. The images were taken with the ICCD camera at a time resolution of 2 ns. Amplitude of the voltage pulse U_0 = 10 kV; duration of the pump pulse Δt = 30 ns; pulse repetition frequency f = 10 Hz [70].

represented microdischarges randomly distributed throughout the discharge volume, which existed against a background of less bright volumetric glow. Beginning with time t = 9.5 ns, the glow of the discharge was transformed into separate zones of increased brightness non-homogeneously located in the inter-electrode space. After passing time t = 29 ns from the time of appearance of the radiation, a less bright homogeneous glow was observed in the discharge gap. The color of the discharge was determined by the buffer gas helium.

3.6.1. Oscillogram of the voltage pulse

Figure 3.22 shows an oscillogram of the voltage pulses in the current shunt. The pulse was a set of consecutive pulses (falling and reflected from the impedance loads (gas-discharge plasma and pump generator)). The first pulse was directed towards the electrodes of the gas-discharge cuvette from the pump generator; the second pulse was reflected from the load (gas-discharge plasma). The third peak corresponds to the pulse reflected from the internal resistance of the generator, etc. up to full attenuation.

The main energy input into the gas-discharge plasma was performed during the time of the second, fourth, and sixth pump pulses. It was calculated as the difference between the areas of the incident and reflected pump pulses:

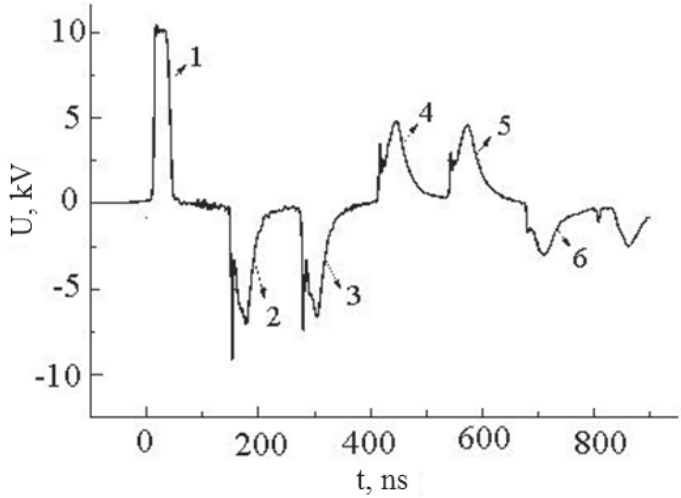

Figure 3.22. Oscillogram of the voltage pulses at the current shunt: 1 - pulse of the pump generator; 2, 4, 6 - pulses reflected from the gas-discharge plasma; 3, 5 - pulse reflected from the internal resistance of the generator.

$$E=E_1+E_2+E_3 = \left(\int \frac{(U_1)^2}{\rho} dt - \int \frac{(U_2)^2}{\rho} dt \right)_+ \left(\int \frac{(U_3)^2}{\rho} dt - \int \frac{(U_4)^2}{\rho} dt \right)_{++} \left(\int \frac{(U_5)^2}{\rho} dt - \int \frac{(U_6)^2}{\rho} dt \right), \quad (3.20)$$

where E_1, E_2, E_3 are the portions of energy deposited into the plasma during the second, fourth and sixth pump pulses and ρ is the wave resistance of the cable. The energy deposited into the plasma was as high as 42 mJ.

3.6.2. Spectra of plasma radiation in the mixture $HgBr_2$:Kr:He. The dependency of the radiation spectrum on temperature

The spectral characteristics of gas-discharge plasma in the $HgBr_2$:Kr:He mixture were studied at temperatures of 45 °C, 55 °C and 65 °C. Depending on the temperature of the mixture, the partial pressure of the mercury dibromide vapor varied in the range 0.1–1.1 Pa [51]. The partial pressures of krypton and helium were 10 and 110 kPa, respectively.

Figures 3.23a and 3.23b show regions of the emission spectra of gas-discharge plasma in the wavelength ranges of 480–515 nm and 200–215 nm at mixture temperatures of 45 °C, 55 °C and 65 °C. In the wavelength range 480–515 nm, spectral emission bands of the mercury monobromide HgBr* exciplex molecule (with the electron-vibrational transition $B^2\Sigma^+_{1/2}\rightarrow X^2\Sigma^+_{1/2}$) were observed [21]. In the 200–215 nm range, spectral emission bands of the exciplex KrBr* molecule were observed, which correspond to the $B^2\Sigma^+_{1/2}\rightarrow X^2\Sigma^+_{1/2}$ electron-vibrational transition [49]. In the studied spectra, the emission of exciplex molecules HgBr* ($B^2\Sigma^+_{1/2}\rightarrow X^2\Sigma^+_{1/2}$); KrBr* ($B^2\Sigma^+_{1/2}\rightarrow X^2\Sigma^+_{1/2}$, $C_{3/2}$–$A_{3/2}$, $D_{3/2}$–$A_{3/2}$); OH* ($A^2\Sigma^+\rightarrow X^2\Pi$) molecules; and Hg atoms ($6^1S_0\rightarrow 6^3P_1$) was observed. An increase in the emission intensity of the exciplex molecules HgBr* ($\lambda_{max.}$ = 502 nm) and KrBr* ($\lambda_{max.}$ = 207 nm) was observed with a change in the temperature of the mixture in the temperature range 45–65 °C by a factor of three and one and a half, respectively. In addition, changes were observed in the spectral bands of these molecules, namely, the electron-vibrational structure. Figure 3.24 shows the region of the emission spectrum of the mixture in the spectral range 200–300 nm, with the spectral band emissions of the electron-vibrational transitions $B^2\Sigma^+_{1/2}\rightarrow X^2\Sigma^+_{1/2}$ of the exciplex molecule HgBr*; the $C_{3/2}$–$A_{3/2}$ exciplex molecule KrBr*; and $A^2\Sigma^+\rightarrow X^2\Pi_i$

OH* molecules, as well as the spectral line of the mercury atom transitions $6^1S_0 \rightarrow 6^3P_1$.

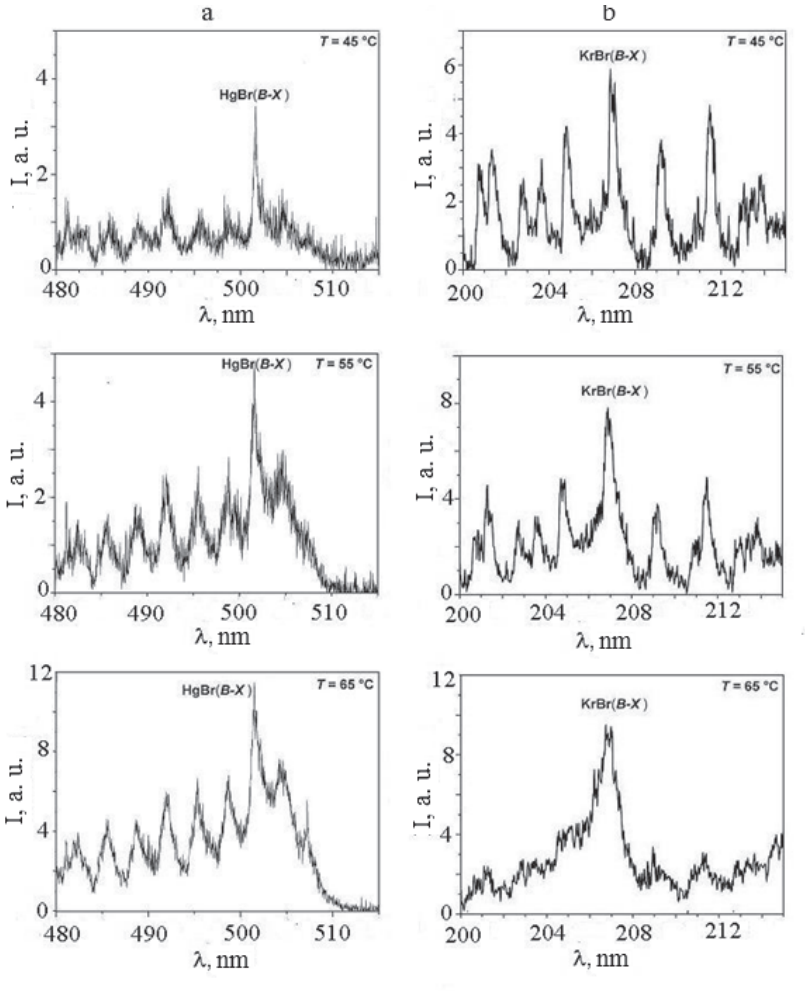

Figure 3.23. The regions of the plasma emission spectrum in the mixture $HgBr_2$:Kr:He at T = 45 °C, 55 °C, 65 °C; Kr = 10 kPa; He = 110 kPa in the wavelength ranges: a - 480–515 nm; b - 200–215 nm. Amplitude of the voltage pulse U_0 = 10 kV; duration of the pump pulse Δt = 30 ns; pulse repetition rate f = 10 Hz [68].

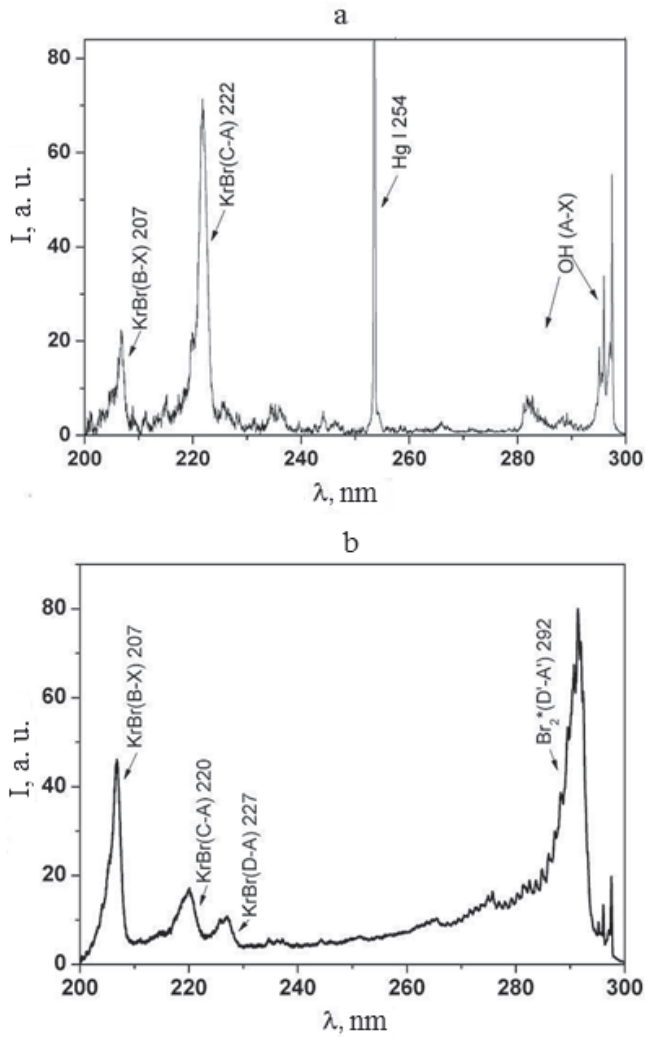

Figure 3.24. The regions of the plasma emission spectrum in the $HgBr_2$:Kr:He mixture: discharge spectra in the $HgBr_2$:Kr/He mi;xture: a - after 1 hour of operation; b - after 15 hours of operation. The temperature was stabilized by an external heater at 65 °C; partial pressures: Kr = 10 kPa; He = 110 kPa. Amplitude of the voltage pulse U_0 = 10 kV; duration of the pump pulse Δt = 30 ns; pulse repetition rate f = 10 Hz [68].

3.6.3. Temporal characteristics of plasma current and radiation of mercury monobromide and krypton bromine exciplex molecules

Figures 3.25 and 3.26 present the results of the investigation into the temporal characteristics of the plasma current and radiation of HgBr* and KrBr* exciplex molecules. The radiation pulses of HgBr* and KrBr* exciplex molecules are similar in shape and duration, but they are different in amplitude.

The radiation power of the exciplex HgBr* molecules exceeded, by four times, the radiation power of KrBr* exciplex molecules. The duration of the pulses at half-maximum was 21 ns. The time delay of the radiation pulse of the exciplex molecule HgBr* relative to the current pulse was 11 ns; for the radiation pulse of the exciplex molecule KrBr* it was 11.5 ns (Figure 3.26).

3.6.4. Discussion of research results

The delay in the time of recording the emission of the gas-discharge plasma with respect to the discharge ignition time was caused by the limited rate of the occurrence of the physicochemical processes that lead to the creation of the necessary concentration of excited helium and krypton atoms, and mercury monobromide and krypton bromide molecules [1].

The value of the time delay for the emission of gas-discharge plasma with respect to the initiation time of a discharge was determined by the sum of the flow times of all physicochemical processes that lead to the emission of gas-discharge plasma.

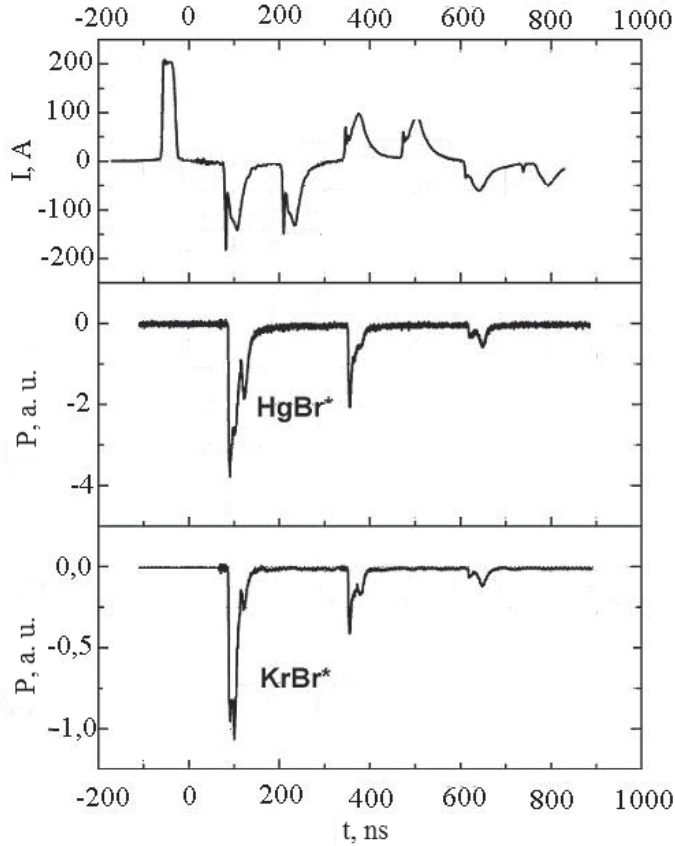

Figure 3.25. Oscillograms of the current pulse (top) and radiation pulses (bottom) of the exciplex molecules HgBr* and KrBr* in the mixture $HgBr_2$:Kr:He = 0.1 Pa:10 kPa:110 kPa. Amplitude of the voltage pulse U_0 = 10 kV; duration of the pump pulse Δt = 30 ns; pulse repetition frequency f = 10 Hz [71].

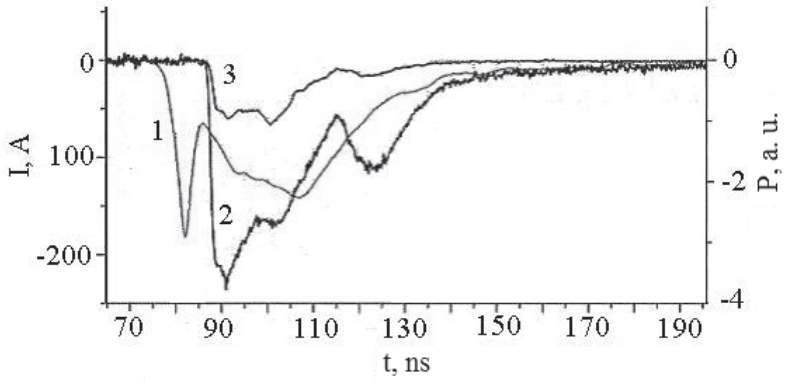

Figure 3.26. Oscillograms of the plasma current pulse (1) and radiation pulses of exciplex molecules HgBr* (2) and KrBr* (3) in the mixture $HgBr_2$:Kr:He = 0.1 Pa:10 kPa:110 kPa. Amplitude of the voltage pulse U_0 = 10 kV; duration of the pump pulse was Δt = 30 ns; pulse repetition frequency f = 10 Hz [68, 71].

Changes in the time of the number of microdischarges (Figure 3.21) and their spatial distribution inside the interelectrode gap were caused by processes of ignition and burning of the barrier discharge, as well as by the accumulation of a charge on the dielectric surface and its resorption during the flow of the charging current of the dielectric surface [16, 49].

The presence on the oscillogram (Figure 3.22) of a set of consecutive pulses was caused by a mismatch between the loads of the impendances of the gas-discharge plasma and pump generator, leading to the appearance of reflected waves. Their propagation along a coaxial cable gives characteristic pulses of voltage drop in the shunt resistance. Such a process operates until the wave energy in the load is completely absorbed.

The appearance in the spectra of gas-discharge plasma emission of exciplex molecules HgBr* ($B^2\Sigma^+_{1/2}$–$X^2\Sigma^+_{1/2}$); KrBr* ($B^2\Sigma^+_{1/2}$–$X^2\Sigma^+_{1/2}$, $C_{3/2}$–$A_{3/2}$, $D_{3/2}$–$A_{3/2}$); molecules Br_2* ($^3\prod_{2g}$–$^3\prod_{2u}$) and OH* ($A^2\Sigma^+ \rightarrow X^2\Pi_i$); and

mercury atoms ($6^1S_0 \rightarrow 6^3P_1$) was caused by the following basic plasma-chemical processes 3.1–3.4, 3.16–3.18, and:

$$HgBr_2+Kr(^3P_2) \rightarrow HgBr(B^2\Sigma^+_{1/2})+Br+Kr \quad (3.21)$$

$$HgBr_2+Kr(^3P_2) \rightarrow KrBr(B^2\Sigma^+_{1/2}, C_{3/2}, D_{3/2})+Br+Kr \quad (3.22)$$

$$Kr^*(Kr_2^*)+Br_2 \rightarrow KrBr^*+(Kr)+Br \quad (3.23)$$

$$Kr^+(Kr_2^+, Kr_3^+)+Br_2^-+M \rightarrow KrBr^*+Br+(Kr, 2Kr)+M \quad (3.24)$$

$$Kr^++Br^-+M \rightarrow KrBr^*+M \quad (3.25)$$

$$KrBr\ (B^2\Sigma^+_{1/2}, C_{3/2}, D_{3/2}) \rightarrow KrBr\ (X^2\Sigma^+_{1/2})+h\nu \quad (3.26)$$

$\lambda_{max.}$ = 207 nm, 222 nm, 228 nm

$$KrBr(B^2\Sigma^+_{1/2}, C_{3/2}, D_{3/2})+M \rightarrow KrBr(X^2\Sigma^+_{1/2})+M+\Delta E_{1,2,3} \quad (3.27)$$

where M is the concentration of quenching molecules and atoms ($HgBr_2$, He, Kr), respectively; and $\Delta E_{1,2,3}$ is the energy difference in the reactions [3, 26, 30, 41–43, 49].

Reactions (3.1) and (3.2) are the main sources for the formation of HgBr* molecules [3, 26, 30, 41–43]. In addition, mercury monobromide molecules are formed by reaction (3.8) due to the excitation of mercury dibromide molecules by electrons in the D-state. This state of the mercury dibromide molecules is the sum of all states that lie between 6.4 and 10.6 eV (where E_i = 10.6 eV is the ionization energy) with an electron scattering threshold of 7.9 eV. Emission from the D-states of the $HgBr_2$ molecules was not observed, because these states pre-dissociate to (C, D) states of HgBr molecules. Emission from the C and D-states of mercury monobromide molecules under the conditions of our experiment was not observed because of the high efficiency of the quenching process (atmospheric pressure discharge). The population of these states was transferred to the $B^2\Sigma^+_{1/2}$ state

of mercury monobromide molecules or to other non-optical channels [3, 30].

The collision of krypton atoms in the metastable state $^3P_2$ with mercury dibromide molecules (3.21) offered a possible, but not very effective, channel for the formation of exciplex HgBr* molecules. [37].

The collision of krypton atoms in the metastable state $^3P_2$ with mercury dibromide molecules (3.22) is the main channel for the formation of KrBr* exciplex molecules in $B^2\Sigma^+_{1/2}$, $C_{3/2}$, and $D_{3/2}$ states.

Excited mercury atoms are formed from reactions (3.16–3.18) due to the large effective cross section for the dissociative excitation of $HgBr_2$ molecules by slow electrons [3, 29, 30]. The exciplex molecules KrBr* (reactions 3.23–3.24) at atmospheric pressures are formed both through a "harpoon" reaction and ion-ion recombination reactions [49].

Weak OH* ($A^2\Sigma^+ \rightarrow X^2\Pi$, 3.24a) emission can be explained by the presence of a trace concentration of water molecules desorbed from the walls of the discharge tube during heating. Emission is caused by the process of dissociative excitation of water molecules upon collision with electrons. The relatively strong Br_2* ($\prod_{2g} \rightarrow {}^3\prod_{2u}$), 3.24b) emission, which appears in the late stage of the discharge, is explained by the accumulation of Br_2 molecules (for example, in reaction (3.16)) and subsequent excitation of Br_2 by electron impact with a transition to the $^3\prod_{2g}$ state, and the decrease in the intensities of the spectral bands of the KrBr (C-A) and (D-A) molecules; the $\lambda = 254$ nm mercury line is due to the apparent absorption of their photons by bromine molecules.

An increase in the emission intensity of exciplex HgBr* molecules by a factor of three and KrBr* by a factor of one and half, with a change in the temperature of the mixture in the temperature range 45–65 °C was

associated with an increase in mercury dibromide vapor pressure and, accordingly, an increase in the concentration of mercury dibromide molecules, leading to an increase in the concentration of exciplex molecules of mercury monobromide and krypton bromide (reactions 3.1–3.2, 3.21 and 3.22) and, correspondingly, the emission intensities of spectral bands increased. The difference in the radiation intensities of the HgBr* and KrBr* molecules was determined by the greater efficiency of processes (3.1–3.4) compared to processes (3.22, 3.23–3.25) [3, 30, 49].

The transformation of the emission spectrum (Figure 3.23), namely the change in the electronic-vibrational structure of the spectral bands of exciplex molecules with an increasing temperature of the gas mixture, was caused by an increase in the rate of relaxation through collision from the upper vibrational levels of mercury monobromide molecules and krypton bromine to the lower ones, followed by a radiative transition to the ground ($X^2\Sigma^+_{1/2}$) weakly bound state [35].

The closeness of the temporal characteristics of the radiation pulses of exciplex molecules HgBr* and KrBr*, as well as their total duration, was primarily due to the fact that these characteristics were determined by the same formation processes in time. The concentration of electrons and drift velocities under the influence of both the field and diffusion effects in the inter-electrode space were also close. At the same time, a difference in the dependency was caused by different mechanisms in the population of the upper states. The excitation of exciplex molecule mercury monobromide $B^2\Sigma^+_{1/2}$ states occurs mainly as a result of the process of dissociative excitation by electrons in collision with mercury dibromide molecules (reactions 3.1–3.2); and excitation of exciplex molecule krypton bromide $B^2\Sigma^+_{1/2}$ states in the “harpoon” reaction of krypton molecules in the metastable state ($^3P_2$) with mercury dibromide molecules (reaction 3.22).

Differences in the mechanisms of the formation of excited states of exciplex molecules HgBr* and KrBr* caused a time delay between radiation pulses.

3.7. The dependency of the radiation power of gas-discharge plasma on the pump conditions and the design of the emitter device

The results of investigation into the radiation power of the energy stored in the dielectric capacitance (7 pF, quartz glass); the repetition rate of the pump pulses; and the operating time of the mixture are shown in Figure 3.27, 3.28 and 3.29. With an increase in energy from 0.1 mJ/cm^3 to 0.8 mJ/cm^3, the average radiation power increased (Figure 3.27). The rate of its growth for each mixture was different, which is associated with unequal losses of discharge power in elastic and inelastic processes occurring in plasma of different composition (see Chapter 4). The highest average power was attained for a discharge in a four-component mixture: $HgBr_2$:SF_6:N_2:He. When the pulse repetition frequency was changed from 3 kHz to 9 kHz, a linear increase in the average radiation power was observed (Figure 3.28). This dependency was caused by a linear increase in the number of photons entering the photodetector with a linear increase in the repetition rate of the pump pulses. The increase in the average radiation power (Figure 3.29) acting on the number of pulses was more intense for discharges in the mixtures $HgBr_2$:SF_6:N_2:He and $HgBr_2$:SF_6:He (curves 1, 2), than for a discharge in the $HgBr_2$:N_2:He mixture (curve 3). This dependency is caused by the unequal rate of increase in the concentration of mercury dibromide vapor for mixtures of different component compositions, which in turn depends on the fraction of power that is deposited in the elastic collisions of plasma electrons with respect to the inelastic scattering of electrons by plasma components (Chapter 4). For

discharge in the four-component mixture $HgBr_2$:SF_6:N_2:He, the concentration growth rate of mercury dibromide vapor was the smallest, which is associated with increased losses of discharge power for inelastic processes in sulfur hexafluoride and nitrogen molecules.

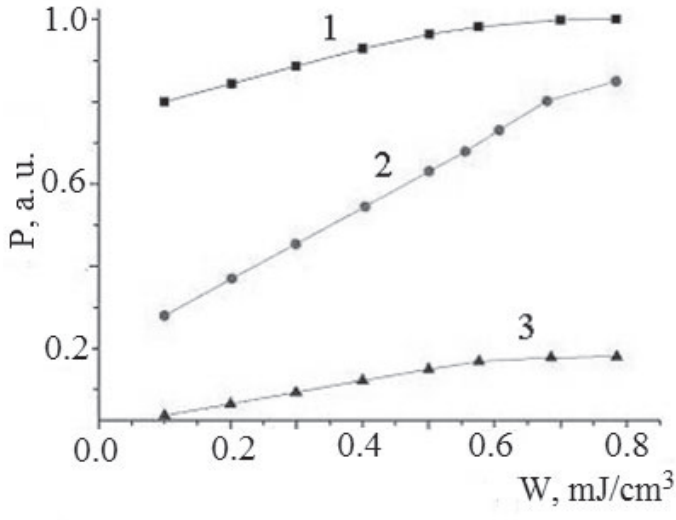

Figure 3.27. The dependency of the average radiation power of a barrier discharge on the specific energy, which is stored on the dielectric capacitance for discharge in the mixtures: 1 - $HgBr_2$:SF_6:N_2:He; 2 - $HgBr_2$:SF_6:He; 3 - $HgBr_2$:N_2:He [59].

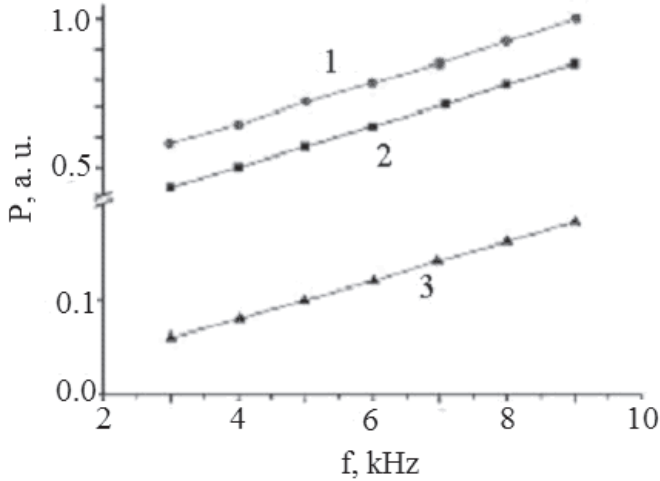

Figure 3.28. The dependency of the average radiation power of the barrier discharge on the repetition rate of the pump pulses for the mixtures: 1 - $HgBr_2$:SF_6:N_2:He; 2 - $HgBr_2$:SF_6:He; 3 - $HgBr_2$:N_2:He [59].

This led to a slower increase in the temperature of the mixture and, correspondingly, to a slow increase in the partial pressure of the mercury dibromide vapor; the concentration of mercury dibromide molecules; and, ultimately, a slow increase in the radiation power up to 1.5 million pulses. Starting from this value of the number of pulses, a sharp increase in the rate of increase in the radiation power was observed, which was caused by the competition of the dynamics of the growth of the concentration of mercury dibromide vapor and heat transfer to the walls of the emitter cell (cuvette with gas discharge plasma). The concentration of mercury dibromide vapor grew faster with an increase in the number of pulses than the loss of heat through the dielectric surface (emitter housing). At pulse counts of 1, 1.5 and 3×10^6 (Figure 3.29), an equilibrium in the rates of increase in the concentration of mercury dibromide molecules and heat loss was achieved,

which led to saturation in the dependency of the radiation power on the number of pulses.

The experimental studies were carried out in experimental installations in which the device (cuvette) was used to produce gas-discharge plasma in the form of a tube (Figure 2.2, Chapter 2). In the course of the study of the optical characteristics of gas discharge plasma in mixtures of mercury dibromide vapor and gases, the possibility of increasing the radiation power in the blue-green spectral range was established. This consisted in applying a special heat-insulating element in the design of the emitter device, for visible and ultraviolet radiation in the cuvette housing. Figure 3.30 shows the radiation spectrum of a barrier discharge for a discharge in the mixture $HgBr_2$:He = 0.1:117 kPa using a heat insulator in the design of the cell (a) and without it (b). Measurement of the average radiation power of a barrier discharge when using a thermal insulator in the radiator design showed an increase of 40 % for all mixtures. The efficiency increased and reached a value of ~10 % for the four-component mixture.

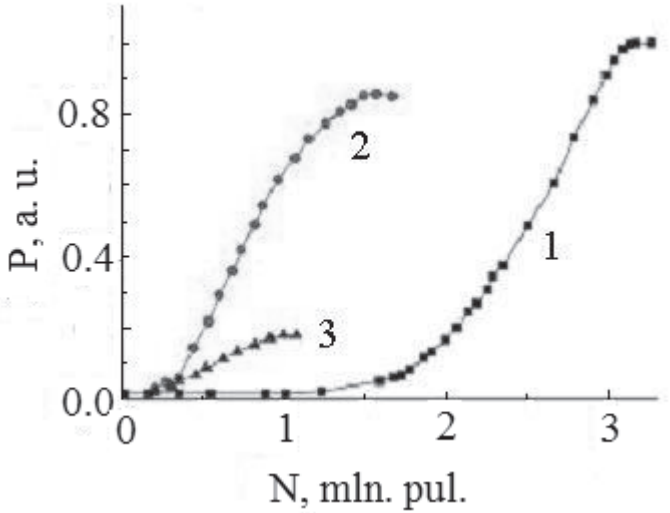

Figure 3.29. The dependency of the average radiation power of a barrier discharge on the total number of pulses for mixtures: 1 - $HgBr_2$:SF_6:N_2:He; 2 - $HgBr_2$:SF_6:He; 3 - $HgBr_2$:N_2:He [59].

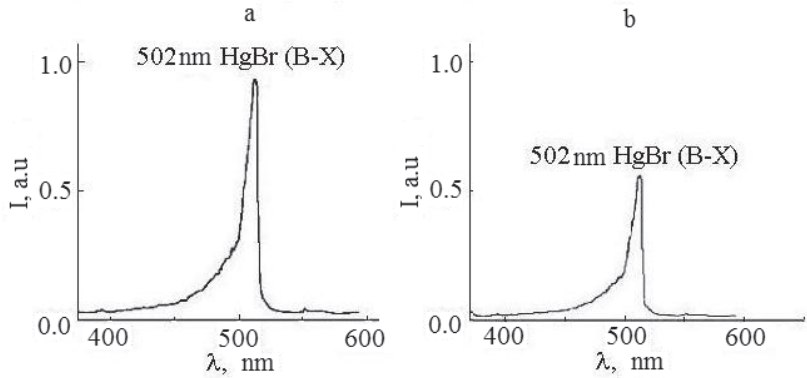

Figure 3.30. The radiation spectrum of a barrier discharge for a discharge in the mixture $HgBr_2$:He = 0.1:117 kPa: a) using a heat insulator; b) without a heat insulator. The total pressure of the mixture was P = 117.1 kPa; the repetition rate of the pump pulses was f = 6 kHz at a voltage amplitude U_a = 9 kV [73, 74].

3.8. The efficiency of quenching of exciplex HgBr* molecules

When studying the optical characteristics of the radiation of gas-discharge plasma in mercury dibromide vapor mixtures with gases (Chapter 3.1–3.4), it was found that with an increase in the partial pressure of the mercury dibromide vapor, nitrogen and sulfur hexafluoride in the working mixtures of the HgBr* emitter, the emission intensity of the mercury monobromide molecules increased, reached a maximum, and then decreased. These changes in the dependency of the emission intensity of HgBr* molecules on the partial pressures of mercury dibromide, nitrogen and sulfur hexafluoride were determined by the kinetics of the processes that led to the excitation and quenching of the $B^2\Sigma^+_{1/2}$ state of these molecules, as well as by the rate constants of these processes [3, 87, 93].

The aim of our research was to establish the efficiency of the quenching process of HgBr* exciplex $B^2\Sigma^+_{1/2}$-state molecules by molecules of mercury dibromide, nitrogen, and sulfur hexafluoride ($HgBr_2$, N_2, SF_6) in the barrier discharge plasma of the HgBr* emitter in three-component and four-component mixtures: $HgBr_2$:SF_6:He; $HgBr_2$:N_2:He and $HgBr_2$:SF_6:N_2:He, respectively, which are quantitative measures of the values of the quenching rate constants.

3.8.1. A method for determining the efficiency of the quenching process of $B^2\Sigma^+_{1/2}$-state exciplex HgBr* molecules

To establish the efficiency of the quenching process of $B^2\Sigma^+_{1/2}$-state exciplex HgBr* molecules by mercury dibromide, nitrogen, and sulfur hexafluoride, we used a gas-discharge method to measure the rate constant of the quenching of $B^2\Sigma^+_{1/2}$-state mercury monobromide molecules by halogen-containing molecules and nitrogen molecules [3, 36]. We

considered the gas-discharge method for multicomponent mixtures of the vapor of mercury dibromide molecules, nitrogen, sulfur hexafluoride and helium (Chapter 3.1–3.4).

In determining the expression for the radiation intensity of exciplex molecules of mercury monobromide, based on the processes that lead to the excitation and quenching of the $B^2\Sigma^+_{1/2}$ state of mercury monobromide, we used the kinetic equation for the population of HgBr* $B^2\Sigma^+_{1/2}$:

$$d[HgBr^*]/dt=k_{d1}[HgBr_2][N_e]+k_{d2}[HgBr_2][N_2^*]+k_q[HgBr(C, D)][SF_6,N_2,HgBr_2]-\tau_r^{-1}[HgBr^*]-k_{q1}[HgBr^*][M] \quad (3.28)$$

where k_{d1} is the rate constant of the dissociative excitation of HgBr* molecules by electron impact; k_{d2} is the rate constant of the dissociative excitation of HgBr* molecules upon the collision of mercury dibromide molecules with nitrogen molecules excited to metastable states $A^3\Sigma^+_u$ and $B^3\Pi_g$; k_q is the sum of rate constants of quenching C and D-state molecules of HgBr; τ_r is the radiative lifetime of the $B^2\Sigma^+_{1/2}$ state of HgBr* molecules; k_{q1} is the rate constant of the quenching of the $B^2\Sigma^+_{1/2}$ state of HgBr* molecules; [HgBr*], [HgBr(C, D)], [$HgBr_2$], [N_2*], [N_e], [M] are the concentrations of molecules: HgBr* in the states $B^2\Sigma^+_{1/2}$, $C^2\Pi_{1/2}$, and $D^2\Pi_{3/2}$; $HgBr_2$, N_2*, electrons and quenching molecules and atoms ($HgBr_2$, SF_6, N_2, He), respectively.

For the quasi-stationary case, (3.28), the emission intensity is:

$$I^{-1}_{HgBr^*} = \alpha(+k_{T1}\,\tau_r\,[M]) \quad (3.29)$$

where $\alpha = (k_{d1}h\nu\,[HgBr_2][N_e]+k_{d2}\,h\nu\,[HgBr_2][N_2^*]+k_q\,h\nu[HgBr^*(C, D)]$

$$[SF_6, N_2, HgBr_2])^{-1} \quad (3.30)$$

The pulsed discharge regime can be considered steady for a mixture of mercury dibromide vapor with nitrogen, sulfur hexafluoride and helium, provided that the duration of the exciting pulse exceeds the characteristic times of the processes that affect the concentration of excited HgBr* molecules ($B^2\Sigma^+_{1/2}$ state). The following must be greater: the characteristic time of establishment of the quasi-stationary electron energy distribution function (EEDF); the time of establishment of the electron concentration; the radiation lifetime of the $B^2\Sigma^+_{1/2}$ state of the molecule HgBr*; and the quenching time of the same state [1, 3].

The time of establishment of the quasi-stationary electron distribution, i.e. the time of "tracking" the EEDF in terms of changes in the electric field strength and concentration of plasma components is approximately equal to the relaxation time of mean electron energy [94]. The time for the establishment of the EEDF for working mixtures ($HgBr_2$:N_2:He; $HgBr_2$:SF_6:He; $HgBr_2$:SF_6:N_2:He) was determined by us using the well-known software program Bolsig+ [73]. They did not exceed 10 ns for the values of the parameter E/N = 10–40 Td (where E is the electric field strength and N is the total concentration of the working mixture), in the range of which the HgBr* emitter operates.

The quenching time (τ_{q1}) of $B^2\Sigma^+_{1/2}$-state HgBr* molecules by mercury dibromide, nitrogen, and sulfur hexafluoride was estimated using the expression:

$$\tau_{q1} \approx (k_{q1}\,[M])^{-1} \quad (3.31)$$

To estimate the quenching time of the $B^2\Sigma^+_{1/2}$-state HgBr* molecule by mercury dibromide, nitrogen and sulfur hexafluoride, we used data on the quenching rate constants k_{q1} and the concentration of mercury dibromide vapor, nitrogen and sulfur hexafluoride [33–36, 96]. The estimate τ_{q1} gives a value of no more than 50 ns.

The radiative lifetime of the $B^2\Sigma^+_{1/2}$-state HgBr* molecule has the value: 23.2 ns [97].

We now clarify the conditions under which the coefficient α (see (9)) does not change with the increasing concentration of quenching molecules. In the case of an increase in the concentration of mercury dibromide molecules in plasma based on mixtures with nitrogen, sulfur hexafluoride and helium, when the partial pressures of nitrogen and sulfur hexafluoride are constant, the increase is compensated by a decrease in the electron concentration N_e due to the process of dissociative attachment (3.2). (The rate constant of this process is approximately 10^{-10} cm^3/s at low (up to 10 eV) mean electron energies in the discharge [13].) However, with an increase in the concentration of mercury dibromide, an increase in the electron concentration during the ionization of mercury dibromide molecules by electrons is also possible; but this process contributes insignificantly, since its efficiency is low at low mean electron energy values, which are characteristic for the barrier discharge applicable for excitation of $B^2\Sigma^+_{1/2}$-state exciplex HgBr* molecules in the working mixtures of the HgBr* emitter [3, 32]. The rate constant of the dissociation of $HgBr_2$ molecules by electron impact k_{d1} can remain constant if the electron distribution function does not change. To do this experimentally, a constant field strength E was applied to the electrodes of the radiator during the pump pulse. As for the total concentration N, this is mainly set by the buffer gas helium. It was $N>10^{19}$ cm^{-3}, which was higher by two orders of

magnitude than the mercury dibromide vapor concentration. In light of this, it can be assumed that the distribution function of plasma electrons varies insignificantly. The numerical calculation of the electron distribution function, as well as the rate constants of the dissociation of $HgBr_2$ molecules by electron impact, performed for the working mixtures of the HgBr* emitter, confirm these assumptions [54, 57, 60]. The rate constant of the dissociative excitation of HgBr* molecules by nitrogen molecules excited to metastable $A^3\Sigma^+_u$ and $B^3\Pi_g$ states in collisions with mercury dibromide molecules remains constant, with an insignificant change in the electron distribution function [37]. The quenching rate constants (k_q) of HgBr* molecule C and D-states by sulfur hexafluoride are not known. Estimation of their value gives a value higher than the value of the quenching rate constant of $B^2\Sigma^+_{1/2}$-state exciplex HgBr* molecules [3].

The coefficient α does not change either with an insignificant (<10 %) increase in the concentration of quenching nitrogen or hexafluoride molecules, since the electron distribution function changes insignificantly with a decrease in the E/N parameter by <10 % [54, 57, 60].

To provide constancy in the quantities of the coefficient α (9) in gas-discharge plasma, with an increase in the partial pressures of quenching molecules, the concentrations of which are insignificant in comparison to the total concentration of the working mixture of the HgBr* radiator, expression (3.29) coincides with the well-known Stern-Volmer method for quenching the luminescence of molecules [93].

3.8.2. The results of studies into the quenching efficiency of $B^2\Sigma^+_{1/2}$-state exciplex HgBr* molecules

From the experimental data it follows that the pump pulse durations of the working mixtures (400 ns and 50 ns—voltage and current, respectively)

exceed the characteristic times of the processes affecting the population of the $B^2\Sigma^+_{1/2}$ state of mercury monobromide molecules. It is known that the helium buffer gas “weakly” quenches HgBr* molecules (quenching rate constant $<10^{-14}$ cm^3/s) [98, 99]. This allows for measurement of the characteristics of the HgBr* emitter at atmospheric pressures of the buffer gas and small partial pressures of mercury dibromide, nitrogen, and sulfur hexafluoride (<10 %). In addition, experimental conditions were provided for which the value of the parameter E/N remained practically unchanged (the amplitude of the voltage pulse applied to the electrodes did not change during its duration, but there was no more than a 10 % increase in the concentration of mercury dibromide, sulfur hexafluoride or nitrogen in comparison to the concentration of the buffer gas helium).

To determine the quenching efficiency of the $B^2\Sigma^+_{1/2}$ state of mercury monobromide molecules in the HgBr* emitter gas discharge plasma, results were obtained on the dependency of the radiation power of mercury monobromide molecules on the partial pressures of nitrogen molecules and sulfur hexafluoride in the discharge in the mixtures: $HgBr_2$:N_2:He; $HgBr_2$:SF_6:He; and $HgBr_2$:SF_6:N_2:He (figures 3.6, 3.10, 3.14). For the partial pressure of mercury dibromide molecules we used the experimental data shown in Figure 3.31. Figure 3.32 shows the dependency of the inverse radiation intensity of exciplex HgBr* molecules on the concentration of nitrogen molecules, sulfur hexafluoride and mercury dibromide for discharge in the three-component mixtures $HgBr_2$:SF_6:He; $HgBr_2$:N_2:He; and $HgBr_2$:SF_6:N_2:He. For inverse values of radiation intensity, a change in the angle of inclination to the abscissa axis is characteristic, depending on the component composition of the mixture and the concentration of molecules that quench the $B^2\Sigma^+_{1/2}$ state of mercury monobromide exciplex molecules.

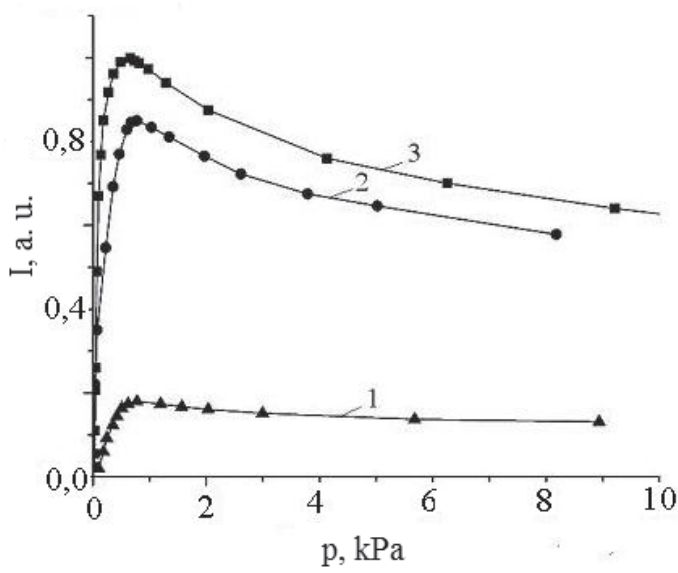

Figure 3.31. The dependency of the emission intensity of the spectral band λ = 502 nm of exciplex HgBr* molecules on the partial pressure of dibromide vapors in the mixtures: 1 - $HgBr_2$:N_2:He, with partial pressures of nitrogen 4 kPa and helium 120 kPa; 2 - $HgBr_2$:SF_6:He, with partial pressures of sulfur hexafluoride 70 Pa and helium 117 kPa; 3 - $HgBr_2$:SF_6:N_2:He, partial pressures of sulfur hexafluoride 70 Pa, nitrogen 4 kPa, helium 117.2 kPa. Repetition rate f = 6 kHz; amplitude of the voltage pulse U_a = 9.5 kV [59].

The value of the product $\alpha k_{T1}\tau_{HgBr^*}$ was determined from the value of the tangent angle slope of these graphs. In turn, the coefficient α was determined at the point of intersection of these dependencies with the ordinate axis upon its continuation.

The results of determining the quenching efficiency of the $B^2\Sigma^+_{1/2}$ state of exciplex HgBr* molecules are presented in Table 3.1. As can be seen from the table data, the efficiency of the quenching process of the

exciplex mercury monobromide molecules by molecules of mercury dibromide, nitrogen and sulfur hexafluoride depends on the composition of the mixture. The four-component mixture ($HgBr_2$:SF_6:N_2:He) was characterized by a lower value of the rate constant for quenching by mercury dibromide molecules than for three-component mixtures of mercury monobromide molecules by nitrogen molecules (reactions 4 and 5, Table 1). In a four-component mixture, the rate constant of the quenching of exciplex mercury monobromide molecules by nitrogen molecules was less important than for the three-component mixture. The highest quenching efficiency of exciplex mercury monobromide molecules can be observed when they are quenched by sulfur hexafluoride molecules (reaction 6, Table 1). The quenching rate constant of this process reached $(71.07 \pm 14.2)\cdot10^{-10}$ $cm^3\cdot s^{-1}$. The regularity of the decrease in the quenching efficiency of exciplex

Table 3.1. Parameters of quenching reactions

№	Quenching reactions	Mixture	$k_q\times10^{10}$, $cm^3\cdot s^{-1}$
1	HgBr* + $HgBr_2$	$HgBr_2$:SF_6:N_2:He	0,22 ± 0,04
2	HgBr* + $HgBr_2$	$HgBr_2$:SF_6:He	0,24 ± 0,05
3	HgBr* + $HgBr_2$	$HgBr_2$:N_2:He	0,29 ± 0,06
4	HgBr* + N_2	$HgBr_2$:SF_6:N_2:He	0,04 ± 0,01
5	HgBr* + N_2	$HgBr_2$:N_2:He	0,55 ± 0,11
6	HgBr* + SF_6	$HgBr_2$:SF_6:He	71,1 ± 14,2

mercury monobromide molecules by mercury dibromide was caused by processes that additionally populate the $B^2\Sigma^+_{1/2}$ state of mercury monobromide molecules [37]. See Table 1 for the quenching of $HgBr_2$:SF_6:He and $HgBr_2$:N_2:He (reactions 1, 2 and 3 in Table 1). The same regularity was observed for the quenching efficiency of exciplex overlying energy states (C and D) by sulfur hexafluoride molecules with transfer of the population to the $B^2\Sigma^+_{1/2}$ state, which is more efficient than the process of populating this state of exciplex mercury monobromide molecules, as a result of collisions of metastable nitrogen molecules (state $A^3\Sigma^+_u$) with mercury dibromide molecules. Therefore, its rate constant (see Table 1, reaction 2) was less important than reaction 3 (Table 1). The regularity in the quenching efficiency in reactions 5 and 6 (Table 1) was related to the difference in the molecular masses of the molecules of sulfur hexafluoride and nitrogen; for molecules with a molecular weight closer to the molecular weight of mercury monobromide, the quenching efficiency was higher [93].

The same regularity for the rate constants of quenching the $B^2\Sigma^+_{1/2}$ state of exciplex mercury monobromide molecules was observed in the work of the authors in [33, 80] for plasma in other mixtures of mercury dihalide vapor and helium. The quenching process 4 (Table 1) was less effective, which is connected to the processes for populating the $B^2\Sigma^+_{1/2}$ state of exciplex mercury monobromide molecules, as well as the lower molecular weight of nitrogen molecules compared to molecules of mercury dibromide and sulfur hexafluoride.

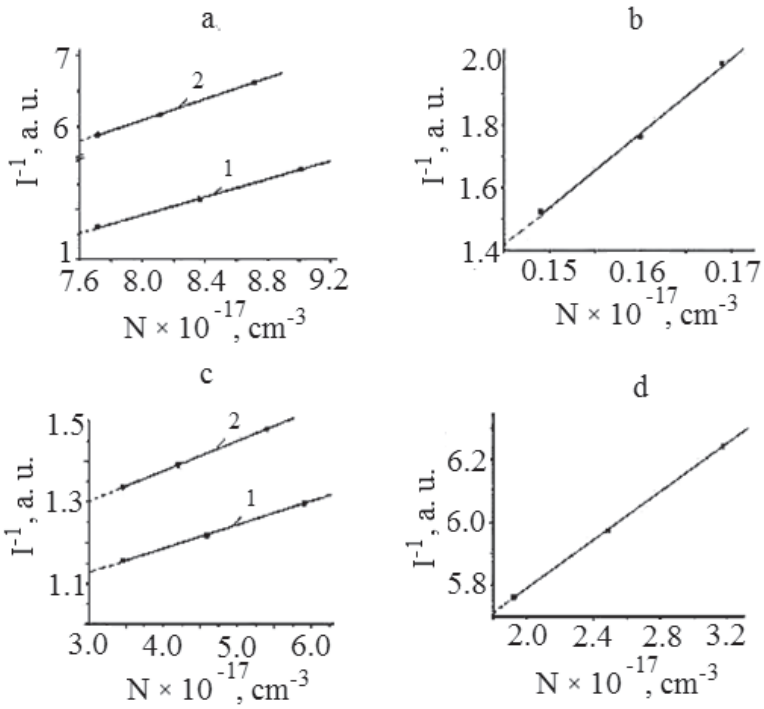

Figure 3.32. The dependency of the inverse intensity of the emission of spectral band λ = 502 nm of HgBr* molecules on the concentration of molecules: a) nitrogen for the mixture $HgBr_2$:SF_6:N_2:He (1) and $HgBr_2$:N_2:He (2); b) sulfur hexafluoride for the mixture $HgBr_2$:SF_6:He; c) mercury dibromide for the mixture $HgBr_2$:SF_6:N_2:He (1) and for the mixture $HgBr_2$:SF_6:He (2); d) mercury dibromide for the mixture $HgBr_2$:N_2:He [59].

3.9. Optical characteristics of gas-discharge plasma in a mixture of mercury dibromide vapor with argon

This section presents our research into the optical characteristics of gas-discharge plasma in a mixture of mercury dibromide vapor with a buffer gas "heavier" than helium, namely argon. The need for such research is due to

the fact that argon has a lower penetrative power through the walls of the emitter and can thus provide a longer lamp life.

The partial vapor pressure of mercury dibromide in the experiments was kept constant at 0.6 kPa. This was chosen as optimal for the maximum radiation intensity observed in our experiments to study the optical characteristics of gas-discharge plasma in the $HgBr_2$:He mixture (Fig. 3.3b). The argon pressure was varied in the range 106–123 kPa.

Immediately after the initiation of the barrier discharge, the filamentous mode of BR burning was observed, with a set of microdischarges between the metal electrode and the inner surface of the quartz tube (4, Fig. 2.4) of the radiator. The color of the discharge in the initial stage (the first 30 s) was determined by the argon buffer gas. In the subsequent time period, the discharge glowed blue-green. In this case, a mainly diffuse and uniform discharge pattern was observed.

In the spectra obtained in the visible range, the spectral band with a maximum wavelength of $\lambda = 502$ nm was seen, which has a weakly resolved vibrational structure and corresponds to the $B^2\Sigma^+_{1/2} \rightarrow X^2\Sigma^+_{1/2}$ electron-vibrational transition of the HgBr* exciplex molecule [21]. The main part of the intensity of the radiation of the spectral band was concentrated in the wavelength range 512–475 nm. The band shape and its width at half-height (15–16 nm) was similar to the bands corresponding to the $B \rightarrow X$ transition of mercury monobromide shown in previous research in which a barrier discharge was created in mixtures of mercury dibromide vapor, helium and other gases using large-sized quartz tubes and small-sized radiation sources. A sharp increase in the intensity of the radiation in the spectrum was observed from the side of the region with long wavelengths and its slow decrease in the region of smaller wavelengths.

3.9.1. The dependency of the average radiation power of exciplex HgBr* molecules on the partial pressure of argon

Figure 3.33 presents the results of research into the dependency of the radiation power of exciplex HgBr* molecules on the partial pressure of argon. In addition, Fig. 3.33 shows the dependency of the radiation power of HgBr* on the partial pressure of helium, which was determined in order to compare the results of the emission of mercury monobromide molecules for two different gases. An increase in the radiation power of the HgBr* exciplex molecule was observed with an increase in the partial pressures of both argon and helium, from 106.5 kPa to 114.4 and 122.2 kPa for argon and helium, respectively. A further increase in the partial pressures of both argon and helium led to a decrease in radiation power. In addition, there was a shift in the maximum radiation power to a region of lower pressure in the mixture with argon and a larger value (~1.3 times) compared to the mixture with helium. The efficiency of the radiation source was ~4 %. The measurement error of the radiation power did not exceed 5 %.

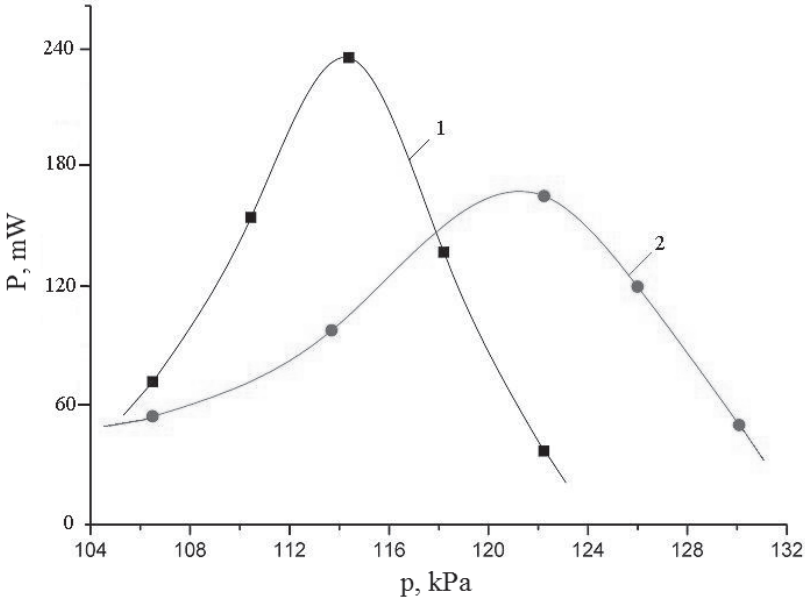

Figure 3.33. The dependency of the radiation power of the exciplex molecule HgBr* (λ = 502 nm) on the partial pressure of the buffer gas for the mixtures: 1 - $HgBr_2$:Ar; 2 - $HgBr_2$:He. Saturated vapor pressure of $HgBr_2$ was equal to 0.6 kPa. The amplitude of the voltage pulse was 2,500 V. The repetition rate of the pump pulses was f = 6,000 Hz.

3.9.2. Current waveform oscillogram

Figure 3.34 presents an oscillogram for a pulsed discharge current pulse for the ratio of the components of the mixture at which maximum radiation power was reached. The oscillatory structure of the current pulse is caused by multiple discharges of the dielectric capacitance during a voltage pulse with an amplitude sufficient to break the discharge gap. The difference in the oscillatory structure of current pulses is due to the opposite directions of current flow through the gas-discharge gap and, as a result, different charge

dissipation conditions on the inner dielectric surface with one barrier discharge, as in our experiment. The maximum value of the amplitude of the current pulse was 8.6 A. The duration of the leading edge was 10 ns, and the half-height duration was 50 ns (measurement error was 10 %).

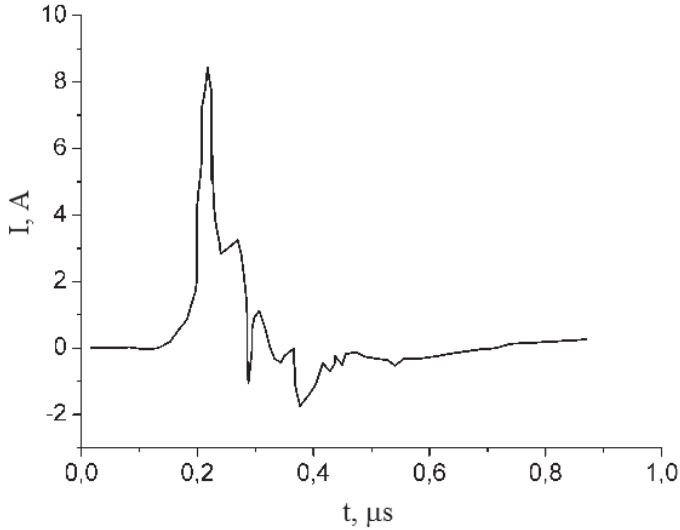

Figure 3.34. Oscillogram of the current pulse in the mixture of $HgBr_2$:Ar = 0.6:114.4 kPa. The amplitude of the voltage pulse was 2,500 V. The repetition rate of the pump pulses was f = 6,000 Hz.

3.9.3. Discussion of research results

The appearance of spectral band emissions with a maximum wavelength of λ = 502 nm of the electron-vibrational transition $B^2\Sigma^+_{1/2} \rightarrow X^2\Sigma^+_{1/2}$ of the exciplex HgBr* molecule in gas-discharge plasma in a mixture of mercury dibromide vapor with argon occurs due to processes leading to to the formation and destruction of the $B^2\Sigma^+_{1/2}$ state of mercury monobromide; the main processes are given in [36, 42, 43]:

(3.28) $HgBr_2+e \rightarrow HgBr^*+ Br+e$

(3.29) $HgBr_2+e \rightarrow HgBr^*+ Br^-$

(3.30) $HgBr^* \rightarrow HgBr+h\nu$

(3.31) $HgBr^*+M \rightarrow HgBr+M+\Delta E$

The cross-sections of the processes (3.28) and (3.29) are $7.5 \cdot 10^{-21}$ m^2 and $1 \cdot 10^{-21}$ m^2 for electron energies of 9.0 eV and 3.0 eV, respectively [3, 41].

The kinetic equation for population of the $B^2\Sigma^+_{1/2}$ states of HgBr* is:

$$\frac{d[HgBr^*]}{dt} = k_D [HgBr_2][N_e] - \tau_r^{-1} [HgBr^*] - k_Q [HgBr^*][M] \quad (3.32)$$

where k_D is the rate constant of the dissociation of $HgBr_2$ molecules by electron impact; τ_r is the radiation lifetime of the $B^2\Sigma^+_{1/2}$ state of HgBr*; k_Q-quenching is the rate constant of the $B^2\Sigma^+_{1/2}$ state of HgBr*; [HgBr*], [$HgBr_2$], [N_e], and [M] are the concentrations of HgBr*, $HgBr_2$, electrons and quenching molecules and atoms ($HgBr_2$, Ar), respectively.

For the quasi-stationary case in equation (5), the emission intensity is:

$$I_{HgBr^*}^{-1} = \alpha(1+k_Q \tau_r [M]) \qquad (3.33)$$

where $\alpha = (k_D h\nu [HgBr_2][N_e])^{-1}$

The rate constants of the processes leading to the formation and destruction of HgBr* molecules for the reduced electric field (E/N) = 20 Td, as well as the lifetime of the HgBr* state, are presented in Table 3.2.

The sharp increase in intensity from the part of the spectrum with long wavelengths and its slow decrease in the short-wavelength region (Fig. 2) can be explained by the course of potential curves (excited $B^2\Sigma^+_{1/2}$ state shifts towards large internuclear distances relative to the $X^2\Sigma^+_{1/2}$ state) and processes of relaxation of the population of the upper vibrational levels of the excited electronic state, which occur faster than the electronic-vibrational transition to the ground $X^2\Sigma^+_{1/2}$ state [3, 24].

Table 3.2. The rate constants of the processes leading to the formation and destruction of HgBr* molecules for the reduced electric field (E/N) = 20 Td, as well as the lifetime of the $B^2\Sigma^+_{1/2}$ state of HgBr*.

Process	Rate constant of the process. Lifetime $B^2\Sigma^+_{1/2}$-state HgBr*	Source
$HgBr_2+e \rightarrow HgBr^*+Br+e$	$8.1 \cdot 10^{-15}$ m^3/s	E/N = 20 Td, calculation
$HgBr_2+e \rightarrow HgBr^*+Br^-$	$1.6 \cdot 10^{-16}$ m^3/s	E/N = 20 Td, calculation
$HgBr^* \rightarrow HgBr+h\nu$	23.7 ns	[97]
$HgBr^*+Ar \rightarrow HgBr+Ar+\Delta E$	$7.2 \cdot 10^{-20}$ m^3/s	[34]
$HgBr^*+HgBr_2 \rightarrow HgBr+HgBr_2+\Delta E$	$2.7 \cdot 10^{-16}$ m^3/s	[36]

The dependency of the radiation power of the exciplex molecule HgBr* on the argon partial pressure (Fig. 3.33) is primarily caused by the following processes: an increase in the electron concentration with an increase in the argon partial pressure in the mixture; a change in the fraction of the discharge energy that is spent on heating the working mixture; a change in mean electron energy and the rate constant of the excitation of mercury

monobromide, depending on the values of the parameter E/N; and the quenching process of the $B^2\Sigma^+_{1/2}$ state of HgBr* molecules in collisions with argon atoms [1, 34]. With an increase in the partial pressure of argon in the mixture, the value of the parameter E/N decreases. This leads to an increase in the fraction of the discharge power going to the elastic scattering of electrons in argon atoms and mercury dibromide molecules, which leads to heating of the mixture and, accordingly, to an increase in the partial pressure of the mercury dibromide vapor and the emission intensity of exciplex HgBr* molecules. In addition, an increase in the electron concentration, which increases with an increase in the concentration of the components of the working mixture, also contributes to an increase in the brightness of the radiation with an increase in the partial pressure of argon [1]. The presence of a maximum and a further decrease in the emission brightness of the exciplex HgBr* molecules with an increase in the partial pressure of argon are caused by the quenching of this state of mercury monobromide molecules when they collide with argon atoms [34].

$$HgBr^* + Ar \rightarrow HgBr + Ar + \Delta E \qquad (3.34)$$

where ΔE is the energy difference in the reaction.

Above a certain value of the partial pressure of argon, the quenching process (3.34) plays a significant role in connection with which the radiation power decreases.

The rate constant of this process is $7.2 \cdot 10^{-20}$ m^3/s [34].

An increase in the radiation power in the discharge of the mercury dibromide vapor with argon mixture, compared to a mixture of mercury dibromide vapor and helium (Fig. 3.33), is caused by the process of

quenching the overlying $C^2\Pi_{1/2}$ and $D^2\Pi_{3/2}$ states of mercury monobromide molecules with excitation transfer to the $B^2\Sigma^+_{1/2}$ state:

$$HgBr_2+e\rightarrow HgBr_2(D)\rightarrow HgBr(C^2\Pi_{1/2},$$
$$D^2\Pi_{3/2})+M\rightarrow HgBr(B^2\Sigma^+_{1/2})+M+\Delta E_{1,2} \quad (3.35)$$

where $\Delta E_{1,2}$ is the difference between the excitation energies of $C^2\Pi_{1/2}$, $D^2\Pi_{3/2}$ and $B^2\Sigma^+_{1/2}$ states of mercury monobromide molecules. This process is indicated by the value of the excitation rate constant of the sum of the states of mercury dibromide molecules above the threshold of 7.9 eV, which is an order of magnitude higher than the excitation rate constant of the $B^2\Sigma^+_{1/2}$ state (Fig. 4.28, Section 4); accordingly, the population of $C^2\Pi_{1/2}$ and $D^2\Pi_{3/2}$ states of mercury monobromide, into which it decomposes, is an order of magnitude higher than the population of the B-state. In the process of quenching, this can lead to a significant increase in the radiation power of the exciplex HgBr*molecules. A necessary condition in this case should first of all be a larger value of the rate constant for quenching with argon compared to that with helium on the $C^2\Pi_{1/2}$ and $D^2\Pi_{3/2}$ states of mercury monobromide. A similar process (the process of quenching of the overlying $C^2\Pi_{1/2}$ state) with the transfer of the population to the lower lying $B^2\Sigma^+_{1/2}$ state has previously been observed for the exciplex mercury mono-iodide molecule [84–86].

3.10. Optical characteristics of gas-discharge plasma in a mixture of mercury dibromide vapor with neon

This section presents our research into the optical characteristics of gas-discharge plasma in a mixture of mercury dibromide vapor with a buffer gas “heavier” than helium: neon. The need for such research was due to the fact that neon has less penetrative power through the walls of the emitter and thus can provide a longer lamp life. In addition, in studies of the optical

characteristics of gas-discharge plasma in a mixture of mercury dibromide vapor with gases, which is the working medium of exciplex lamps, the design of the emitters was coaxial and, as a rule, the side surface was the radiating zone. For a number of scientific and technological applications, it is necessary to achieve high radiation density, which is provided by another type of lamp design [16], and this was the purpose of our research.

3.10.1. The design of the radiator

Gas-discharge plasma in mixtures of mercury dibromide vapor and neon was created using a barrier discharge (BR) in the radiator (I), which was made of a quartz tube (2, Fig.3.35) with a diameter of 34 mm and a length of 200 mm. Two tungsten electrodes (4) with a diameter of 5 mm were located along the axis of the gas-discharge radiator at a distance of 15 mm. One of the electrodes was placed in a quartz tube (3) with a diameter of 9 mm. To reduce the release of mercury dibromide vapor from the gas-discharge cuvette in the VPGFS, a nozzle (6) was welded to the gas-discharge cuvette, with a capillary of 0.5 mm diameter in the middle.

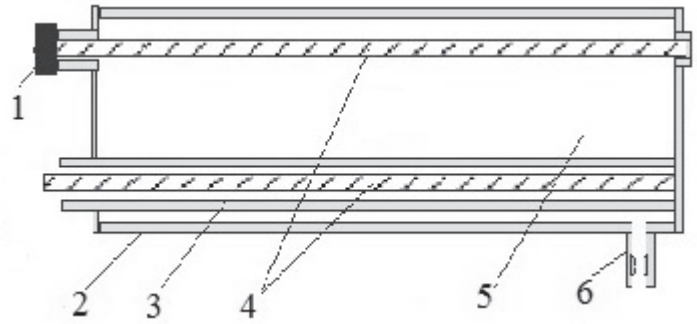

Figure 3.35. Radiator design: 1 - high-voltage input; 2 - quartz tube with a diameter of 34 mm; 3 - quartz tube with a diameter of 9 mm; 4 - electrodes; 5 - working volume; 6 - nozzle with a capillary.

3.10.2. Plasma emission spectrum

The partial vapor pressure of mercury dibromide in the experiments was kept constant at 0.8 kPa. This was chosen as the optimal value at which the maximum intensity of radiation was observable in our experiments into the optical characteristics of a discharge plasma in the $HgBr_2$:He mixture [52]. The pressure of neon varied in the range of 10–120 kPa.

Immediately after the initiation of the barrier discharge, the filamentous mode of burning of the BR was observed, a set of cone-shaped microdischarges with the tip on the metal electrode and the base on the inner surface of the quartz tube (3) of the radiator occurred. The red color of the discharge in the initial stage (first 30 s) was determined by the neon buffer gas. Subsequently, the discharge glowed blue-green. In this case, a mainly diffuse and uniform discharge pattern was observed; the number of filaments sharply decreased, and did not exceed three in number.

In the spectra obtained in the visible range, a spectral band with a maximum at a wavelength of λ = 502 nm (Fig. 3.36) was distinguishable, which has a weakly resolved vibrational structure and corresponds to the $B^2\Sigma^+_{1/2} \rightarrow X^2\Sigma^+_{1/2}$ electronic-vibrational transition of exciplex HgBr* molecules [24]. The main part of the intensity of the radiation of the spectral band was concentrated in the wavelength range 512–475 nm. The band shape and its width at half-height (15–16 nm) was similar to the bands corresponding to the B→X transition of mercury monobromide, as shown in previous research in which the creation of a barrier discharge in mixtures of mercury dibromide vapor, helium and other gases was carried out using large-sized quartz tubes and small-sized radiation sources. A sharp increase in the intensity of the radiation in the spectrum was observed from the side

of the region with long wavelengths and its slow decrease in the region of smaller wavelengths.

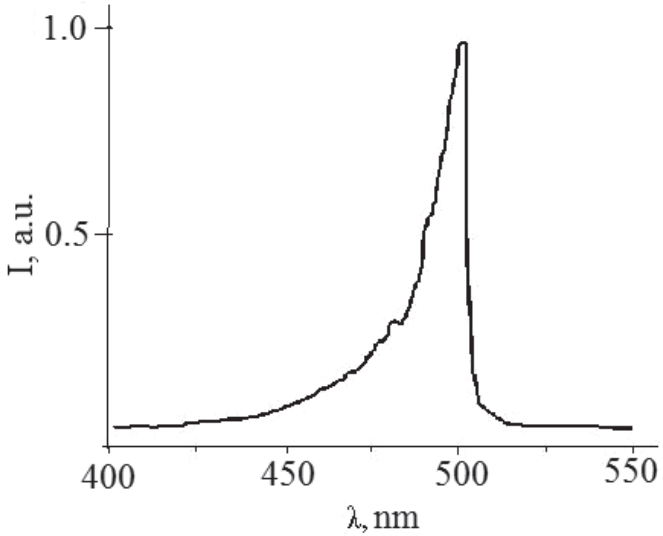

Figure 3.36. The emission spectrum of the barrier discharge for the mixture $HgBr_2$:Ne = 0.8:100 kPa. The total pressure of the mixture was P = 100.8 kPa. The pump pulse repetition rate was f = 1 kHz; the voltage pulse amplitude was U_a = 30 kV.

3.10.3. The dependency of the emission brightness of exciplex HgBr* molecules on neon partial pressure

Figure 3.37 presents the results of research into the dependency of the emission brightness of the exciplex HgBr* molecule on the partial pressure of neon. Fig. 3.37 shows the dependency of the brightness of HgBr* radiation on the partial pressure of helium. This was determined in order to compare the results of mercury monobromide emissions for two different gases. An increase in the emission brightness of the HgBr* exciplex molecule was observed with an increase in the partial pressures of both neon

and helium from 10 kPa to 117–120 kPa. A further increase in the partial pressures of both neon and helium led to a decrease in the emission brightness. In addition, there was a shift in the emission brightness maximum to the region of low pressure in a mixture with neon, as well as a smaller value (by ~10%) compared to a mixture with helium. The average radiation power using helium as a buffer gas was 170 mW (discharge burning volume 14 cm^3) with an efficiency of 1.1 %. In a mixture of mercury dibromide vapor with neon, the average radiation power of the exciplex HgBr* molecule did not exceed 153 mW and an efficiency <1 %.

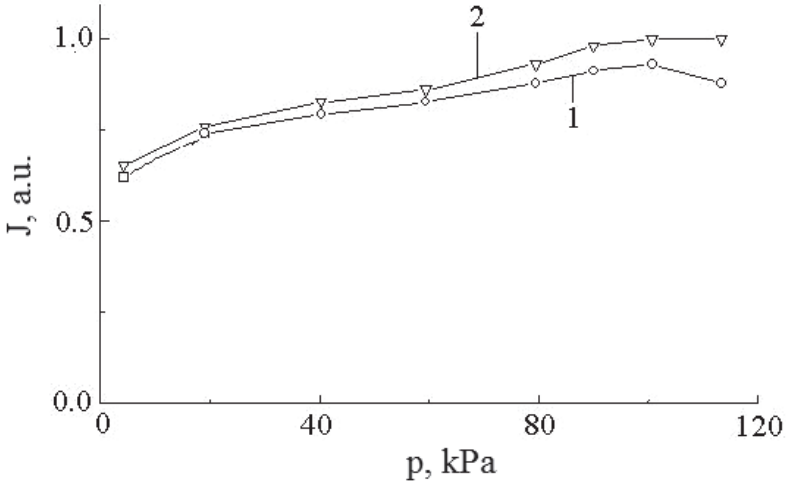

Figure 3.37. The dependency of the emission brightness of the exciplex HgBr* molecule (λ = 502 nm) on the partial pressure of the buffer gas for the mixture: 1 - $HgBr_2$:Ne; 2 - $HgBr_2$:He. Saturated vapor pressure of $HgBr_2$ = 0.8 kPa. Pump pulse repetition rate f = 1,000 Hz.

3.10.4. Current pulse waveform

Figure 3.38 presents oscillograms for the current pulses of a barrier discharge and radiation for the ratio of the components of the mixture at which the maximum brightness of radiation was reached. An oscillatory mode was observed for the energy input of the pump source into the plasma. The maximum value of the amplitude of the current pulse was 300 A. The current pulses were twofold and of different polarity; the delay between them in our experimental conditions was 150 ns. The leading edge was 10 ns and the duration was 50 ns. The radiation pulses were also twofold with a time shift relative to each other of 150 ns. Their amplitudes were different in magnitude, with the amplitude of the second pulse exceeding the magnitude of the first. An increase in the neon partial pressure in the range of 10–100 kPa led to an increase in the amplitude of both pulses.

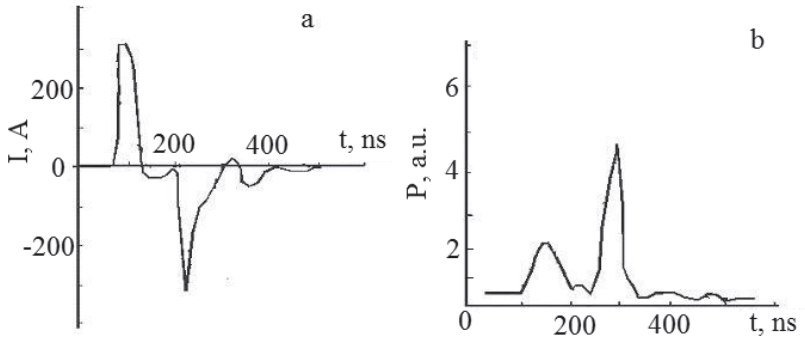

Figure 3.38. Oscillograms of current (a) and radiation (b) pulses of HgBr* molecules (λ = 502 nm) in the mixture $HgBr_2$:Ne = 0.8:100 kPa. Pump pulse repetition rate f = 1 kHz.

3.10.5. Discussion of research results

The appearance of spectral band emissions with a maximum wavelength of λ = 502 nm of the electron-vibrational transition $B^2\Sigma^+_{1/2} \rightarrow X^2\Sigma^+_{1/2}$ of the exciplex HgBr* molecule in gas-discharge plasma in a mixture of mercury dibromide vapor with neon occurs due to processes leading to the formation and destruction of the $B^2\Sigma^+_{1/2}$ state of mercury monobromide. The main processes are given in [36, 42, 43]:

(3.36) $HgBr_2+e \rightarrow HgBr^*+ \begin{cases} Br+e \\ Br^- \end{cases}$

(3.37)

(3.38) $HgBr^* \rightarrow HgBr+h\nu$

(3.39) $HgBr^*+M \rightarrow HgBr+M+\Delta E$

The kinetic equation for the population of the $B^2\Sigma^+_{1/2}$ states of HgBr* is:

$$\frac{d[HgBr\ ^*]}{dt} = k_D\,[HgBr_2][N_e]-\tau_r^{-1}\,[HgBr^*]-k_Q\,[HgBr^*][M] \quad (3.40)$$

where k_D is the rate constant for the dissociation of $HgBr_2$ molecules by electron impact; τ_r is the radiation lifetime of the $B^2\Sigma^+_{1/2}$ state of HgBr *; k_Q is the quenching rate constant of the $B^2\Sigma^+_{1/2}$ state of HgBr*; [HgBr*], [$HgBr_2$], [N_e], and [M] are the concentrations of HgBr*, $HgBr_2$, electrons and quenching molecules and atoms ($HgBr_2$, Ne), respectively.

For the quasi-stationary case in equation (5), the emission intensity is:

$$I_{HgBr^*}^{-1} = \alpha(1+k_Q \tau_r [M]) \qquad (3.41)$$

where $\alpha = (k_D h\nu [HgBr_2][N_e])^{-1}$

The sharp increase in intensity from the part of the spectrum with long wavelengths and its slow decrease in the short-wavelength region (Fig. 2) can be explained by the progress of potential curves (the excited $B^2\Sigma^+_{1/2}$ state shifts towards large internuclear distances relative to the $X^2\Sigma^+_{1/2}$ state) and processes of relaxation of the population of the upper vibrational levels of the excited electronic state, which occur faster than the electronic-vibrational transition to the ground $X^2\Sigma^+_{1/2}$ state [3, 22, 24].

The dependency of the brightness of the HgBr* exciplex molecule on the partial pressure of neon (Fig. 3.37) was caused primarily by the following processes: an increase in the electron concentration with an increase in the partial pressure of neon in the mixture; a change in the fraction of the discharge energy that is spent on heating the working mixture; a change in mean electron energy and the rate constant of the excitation of mercury monobromide depending on the values of the parameter E/N; and the quenching process of the $B^2\Sigma^+_{1/2}$ state of the HgBr* molecule in collisions with neon atoms [1, 3]. With an increase in the partial pressure of neon in the mixture, the value of the parameter E/N decreases. This leads to an increase in the specific discharge power losses in the elastic scattering of electrons on neon atoms and mercury dibromide molecules, leading to heating of the mixture and, accordingly, to an increase in the partial pressure of the mercury dibromide vapor and the radiation intensity of exciplex HgBr* molecules. In addition, an increase in the electron

concentration, which increases with an increase in the concentration of the components of the working mixture, also contributes to an increase in the brightness of the radiation with an increase in the partial pressure of neon [1]. The presence of a maximum and then a decrease in the emission brightness of the exciplex HgBr* molecules with an increase in the neon partial pressure was caused by the process of quenching this state of mercury monobromide molecules through collision with neon atoms [3].

$$HgBr^* + Ne \rightarrow HgBr + Ne + \Delta E \qquad (3.42)$$

where ΔE is the energy difference in the reaction.

Above a certain value of the partial pressure of neon, the quenching process (3.42) plays a large role in connection with which the radiation brightness decreases. The rate constant of this was $<3.4 \cdot 10^{-14}$ cm^3/s [34].

The oscillatory structure of the current pulse (Fig. 3.38a) was caused by the charging and discharging of the dielectric capacitance during a voltage pulse with an amplitude sufficient to break the discharge gap [75]. The difference in the form of current pulses at the front and trailing edge was associated with opposite directions of current flow through the gas-discharge gap (14 mm). As a result, unequal charge resorption conditions appeared on the inner dielectric surface under the conditions of the barrier discharge used in our experiment.

The regularity of the difference in the amplitudes of the first and second radiation pulses (Fig. 3.38b) can be explained as follows. The first and second pump pulses (current) form mercury monobromide molecules in the $B^2\Sigma^+_{1/2}$ and $X^2\Sigma^+_{1/2}$ states due to the dissociation of mercury dibromide molecules upon collision with electrons. The second pump pulse (current)

leads to an additional increase in the population of the $B^2\Sigma^+_{1/2}$ state of mercury monobromide molecules due to the process:

$$e+HgBr(X^2\Sigma^+_{1/2})\rightarrow e+HgBr(B^2\Sigma^+_{1/2}) \qquad (3.43)$$

with HgBr ($X^2\Sigma^+_{1/2}$) mercury monobromide molecules in the ground state. These do not have time to recover into a triatomic molecule (mercury dibromide) in the inter-pulse period (150 ns) of the process:

$$HgBr(X^2\Sigma^+_{1/2})+Br+Ne\rightarrow HgBr_2+Ne \qquad (3.44)$$

leading to an increase in the amplitude of the second radiation pulse.

The second regularity (an increase in the amplitudes of both radiation pulses with an increase in the neon partial pressure) may be associated with a decrease in the parameter E/N, which leads to an increase in the excitation rate constant of the $B^2\Sigma^+_{1/2}$ state of mercury monobromide molecules (Fig. 4.32, Chapter 4) and a consequent increase in the amplitudes of the radiation pulses.

3.11. Conclusions to Chapter 3

1. In a low-temperature plasma based on mixtures of mercury dibromide vapor with nitrogen, sulfur hexafluoride, and helium, created by a barrier discharge, the exciplex HgBr* molecule was efficiently excited at pulse repetition rates of 3 to 9 kHz.

2. Studies into the radiation spectra of discharges in two, three and four-component mixtures of mercury dibromide vapor with helium, argon, neon, nitrogen,sulfur hexafluoride show us that the $B^2\Sigma^+_{1/2}$ state of the exciplex molecule HgBr* is effectively excited in the barrier discharge and at high

repetition rates. The difference in the value of radiation intensity for the wavelength $\lambda = 502$ nm in a system of spectral bands is associated with the additional mechanisms (in addition to the dissociative excitation of mercury dibromide molecules by electrons) of the population of $B^2\Sigma^+_{1/2}$ states of exciplex HgBr* molecules. At higher frequencies (120 kHz), the fragmentation of mixture components was observed and the mercury monobromide molecules did not have time to recover to mercury dibromide molecules and decompose into mercury and bromine atoms through collisions with electrons.

3. Optimal conditions for the formation and emission of HgBr* and XeBr* exciplexes in the visible ($\lambda_{max.} = 502$ nm) and ultraviolet ($\lambda_{max.} = 281$ nm) spectral regions were detected in a discharge in a mixture of mercury dibromide vapor, krypton and xenon. The optimal temperature range was found at which simultaneous emission of exciplex molecules HgBr* and XeBr* could be observed.

4. The conditions for the formation and emission of HgBr* and KrBr* exciplexes in the visible ($\lambda_{max.} = 502$ nm) and ultraviolet ($\lambda_{max.} = 207$ nm) spectral regions were revealed in a discharge in a mixture of mercury dibromide vapor, krypton and helium. This allowed us to establish the formative mechanism of exciplex molecules of krypton bromide.

5. In all mixtures, an increase in the radiation power to a maximum value was observed, and subsequently, with increasing partial pressure of the mixture components, the radiation power decreased.

6. The dependency of the radiation power of exciplex molecules HgBr* on the partial pressure of the components of the mixture was related to the following processes: an increase in the electron concentration with increasing partial pressure of He, Ar, Ne, N_2, SF_6, and $HgBr_2$ in the mixture; a change in the fraction of the discharge energy consumed in heating the

working mixture; the change in the mean electron energy; the rate constant of excitation of HgBr* exciplex as a function of the value of the parameter E/N; and the quenching of the $B^2\Sigma^+_{1/2}$ state of HgBr* molecules through collision with helium atoms, nitrogen molecules, sulfur hexafluoride and mercury dibromide.

7. The quenching efficiency of HgBr* by nitrogen molecules, sulfur hexafluoride and mercury dibromide was determined to be within the range $(0.04 \pm 0.01–71.1 \pm 14.2) \times 10^{-16}$ m^3/s.

8. With an increase in the energy stored in the capacitance 7 pF dielectric, from 0.1 mJ/cm^3 to 0.8 mJ/cm^3, the average radiation power for all mixtures increased proportionally. The rate of increase in the radiation power from the energy stored in the dielectric capacitance for each mixture was different. This was due to various redistributions of the discharge energy into elastic and inelastic processes occurring in the plasma, depending on the composition of the mixture. A proportional increase in the radiation power was also observed with a change in the pulse repetition frequency from 3 kHz to 9 kHz. The highest values of average and pulsed radiation power were achieved for the discharge in the four-component mixture $HgBr_2$:SF_6:N_2:He, which reached 48.8 ± 2.9 mW and 40.6 ± 6.5 W in the self-heating mode, respectively, with an efficiency of ≤ 10 %. With external heating of this mixture, the average power reached a maximum value of ~480 ± 29 mW.

9. A significant increase in the radiation power of exciplex HgBr* molecules in a discharge in mercury dibromide vapor with sulfur hexafluoride, nitrogen and helium mixtures can be explained by the quenching of the overlying energy states ($C^2\Pi_{1/2}$ and $D^2\Pi_{3/2}$) of mercury monobromide and the transfer of their population to the $B^2\Sigma^+_{1/2}$ state.

10. The amplitude of the radiation pulses and their half-width were higher in a four-component mixture in comparision to those achieved when using a two-component mixture. This regularity was caused by the quenching processes of the overlying energy states $C^2\Pi_{1/2}$ and $D^2\Pi_{3/2}$ of mercury monobromide by molecules of sulfur hexafluoride and nitrogen with a transfer of the population to the $B^2\Sigma^+_{1/2}$ state, leading to an increase in the pulse amplitude in three and four-component mixtures in comparison to two-component mixtures.

11. The use of a special heat-insulating element in the structure of the device of the radiator, namely, an additional housing in a transparent cuvette to examine the visible and ultraviolet radiation, saw an increase in the radiation power for all mixtures of 40 %. The efficiency for a four-component mixture reached ~10 %.

CHAPTER 4

PARAMETERS AND CHARACTERISTICS OF GAS-DISCHARGE PLASMA IN MIXTURES OF MERCURY DIBROMIDE VAPOR WITH ATOMIC AND MOLECULAR GASES

The third chapter described our investigations into the optical characteristics of gas-discharge plasma in mixtures of mercury dibromide vapor with helium, argon, neon, nitrogen, sulfur hexafluoride, xenon and krypton. Because of methodical and technical difficulties, measurements of the parameters and characteristics were not carried out. These included: the electron energy distribution; mean electron energy; electron temperature, drift velocity, and concentration; and the efficiency of elastic and inelastic processes of electron collisions with the components of the working mixtures. Additionally, the power losses in the discharge, including the excitation, ionization, attachment and elastic scattering of electrons by atoms and molecules that are the part of plasma working mixtures, were unable to be measured. The measurement of these parameters and the characteristics of plasma in the mixtures being studied at atmospheric pressures is a complex task, both methodologically and technically [100]. As such, we used a theoretical method to establish data on the characteristics and parameters of the plasma, which was then successfully tested in discharges using other mixtures of mercury dihalide vapor with gases [30–32, 48, 49, 87, 101]. According to this method, the parameters and

characteristics of gas-discharge plasma were determined on the basis of the known electron energy distribution function (EEDF). To determine the EEDF, the Boltzmann kinetic equation was used for the quasi-stationary electron energy distribution function [1, 3, 101]:

$$\frac{\partial f}{\partial t} + \mathbf{v}\cdot\nabla_r f - \frac{e}{m}\cdot\mathbf{E}\cdot\nabla_v f = C[f] \qquad (4.1)$$

where f is the electron distribution function in six-dimensional phase space; v is the coordinates of velocity; *e* is the elementary charge; *m* is the electron mass; E is the electric field strength; ∇_r is the gradient operator; ∇_v is the velocity gradient operator; and C is the change in velocity in the EEDF due to collisions.

The kinetic Boltzmann equation (4.1) for the quasi-stationary electron energy distribution function is used for experimental conditions in which the plasma medium is spatially homogeneous, characterized by the constancy of the component composition and in an electric field where the intensity does not change during the time of establishing the electron energy distribution function [1, 3, 101]. These experimental conditions are describe for our experiments in Chapters 2 and 3.

4.1. Results of numerical calculations and their discussion

The parameters of the plasma in the barrier discharge in mixtures of mercury dibromide vapor and gases were determined numerically and calculated as complete integrals of the electron energy distribution function in the discharge for mixtures with optimal component ratios for obtaining maximum radiation power. These were: $HgBr_2$:He (0.5:99.5 %); $HgBr_2$:Ar

(0.5:99.5 %); $HgBr_2$:Ne (0.5:99.5 %); $HgBr_2$:N_2:He (0.6:3.3:96.1 %); $HgBr_2$:SF_6:He (0.6:0.06:99.34 %); $HgBr_2$:SF_6:N_2:He (0.6:0.06:3.3:96.14 %); $HgBr_2$:Xe:Kr (0.3:8:91.7 %); and $HgBr_2$:Kr:He (0.0009:8.3999:91.5992 %). In addition, the rate constants of elastic and inelastic scattering of electrons by molecules and atoms (the components of the mixture) and the power losses of the electric discharge in different elementary processes in the plasma were determined for different values of the parameter E/N (where E/N was the ratios of the electric field strength (E) to the total concentration of the mixture components (N)) in the parameter range E/N = 1–100 Td ($1 \cdot 10^{-17}$–$1 \cdot 10^{-15}$ V·cm^2). The range of the change in the parameter E/N included all the values of the parameter E/N that were realized in the experiment.

Calculation of the electron energy distribution function, as well as the plasma parameters, were carried out using the freely available software program BOLSIG+ on the Internet [95].

For the value of the integral of electron collisions with molecules of helium, argon, neon, krypton, xenon, sulfur hexafluoride and nitrogen, processes from the Bolsig+ database were used. These were the following: elastic scattering and excitation of energy states of helium atoms (2^3S, 2^1S, 2^3P, 2^1P, 3SPD, 4SPD, 5SPD); argon atoms with threshold energies of 11.623 eV, 12.906 eV, and 11.273 eV; neon atoms with threshold energies of 16.62 eV, 16.67 eV (1s4), 16.84 eV (1s2), 18.72 eV (2p), 20.0 eV (2s + 3d), and 20.65 eV (3p); excitation of electronic states of krypton atoms with threshold energies of 9.5 eV, 10 eV, and 11 eV; excitation of electronic states of xenon atoms with threshold energies of 3.4 eV, 8.31 eV, 8.44 eV, 9.69 eV, 10.0 eV, 11.0 eV and 11.7 eV; and the ionization of helium, krypton and xenon atoms. For elastic excitation and excitation of energy states of sulfur hexafluoride molecules, the following were taken from the

Bolsig+ database: excitation of the first vibrational state of the ground electronic state; excitation of electronic states with threshold energies of 10.0 eV, 11.7 eV, 15.0 eV and 15.7 eV; ionization and electron attachment to SF_6 molecules; dissociative attachment of electrons to sulfur hexafluoride molecules with the formation of SF^-_5 ions; dissociative excitation of SF_6 molecules with the formation of negative ions other than SF^-_5. For the elastic scattering and excitation of energy states of nitrogen molecules, the following were taken into account: vibrational $\upsilon = 1–8$; lower electron $A^3\Sigma^+_u$ $\upsilon = 0–4$; $\upsilon = 5–9$; $\upsilon = 10$; $B^3\Pi_g$; $B^3\Sigma^-_g$; $A^1\Sigma^-_u$; $A^1\Pi_g$; $W^1\Delta_u$; $C^3\Pi_u$; $E^3\Sigma^+_g$; A^1 (threshold 12.25 eV); the sum of singlet states with energy above the threshold 13 eV; and the ionization of nitrogen molecules [95]. The interaction processes of electrons and mercury dibromide molecules were taken into account, including: vibrational excitation of $HgBr_2$ molecules, with scattered electron energy equal to 0.0035 eV; resonant vibrational excitation of $HgBr_2$ molecules, with scattered electron energy equal to 0.25 eV; dissociative excitation of electronic states of mercury monobromide ($X^2\Sigma^+_{1/2}$, $B^2\Sigma^+_{1/2}$); excitation of the electronic state of mercury dibromide ($HgBr_2$ (D)) with an electron threshold energy of 7.9 eV, attachment, and ionization. Data on the absolute values of the effective cross-sections of these processes, as well as their dependency on electron energy, were taken from [30, 31, 42, 43].

The numerical calculation of mean electron energies makes it possible to determine their temperature in gas-discharge plasma from the well-known formula [1]:

$$\varepsilon = 3/2 \cdot kT \qquad (4.2)$$

where ε is the electron energy; k is the Boltzmann constant; and T is the temperature in degrees Kelvin.

The electron concentration (N_e) was calculated from the formula [1]:

$$N_e = j/e \cdot V_{dr.} \quad (4.3)$$

where j is the current density in the discharge; e is the electron charge; and $V_{dr.}$ is the drift velocity of electrons.

The electron drift velocity was determined from the expression [1]:

$$V_{dr.} = \mu_e \cdot E \quad (4.4)$$

where μ_e is the electrons mobility and E is the field strength acting on the plasma.

The field strength acting on the plasma E was calculated by the formula:

$$E = U_{pl.}/d \quad (4.5)$$

where $U_{pl.}$ is the voltage acting on plasma and d is the discharge gap.

The voltage acting on plasma was estimated from the expression:

$$U_{pl.} = U \cdot C_{dl.}/(C_{pl.}+C_{dl.}) \quad (4.6)$$

where U is the amplitude of the voltage pulse applied to the electrodes of the radiator; $C_{dl.}$ is the capacitance of the dielectric surface; and $C_{pl.}$ is the capacitance of the plasma gap.

The results of the calculations are published in [52–54, 57, 58, 60, 61, 63, 65, 66, 69, 102, 103].

4.1.1. Transport and energy characteristics of plasma in a mixture of mercury dibromide vapor with helium. The rate constants of electron collision processes with the components of the mixture

In Figure 4.1, the characteristic shape of the EEDF is shown for a change in the parameter E/N in the range 1–100 Td. An increase in the E/N parameter led to an increase in the number of "fast" electrons in the discharge and a decrease in the electron density in the working range of the radiator (E/N = 3–30 Td). Mean energy of the discharge electrons most strongly depended on the value of the parameter E/N = 1–20 Td, which increased linearly from 1 to 6 eV. In the range of the parameter E/N = 20–100 Td, mean electron energy also increased from 6 to 12 eV, but at a lower rate.

The electron temperature increased from 11,600 K to 139,200 K with a change in the E/N parameter from 1 to 100 Td, respectively.

The mobility of electrons (Figure 4.2) decreases sharply in the range of values of the parameter E/N (1 Td) from $4.5 \cdot 10^{24} \cdot N$ (1/m/V/s) and varies slightly within the range $2.2 \cdot 10^{24} \cdot N$–$2.3 \cdot 10^{24} \cdot N$ (1/m/V/s) when changing the E/N parameter in the range 10–100 Td. This gives values for electron drift velocity ranging from $74.4 \cdot 10^4$ m/s to $37.2 \cdot 10^4$ m/s for the amplitude of the voltage pulse 8 kV (with an electric field strength acting on the plasma of $31 \cdot 10^5$ V/m and an electron concentration of $3.9 \cdot 10^{17}$ m^{-3}–$7.8 \cdot 10^{17}$ m^{-3} at a current density through the gas-discharge gap of the radiation source of 4.7 A/cm^2 (on the surface of the inner electrode (S = 1.9 cm^2)).

The distribution of power losses in the discharge of the main processes, with a change in the value of the parameter E/N in the range 1–100 Td, is shown in Figure 4.3a. In the dissociative excitation of mercury monobromide molecules, discharge power losses increased as the E/N

parameter increased, reaching maxima of 14 %, 35 % and 49 % for the electronic states of mercury monobromide $B^2\Sigma^+_{1/2}$, mercury monobromide $X^2\Sigma^+_{1/2}$, and mercury dibromide $HgBr_2(D)$, respectively. With a further increase in the parameter E/N, they decreased. The rate of change in the discharge power losses in these processes and their magnitudes are related to the nature of the dependency of the effective excitation cross-sections of specific states; the electron energies; their absolute magnitudes; the dependency of the electron distribution function for different values of the parameter E/N; and on the threshold energy of the dissociative excitation of electronic states of mercury monobromide molecules. The dependency of discharge power losses on vibrational excitation; the dissociative attachment of electrons to mercury dibromide molecules; and the elastic scattering of

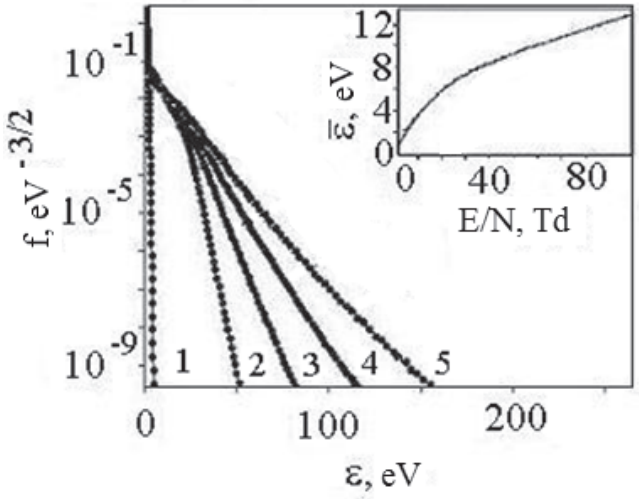

Figure 4.1. Electron energy distribution functions in discharge acting on the mixture $HgBr_2$:He = 0.5:99.5 % at E/N = 1 (1); 25.8 (2); 55.5 (3); 75.3 (4); and 100 Td (5). Insert: the dependency of mean electron energy on the parameter E/N [52].

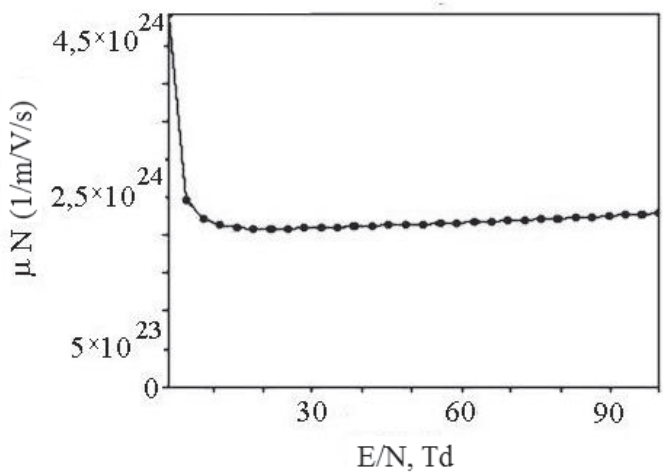

Figure 4.2. The dependency of the reduced mobility of electrons on the parameter E/N for the mixture $HgBr_2$:He = 0.5:99.5 % [52].

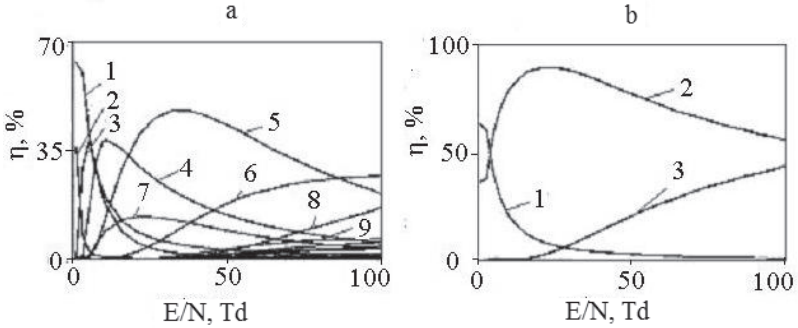

Figure 4.3. a). The dependency of specific power losses on the main electronic processes in the mixture as a function of the parameter E/N: vibrational excitation of mercury dibromide molecules (1); elastic scattering of electrons by helium atoms (2); resonant vibrational excitation of mercury dibromide molecules (3); dissociative excitation of electronic states of mercury monobromide molecules $X^2\Sigma^+_{1/2}$ (4) and mercury dibromide (D) (5); ionization of mercury dibromide molecules (6); dissociative excitation of the $B^2\Sigma^+_{1/2}$ state of mercury monobromide molecules (7); ionization of helium atoms (8); excitation of helium atoms 2^3S state (9). b).

Dependency of the total specific losses of discharge power on the parameter E/N: elastic scattering of electrons (1); inelastic processes: dissociative excitation of energy states of mercury monobromide molecules; vibrational excitation of mercury dibromide molecules and excitation of energy states of helium atoms (2); ionization of mercury monobromide molecules and helium atoms (3) [52].

electrons by helium atoms were significant only at E/N<10 Td. With an increase in the parameter E/N (>10 Td), they decreased sharply. The losses of discharge power in the ionization processes of the discharge were most strongly manifested in the ionization of mercury dibromide molecules. This is due to the smaller value of its ionization potential in comparison to that of helium atoms. The losses of discharge power in the ionization of mercury dibromide molecules began to increase sharply at values of the parameter E/N>20 Td. For E/N>40 Td, they became higher than the power losses of the discharge in the excitation of the $B^2\Sigma^+_{1/2}$ state of mercury monobromide. The losses of discharge power in inelastic processes for helium were noticeable at E/N>30 Td. Their values in the excitation of electronic states did not exceed 7 %; for ionization this was 14 % (E/N = 100 Td). Low losses of discharge power in the inelastic collision of electrons with helium atoms, in comparison to losses in the inelastic collision of electrons with mercury dibromide molecules, were associated with lower absolute values of effective cross-sections of these processes in conjunction with higher energy values and thresholds. The total energy losses of the gas-discharge plasma (Figure 4.3b) in inelastic processes, in terms of the dissociative excitation of energy states of mercury monobromide molecules; the excitation of vibrational energy states of mercury dibromide molecules; and the excitation of electron energy states of helium atoms, increased from the values of the parameter E/N = 1 Td, reached a maximum at E/N = 20–30

Td, reached 90 % and then monotonically decreased to 50 % at E/N = 100 Td. The total energy losses of the gas-discharge plasma during ionization linearly increased with values of the parameter E/N = 10 Td to 100 Td and reached 40 %. Losses in the elastic collision process decreased exponentially from 60 % for low values of the parameter (E/N = 1 Td) and to several percentages in the range of the parameter values E/N = 100 Td. The losses of discharge power in the attachment of electrons to mercury dibromide molecules were insignificant. Even at values of the parameter E/N = 1–20 Td, they did not exceed 1 % of the total losses.

Figure 4.4 presents the results of numerical calculation of the rate constants of the following processes: dissociative excitation of electronic states of mercury monobromide ($X^2\Sigma^+_{1/2}$ and $B^2\Sigma^+_{1/2}$) and states of mercury

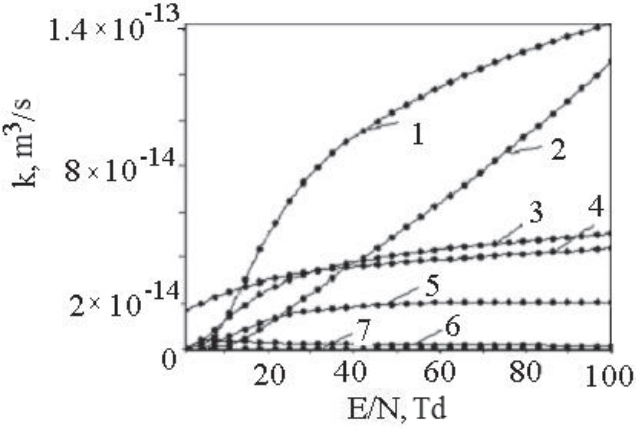

Figure 4.4. Rate constants of the collision of electrons with molecules of mercury dibromide in gas-discharge plasma acting on the mixture $HgBr_2$:He (0.5:99.5 %) at a total pressure of 120 kPa: 1 - excitation of $HgBr_2$ molecule D-state; 2 - ionization of $HgBr_2$ molecules by electrons; 3 - dissociative excitation of HgBr* molecule $X^2\Sigma^+_{1/2}$ state; 4 - vibrational excitation of $HgBr_2$ molecules; 5 - dissociative excitation of HgBr* molecule $B^2\Sigma^+_{1/2}$ state; 6 - resonance vibrational excitation of $HgBr_2$ molecules; and 7 - electron attachment to $HgBr_2$ molecules [52].

dibromide (D); vibrational excitation of mercury dibromide molecules by electrons; dissociative attachment of electrons to mercury dibromide molecules; and ionization of mercury dibromide molecules by electrons for the mixture $HgBr_2$:He (0.5:99.5) % in the component ratio at which the maximum emission power of the spectral band $\lambda_{max} = 502$ nm of the exciplex molecule HgBr* was observed. The rate constants were characterized by high values $k \approx 10^{-14}$–10^{-13} m^3/s, which are connected to the large value of the absolute effective cross-sections of the corresponding processes. In the range of the parameter E/N = 1–100 Td, the excitation constants of the D-state of mercury dibromide and the ionization of mercury dibromide by electrons increased from 10^{-15} to 10^{-13} m^3/s. In the vibrational excitation of mercury dibromide molecules and dissociative excitation of the $X^2\Sigma^+_{1/2}$ and $B^2\Sigma^+_{1/2}$ states of mercury monobromide molecules by electrons, the rate constants increased from 10^{-15} to 10^{-14} m^3/s. For the dissociative attachment of electrons to mercury dibromide molecules, the rate constants increased from 10^{-17} to 10^{-16} m^3/s. In the range of the parameter E/N = 10–40 Td, in which the radiation source operates, the rate constant of $B^2\Sigma^+_{1/2}$ state excitation had a value of $1 \cdot 10^{-14}$ m^3/s, which is a quantitative measure of the excitation efficiency of exciplex HgBr* molecules in the working mixture of the radiation source.

4.1.2. Transport and energy characteristics of plasma in a mixture of mercury dibromide vapor with nitrogen and helium. The rate constants of electron collision processes with the components of the mixture

Figure 4.5 shows the characteristic form of the EEDF when the parameter E/N is in the range 1–100 Td. The increase in the parameter E/N led to an increase in the number of “fast” electrons in the discharge and a decrease in the electron density in the range of the emitter (E/N = 3–30 Td).

Mean energy of the discharge electrons (Figure 4.5) depended most strongly on the parameter E/N = 8–20 Td, while it increased linearly from 1.5 to 5 eV. In the range of the parameter E/N = 20–100 Td, mean electron energy also increased from 5 to 11 eV, but at a lower rate. The slower growth of mean electron energies in the region of the parameter E/N = 1–8 Td is caused by the energy loss of electrons upon excitation of the vibrational energy levels of nitrogen molecules.

Electron temperatures increased from 5,800 K to 127,600 K when the parameter E/N varied from 1 to 100 Td, respectively.

The reduced electron mobility, as shown in the data of the numerical calculation (Figure 4.6), varies within $4.9 \cdot 10^{24} \cdot N$–$2.0 \cdot 10^{24} \cdot N$ (1/m/V/s), when the parameter E/N varies in the range 1–100 Td.

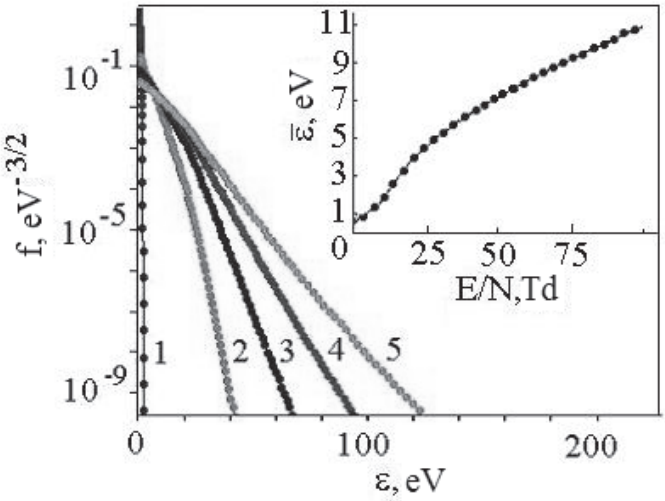

Figure 4.5. Electron energy distribution functions in the discharge for the mixture $HgBr_2$:N_2:He = (0.6:3.3:96.1) % for the following values of the parameter E/N: 1 (1); 25.8 (2); 50.5 (3); 75.3 (4); 100 (5) Td. The insert shows the dependency of the mean electron energy on the parameter E/N [54].

This gives electron drift velocity values of $92.3 \cdot 10^4$ m/s and $39.1 \cdot 10^4$ m/s, respectively, for a field strength acting on the plasma of $35.5 \cdot 10^5$ V/m for a time instant of 150 ns from the beginning of the voltage pulse (the maximum value of the pulse amplitude [Chapter 3, Figure 3.5] and the value of the electron concentration of $3.9 \cdot 10^{17}$ m^{-3}–$9.1 \cdot 10^{17}$ m^{-3} at a current density of 5.7 A/cm^2 on the surface of the internal electrode of the radiation source (1.9 cm^2).

The distribution of specific power losses of the discharge in the main processes with a change in the value of the parameter E/N in the range 1–100 Td is shown in Figure 4.7a. In the dissociative excitation of mercury monobromide molecules, the discharge power losses increased with an increase in the parameter E/N. They reached maxima of 9.5 %, 18.9 % and 35.7 % for E/N parameters equal to 20 Td, 30 Td and 40 Td for electronic states of mercury monobromide $B^2\Sigma^+_{1./2}$, mercury monobromide $X^2\Sigma^+_{1/2}$, and mercury dibromide (D), respectively.

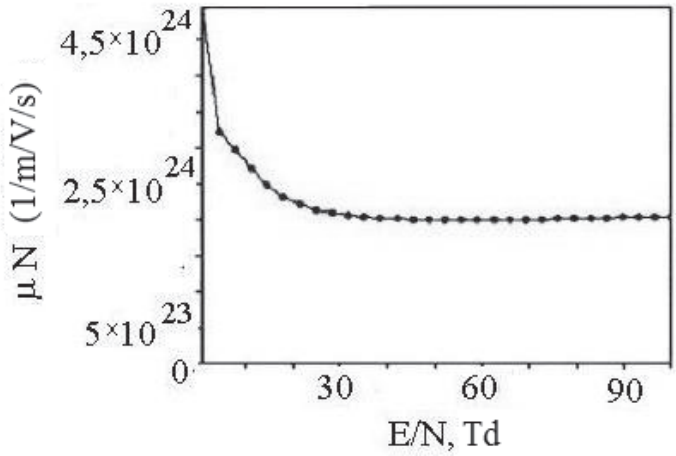

Figure 4.6. The dependency of reduced electron mobility on the parameter E/N for the mixture $HgBr_2$:N_2:He (0.6:3.3:96.1 %) [54].

With a further increase in the parameter E/N, they decreased. The rates of increase and decrease of the discharge power losses in these processes and their magnitudes are related to the nature of the dependency of the effective excitation cross-sections of specific states; the electron energies; their absolute magnitudes; the dependency of the electron distribution function on the parameter E/N; and the threshold energy of the dissociative excitation of the electronic states of mercury monobromide molecules. The losses of discharge power in the vibrational excitation of nitrogen molecules and mercury dibromide; the dissociative attachment of electrons to mercury dibromide molecules; and the elastic scattering of electrons by helium atoms were significant only at E/N<10 Td; with an increase in the parameter E/N>10 Td, they decreased sharply. The losses of discharge power in the excitation of the electronic states of nitrogen molecules were significant only for the $C^3\Pi_u$ states and the sum of singlet states (dependencies (7) and (8)). They were 5.8 % and 3.2 %, respectively, for values of the parameter E/N = 50 Td.

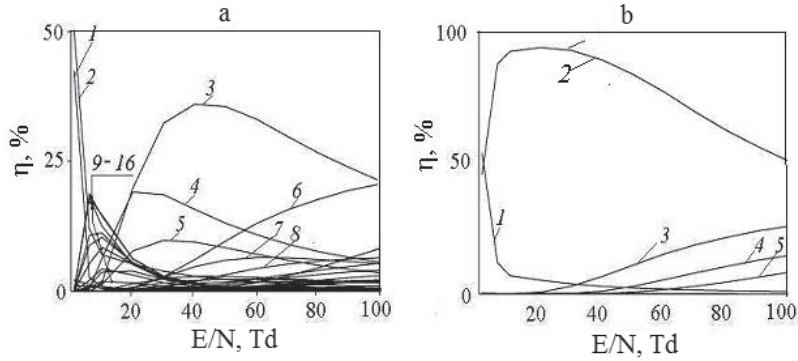

Figure 4.7. a). The dependency of power losses in the processes of electron collisions with mercury dibromide and nitrogen molecules and helium atoms as a function of the parameter E/N for discharges in the mixture $HgBr_2$:N_2:He = (0.6:3.3:96.1) %: the vibrational excitation of mercury dibromide molecules (1); the elastic scattering of electrons by helium atoms (2); the excitation of electronic states of mercury dibromide (D) (3); the dissociative excitation of electronic states of mercury dibromide molecules to form mercury monobromide in the states: $X^2\Sigma^+_{1/2}$ (4) and $B^2\Sigma^+_{1/2}$ (5); the ionization of mercury dibromide molecules (6); the excitation of an electron state $C^3\Pi_u$ of nitrogen molecules (7); the excitation of the sum of singlet states of nitrogen molecules (8); the excitation of vibrational states of the ground state ($X^2\Sigma^+_g$) of nitrogen molecules: ν = 2 (9), ν = 3 (10), ν = 1 (11), ν = 4 (12), ν = 5 (13), ν = 6 (14), ν = 7 (15), and ν = 8 (16). b). The dependency of the total specific power losses of the discharge on the parameter E/N in: the elastic scattering of electrons (1); the inelastic processes of collisions of electrons with molecules of mercury dibromide, nitrogen and helium atoms (2); the ionization of molecules: mercury dibromide (3), nitrogen (4) and the ionization of helium atoms (5) [54].

For other states of nitrogen molecules, these losses did not exceed 2 %. The losses of discharge power in ionization processes was most significant for the ionization of mercury dibromide molecules (dependency (6)). This is due to the low ionization potential of this molecule in comparison to the

ionization potential of the nitrogen molecule and the helium atom and the large effective ionization cross-section. The loss of discharge power in the ionization of mercury dibromide molecules began to increase sharply with parameter values E/N>20 Td; for E/N>45 Td they exceeded (9.5 %) the discharge power losses in the excitation of the $B^2\Sigma^+_{1/2}$ state of mercury monobromide. The losses of discharge power in inelastic processes for helium were noticeable for values of the parameter E/N>30 Td; their values in the excitation of electronic states did not exceed 1 %; for ionization this was 0.8 % at (E/N) = 100 Td. Low losses of discharge power in the inelastic collision of electrons with nitrogen molecules and helium atoms, in comparison to losses in the inelastic collision of electrons with molecules of mercury dibromide, were associated with lower absolute values of the effective cross-sections of these processes and large values in their threshold energies. The total energy losses of gas-discharge plasma (Figure 4.9b) in inelastic processes, in terms of the dissociative excitation of energy states of mercury monobromide molecules; the excitation of vibrational energy states of mercury dibromide molecules; the excitation of energy states of nitrogen molecules; the excitation of vibrational energy states of nitrogen molecules; and the excitation of electron energy states of helium atoms, increased from the value of the parameter E/N = 1 Td. They reached a maximum at E/N = 20–30 Td and 90 %, after which they decreased monotonically to 50 % at E/N = 100 Td. The total energy losses of gas-discharge plasma in ionization increased linearly in the range E/N = 20–100 Td, reaching 19 %. The losses in elastic collisions decreased exponentially from 55% for a low value of the parameter (E/N = 1 Td) and to several percentages in the range of the parameter E/N = 100 Td. The losses of the discharge power in the attachment of electrons to mercury dibromide

molecules were insignificant and even at values of the parameter E/N = 1–20 Td did not exceed 1 % of the total losses.

Figure 4.8 shows the results of numerical calculation of the rate constants for electron collisions with (a) mercury dibromide molecules and (b) nitrogen, which are a quantitative measure of the efficiency of these processes [32]. The efficiency of these processes for mercury dibromide molecules was higher. The values of the rate constant (k) were in the range $1 \cdot 10^{-14}$–$1.2 \cdot 10^{-13}$ m^3/s with an increase in the E/N parameter from 10 to 100 Td. This was caused by the higher absolute effective cross-sections of the corresponding processes in comparison to the data for nitrogen molecules [26–30]. In the range of the parameter E/N = 1–100 Td, the excitation rate constants of mercury dibromide D-state and the ionization of mercury dibromide by electrons (curves 1 and 2, Figure 7a) increased monotonically from $1 \cdot 10^{-15}$ to $1.2 \cdot 10^{-13}$ m^3/s and $1 \cdot 10^{-15}$ to $4 \cdot 10^{-14}$ m^3/s, respectively. The rate constants of the vibrational excitation processes of mercury dibromide molecules increased from $1 \cdot 10^{-15}$ to $4 \cdot 10^{-14}$ m^3/s. The same values were also reached for the rate constants of the dissociative excitation of the $X^2\Sigma^+_{1/2}$ and $B^2\Sigma^+_{1/2}$ states of mercury monobromide molecules. In the process of the dissociative attachment of electrons to molecules of mercury dibromide, they increased from values of $3 \cdot 10^{-18}$ m^3/s, reaching a maximum of $1.2 \cdot 10^{-16}$ m^3/s for parameter values E/N = 20–30 Td, after which they decreased to $1 \cdot 10^{-16}$ m^3/s as the parameter E/N increased to 100 Td. In the range of the parameter E/N = 10–40 Td, where the radiation source operates, the rate constant of the $B^2\Sigma^+_{1/2}$ state excitation of mercury monobromide increased smoothly from $1 \cdot 10^{-15}$ to $1.5 \cdot 10^{-14}$ m^3/s (dependency 5, Figure 4.10a).

The rate constants of the collision processes of electrons with nitrogen molecules (k) varied within the limits $1 \cdot 10^{-17}$–$5 \cdot 10^{-15}$ m^3/s (Figure 4.8b). The rate constants of the excitation of the vibrational levels v = 1–7 and the

rotational level ($E_{thr.}$ = 0.02 eV) of nitrogen molecules increased from $1 \cdot 10^{-17}$ m^3/s, reaching a maximum at $k = 4.3 \cdot 10^{-15}$ m^3/s, (for the excitation of the first vibrational level) with the parameter value E/N = 10–20 Td (dependencies 1, 10–15 and 2, respectively). After that, as the parameter E/N increased, an exponential fall in their values to $1 \cdot 10^{-16}$ m^3/s was observed. The rate constants of the excitation of the electronic states of nitrogen molecules increased sharply from $k \sim 1 \cdot 10^{-16}$ m^3/s to $6 \cdot 10^{-15}$ m^3/s

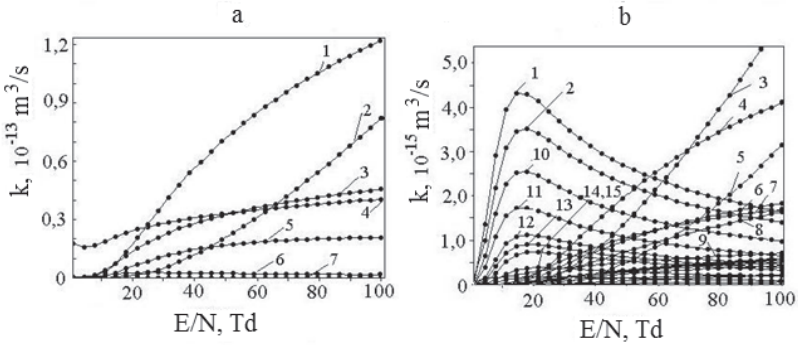

Figure 4.8. a) The rate constants of the collision of electrons with molecules of mercury dibromide in gas-discharge plasma in the mixture $HgBr_2$:N_2:He = (0.6:3.3:96.1) %: 1 - excitation of $HgBr_2$ molecules D-state; 2 - dissociative excitation of $X^2\Sigma^+_{1/2}$-state HgBr* molecules; 3 - ionization of $HgBr_2$ molecules by electrons; 4 - vibrational excitation of $HgBr_2$ molecules; 5 - dissociative excitation of $B^2\Sigma^+_{1/2}$-state HgBr* molecules; 6 - resonant vibrational excitation of $HgBr_2$ molecules; 7 - attachment of electrons to $HgBr_2$ molecules. b) The rate constants of collisions of electrons with nitrogen molecules: 1 - excitation of the vibrational level ν = 1 ($E_{thr.}$ = 0.2910 eV) of the ground state of $X^2\Sigma^+_g$; 2 - excitation of the rotational level ($E_{rot.}$ = 0.02 eV); 3 - excitation of the sum of singlet states; 4 - excitation of the electronic state of $C^3\Pi_u$; 5 - ionization of nitrogen molecules by electrons; 6, 7, 8, 9 - excitation of electronic states of nitrogen molecules $W^3\Delta_u$, $B^3\Sigma^-_g$, $A^1\Pi_g$, and 9-$A^3\Sigma^+_u$; 10, 11, 12, 13, 14, 15 - excitation of the vibrational levels of the ground electronic state $X^2\Sigma^+_g$ ν = 2, ν = 3, ν = 1 ($E_{thr.}$ = 0.29 eV), ν = 5, ν = 6, ν = 7, respectively [54].

in the growth region of the parameter E/N = 1–100 Td (curves 3, 4, 6). In the same region of the change of the parameter E/N, the rate constant of the ionization of nitrogen molecules (curve 5) also sharply increased from $1 \cdot 10^{-17}$ to $3 \cdot 10^{-15}$ m^3/s with an increase in E/N from 1 to 100 Td.

The excitation of helium atoms by electrons had smaller values for the rate constants compared to those for mercury dibromide and nitrogen molecules. They increased from $1 \cdot 10^{-18}$ to $1 \cdot 10^{-16}$ m^3/s in the range of the parameter E/N = 1–100 Td. The rate constant for ionization of helium atoms by electrons monotonically increased within the limits $1 \cdot 10^{-17}$ to $1.6 \cdot 10^{-16}$ m^3/s in the same parameter range of E/N = (1–100 Td). For the elastic scattering of electrons by helium atoms, the value of the rate constant was in the range $3 \cdot 10^{-14}$–$7 \cdot 10^{-14}$ m^3/s (E/N = 1–100 Td).

4.1.3. Transport and energy characteristics of plasma in a mixture of mercury dibromide vapor, sulfur hexafluoride and helium. The rate constants of electron collision processes with the components of the mixture

Figure 4.9 shows the characteristic shape of the EEDF when the parameter E/N is varied in the range 1–100 Td. An increase in the parameter E/N led to an increase in the number of "fast" electrons in the discharge. Mean energy of the discharge electrons most strongly depended on the parameter E/N = 1–20 Td, increasing from 1.37 to 5 eV. In the range of the parameter E/N = 20–100 Td, mean electron energy also increased from 5 to 10.26 eV, but at a lower rate.

The electron temperature increased from 15,892 to 119,016 K with an increase in the parameter E/N from 1 to 100 Td.

The reduced electron mobility (Figure 4.10) varied between $2.86 \cdot 10^{24} \cdot N$ and $2.15 \cdot 10^{24} \cdot N$ (1/m/V/s), with an increase in the parameter

E/N in the range 1–100 Td. This gave electron drift velocity values of $53.4 \cdot 10^4$ m/s and $40.2 \cdot 10^4$ m/s, respectively, with an electric field in the plasma of $35.5 \cdot 10^5$ V/m at time 150 ns from the start of the voltage pulse (maximum voltage value of the pulse amplitude (Figure 3.8, Chapter 3) and an electron concentration of $6.1 \cdot 10^{17}$ m^{-3}–$8.1 \cdot 10^{17}$ m^{-3}, with a current density of 5.26 A/cm^2 at the surface of the internal electrode of the radiation source (1.9 cm^2).

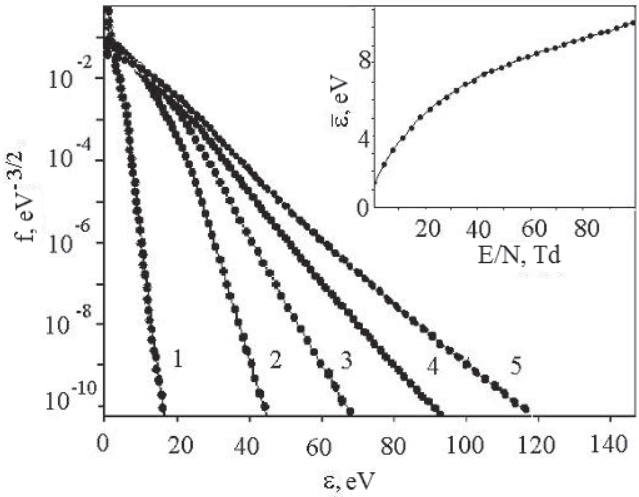

Figure 4.9. Electron energy distribution functions in the discharge for the mixture: $He:SF_6:HgBr_2 = 0.9934:0.0006:0.006$ at total pressure P = 117.17 kPa for the values of the parameter E/N: 1 (1), 25.8 (2), 50.5 (3), 75.3 (4), 100 (5) Td. The insert shows the dependency of mean electron energy on the parameter E/N [57].

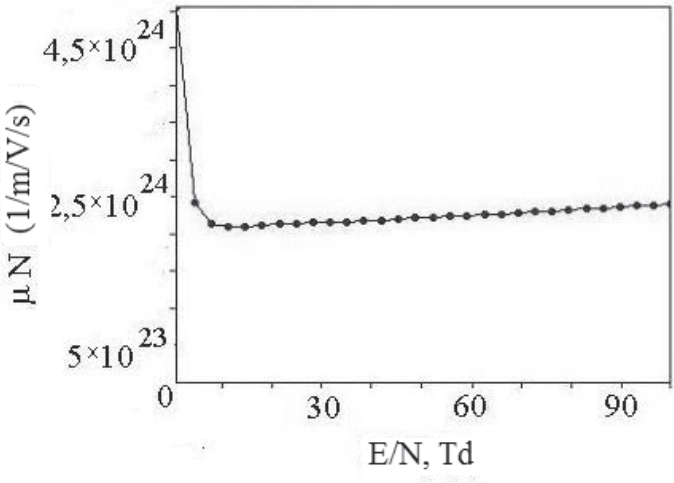

Figure 4.10. The dependency of the reduced mobility of electrons on the parameter E/N for the discharge in the mixture $He:SF_6:HgBr_2 = 0.9934:0.0006:0.006$ [57].

The distribution of specific power losses of the discharge in the main processes at a value of the parameter E/N in the range 1–150 Td are shown in Figure 4.11. In the dissociative excitation of mercury monobromide molecules, discharge power losses increased with an increase in the E/N parameter. They reached maxima of 39.5 %, 13.7 % and 47.0 % for the E/N parameter values 11 Td, 23 Td and 37 Td for electronic states of mercury monobromide $X^2\Sigma^+_{1/2}$, mercury monobromide $B^2\Sigma^+_{1./2}$, and mercury dibromide (D), respectively; with a further increase in the parameter E/N, they decreased. The rates of increase and decrease of the discharge power losses in these processes and their values are related to the nature of the dependency of the effective excitation cross-sections of specific states; the electron energies and their absolute values; and the dependency of the electron distribution function for different values of the parameter E/N in the threshold energy of the dissociative excitation of electronic states of

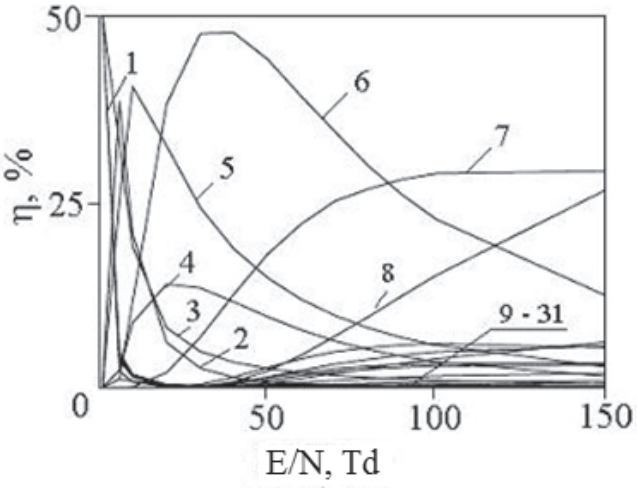

Figure 4.11. The dependency of specific power losses in the collisions of electrons with molecules of mercury dibromide, sulfur hexafluoride and helium atoms as the function of the parameter E/N in the mixture $HgBr_2$:SF_6:He = (0.6:0.1:99.3) % at total mixture pressure P = 117.17 kPa: vibrational excitation of mercury dibromide molecules (1); resonant vibrational excitation of mercury dibromide molecules (2); elastic scattering of electrons by helium atoms (3); dissociative excitation of electronic states of mercury dibromide molecules with formation of mercury monobromide in the states: $B^2\Sigma^+_{1/2}$ (4), $X^2\Sigma^+_{1/2}$ (5), and $D^2\Sigma^+_{1/2}$ (6); ionization of mercury dibromide molecules (7); ionization of helium atoms (8); other processes of electron collision with molecules of sulfur hexafluoride and helium atoms (9 to 31) [57].

mercury monobromide molecules. The losses of discharge power in the vibrational excitation of sulfur hexafluoride and mercury dibromide molecules; the dissociative attachment of electrons to mercury dibromide molecules; and the elastic scattering of electrons by helium atoms were significant only at E/N<5 Td; with an increase in the parameter E/N>5 Td, they sharply decreased. Losses of discharge power in the ionization of mercury dibromide molecules began to increase sharply at E/N>11 Td. For

E/N>43 Td they became higher than the values (13.7 %) of the discharge power losses in the $B^2\Sigma^+_{1/2}$ state excitation of mercury monobromide. In the ionization of helium atoms, they increased linearly, beginning with the value of the parameter E/N = 37 Td; at E/N = 150 Td they reached 26.3 %. The losses of discharge power in inelastic processes for sulfur hexafluoride molecules and the excitation of the energy states of helium atoms were noticeable at E/N>25 Td. Their value did not exceed 6.5 % at E/N = 100 Td. Low losses of discharge power in the inelastic collision of electrons with sulfur hexafluoride molecules and helium atoms, in comparison to the losses in inelastic collisions of electrons with mercury dibromide molecules, are associated with lower absolute values of the effective cross-sections of these processes and high energy values and thresholds.

Figure 4.12 presents the results of numerical calculation of the rate constants of electron collision processes with molecules of mercury dibromide, as a quantitative measure of the efficiency of these processes [29]. The value of the rate constants (k) for them was in the range $4\cdot10^{-17}$–$1.2\cdot10^{-13}$ m^3/s with an increase in the parameter E/N from 1 to 100 Td. This is due to higher values of the absolute effective cross-sections of the corresponding processes [26–30]. In the region of the parameter E/N = 1–100 Td, the excitation rate constants of the mercury dibromide (D) state and the ionization of mercury dibromide by electrons (curves 1 and 2, Figure 7) increased from $1\cdot10^{-15}$ to $1.2\cdot10^{-13}$ m^3/s and $1\cdot10^{-15}$ to $6\cdot10^{-14}$ m^3/s, respectively. In the vibrational excitation of mercury dibromide molecules and the dissociative excitation of $X^2\Sigma^+_{1/2}$ and $B^2\Sigma^+_{1/2}$ states of mercury dibromide molecules by electrons, the rate constants also increased from $1.7\cdot10^{-17}$ to $4.4\cdot10^{-14}$ m^3/s. In the dissociative attachment of electrons to mercury dibromide molecules, they increased from $4.3\cdot10^{-17}$ m^3/s, reaching a maximum $77.6\cdot10^{-17}m^3/s$ at E/N = 100 Td. In the range of the parameter

E/N = 10–40 Td, in which the radiation source operated, the rate constant of the $B^2\Sigma^+_{1/2}$ state excitation of mercury monobromide smoothly increased from $1\cdot10^{-15}$ to $1.5\cdot10^{-14}$ m^3/s (dependency 5).

The values of the rate constants of collision processes of electrons with sulfur hexafluoride molecules (k) varied within the range $1\cdot10^{-17}$–$3\cdot10^{-13}$ m^3/s in the range of the parameter E/N = 1–100 Td. The rate constant for the elastic scattering of electrons by SF_6 molecules was the largest, and in this range of the parameter E/N, it increased from $5.3\cdot10^{-14}$ to $3\cdot10^{-13}$ m^3/s.

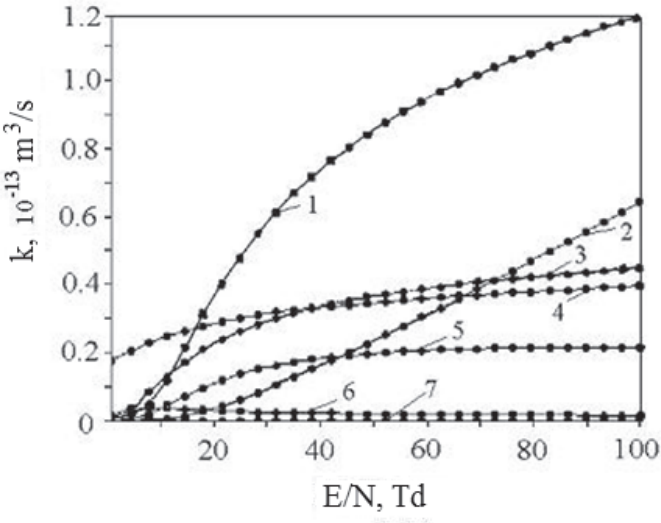

Figure 4.12. The rate constants of electron collisions with molecules of mercury dibromide in a gas-discharge plasma in the mixture $He:SF_6:HgBr_2$ = 0.9934:0.0006:0.006 at a total mixture pressure of P = 117.17 kPa: 1 - excitation $HgBr_2$ molecules (D) state; 2 - ionization of $HgBr_2$ molecules by electrons; 3 - dissociative excitation of $X^2\Sigma^+_{1/2}$-state HgBr* molecules; 4 - vibrational excitation of $HgBr_2$ molecules; 5 - dissociative excitation of $B^2\Sigma^+_{1/2}$-state HgBr* molecules; 6 - resonant vibrational excitation of $HgBr_2$ molecules; and 7 - attachment of electrons to $HgBr_2$ molecules [57].

The rate constant for the excitation of the first vibrational state with the threshold electron energy ($E_{thr.}$ = 0.1 eV) decreased smoothly from $4.5 \cdot 10^{-14}$ m^3/s to $2.3 \cdot 10^{-14}$ m^3/s. The rate constants of the excitation of the electronic states of sulfur hexafluoride molecules with threshold energy 10.0 eV, 11.7 eV, 15.0 eV and 15.7 eV increased sharply from $\sim 1 \cdot 10^{-16}$ m^3/s to $5.5 \cdot 10^{-15}$ m^3/s in the range of the parameter change E/N = 1 to 100 Td. In the same region of E/N variation, the rate constant of the ionization of SF_6 molecules also sharply increased from $1 \cdot 10^{-16}$ to $3.5 \cdot 10^{-15}$ m^3/s with an increase in the E/N parameter from 1 to 100 Td. The rate constant of electron attachment to SF_6 molecules decreased exponentially from $3.5 \cdot 10^{-15}$ m^3/s to $2 \cdot 10^{-16}$ m^3/s. For the process of dissociative attachment of electrons to SF_6 molecules, with the formation of a negative ion SF_5^-, the rate constant also decreased exponentially from $2.5 \cdot 10^{-15}$ m^3/s to $1 \cdot 10^{-16}$ m^3/s. For the sum of the processes of dissociative excitation of SF_6 molecules with the formation of negative ions other than SF_5^-, they increased from $1 \cdot 10^{-17}$ m^3/s to a maximum of $1.3 \cdot 10^{-16}$ m^3/s in the range of the E/N parameter 20–30 Td, and then decreased to $1.1 \cdot 10^{-16}$ m^3/s at E/N = 100 Td.

The values of the rate constants for the excitation of energy states of helium atoms by electrons were smaller than those for mercury dibromide and sulfur hexafluoride molecules. They increased exponentially from $\sim 1 \cdot 10^{-18}$ to $7 \cdot 10^{-17}$ m^3/s in the growth range of the E/N parameter from 1 to 100 Td. The rate constants of the ionization of helium atoms by electrons monotonically increased in the range $9 \cdot 10^{-18}$ to $9 \cdot 10^{-17}$ m^3/s in the same parameter range E/N (1–100 Td). In the elastic scattering of electrons by helium atoms, the value of the rate constant was in the range $4.5 \cdot 10^{-14}$–$8 \cdot 10^{-14}$ m^3/s (E/N = 1–100 Td).

4.1.4. Transport and energy characteristics of plasma in a mixture of mercury dibromide vapor, sulfur hexafluoride, nitrogen and helium. The rate constants of electron collision processes with the components of the mixture

Figure 4.13 shows the characteristic shape of the EEDF when the parameter E/N varies in the range 1–100 Td. An increase in the E/N parameter led to an increase in the number of "fast" electrons in the discharge and a decrease in the electron density in the range of the radiator (E/N = 3–30 Td). The average energy of the discharge electrons (see the insert in Figure 4.13) depended most strongly on the parameter E/N = 1–20 Td, and it increased linearly from 0.5 to 3.5 eV. In the range E/N = 20–100 Td, mean electron energy also increased from 3.5 to 10.1 eV, but at a lower rate. The electron temperature increased from 5,800 K to 117,160 K with an increase in the E/N parameter from 1 to 100 Td.

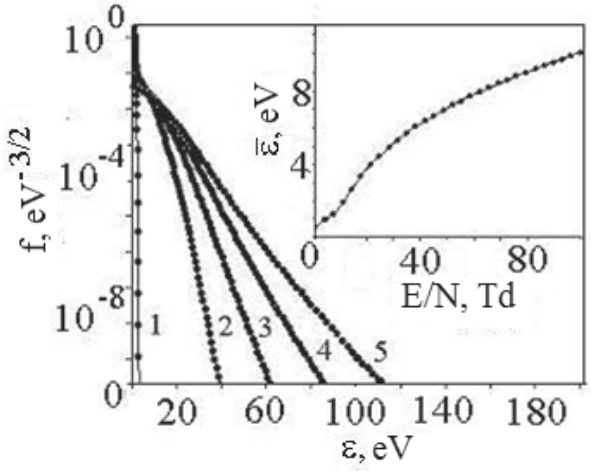

Figure 4.13. Electron energy distribution functions of the discharge in the mixture $HgBr_2$:SF_6:N_2:He = 0.7:0.07:4:117.2 kPa at a total mixture pressure P = 121.97 kPa and E/N parameters: 1 (1), 25.8 (2), 50.5 (3), 75.3 (4), and 100 (5) Td. The insert shows the dependency of mean electron energy on the parameter E/N [60].

Electron mobility (Figure 4.14) reduced, with an exponential change, in the range $5.5 \cdot 10^{24} \cdot N$–$2.0 \cdot 10^{24} \cdot N$ (1/m/V/s). With the increase of the parameter E/N in the range 1–35 Td, and in the range E/N = 35–100 Td, it reached saturation at $2.0 \cdot 10^{24} \cdot N$ (1/m/V/s), which corresponded to the electron drift velocity: $105 \cdot 10^4$ m/s and $37.5 \cdot 10^4$ m/s for E/N = 1-100 Td, respectively. The electric field strength acting on the plasma was $37.5 \cdot 10^5$ V/m for the maximum value of the voltage pulse amplitude (Figure 3.12, Chapter 3) and the electron concentration value of $2.9 \cdot 10^{16}$ m^{-3}–$8 \cdot 10^{17}$ m^{-3} at a current density of 4.8 A/cm^2 on the surface of the internal electrode of the radiation source (1.9 cm^2).

Figure 4.15 presents the rate constants for electron collisions with mercury dibromide molecules, which served as a quantitative measure of the efficiency of these processes [26].

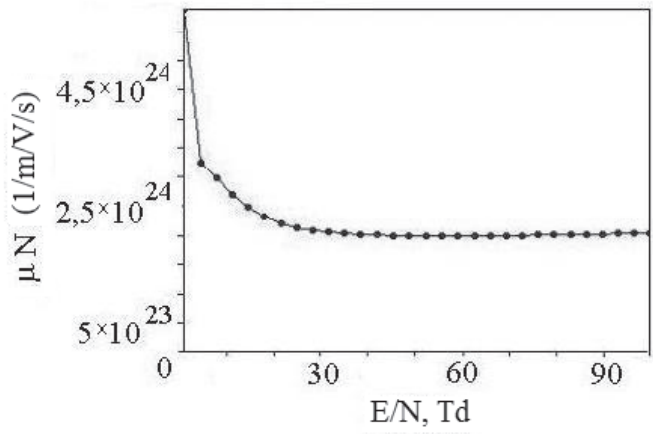

Figure 4.14. The dependency of electron mobility on the parameter E/N for the mixture $HgBr_2$:SF_6:N_2:He = 0.7:0.07:4:117.2 kPa [60].

The value of the rate constant (k) for them was in the range $2 \cdot 10^{-17}$–1.2 10^{-13} m^3/s with an increase in the parameter E/N from 10 to 100 Td. In the range of the parameter E/N = 1–100 Td, the rate constants for the excitation of the electronic state of mercury dibromide ($HgBr_2(D)$) and the ionization of mercury dibromide by electrons (curves 1 and 2, Figure 6) monotonically increased from $1 \cdot 10^{-15}$ to $1.2 \cdot 10^{-13}$ m^3/s and $1 \cdot 10^{-15}$ to $6 \cdot 10^{-14}$ m^3/s, respectively. The rate constants of the vibrational excitation of mercury dibromide molecules increased from $1 \cdot 10^{-17}$ to $4 \cdot 10^{-14}$ m^3/s. The rates of dissociative excitation of $X^2\Sigma^+_{1/2}$ and $B^2\Sigma^+_{1/2}$-state mercury monobromide molecules increased in the ranges ($1 \cdot 10^{-15}$–$4 \cdot 10^{-14}$ m^3/s) and ($1 \cdot 10^{-15}$–$2.2 \cdot 10^{-14}$ m^3/s) with an increase in the parameter E/N in the range 1–100 Td. For the process of dissociative attachment of electrons to mercury dibromide molecules, they increased from $9 \cdot 10^{-18}$ m^3/s, reaching a maximum of $1.2 \cdot 10^{-16}$ m^3/s for the parameter E/N = 20–30 Td, then dropped to $7.0 \cdot 10^{-17}$ m^3/s with an increase in the parameter E/N to 100 Td. In the range of the parameter E/N = 10–40 Td, the excitation constant of $B^2\Sigma^+_{1/2}$-state mercury monobromide molecules gradually increased from $1 \cdot 10^{-15}$ to 1.4 10^{-14} m^3/s (dependency 5, Figure 4.17).

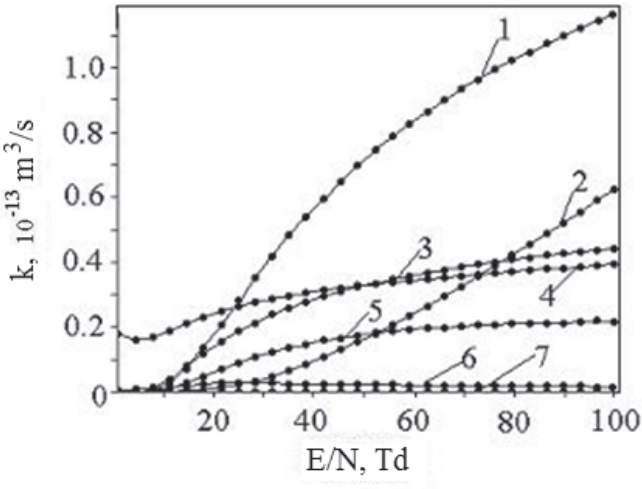

Figure 4.15. The dependencies of the rate constants of electron collisions with mercury dibromide molecules on the parameter E/N in a gas-discharge plasma in a mixture $HgBr_2$:SF_6:N_2:He = 0.7:0.07:4:117.2 kPa: 1 - excitation of the electronic state of mercury dibromide ($HgBr_2$(D)); 2 - ionization of $HgBr_2$ molecules by electrons; 3 - dissociative excitation of $X^2\Sigma^+_{1/2}$-state HgBr* molecules; 4 - vibrational excitation of $HgBr_2$ molecules; 5 - dissociative excitation of $B^2\Sigma^+_{1/2}$-state HgBr* molecules; 6 - resonant vibrational excitation of $HgBr_2$ molecules; and 7 - attachment of electrons to $HgBr_2$ molecules [60].

4.1.5. Transport and energy characteristics of plasma in a mixture of mercury dibromide vapor, xenon and krypton. The rate constants of electron collision processes with the components of the mixture

Figure 4.16 shows the characteristic shape of the EEDF when the E/N parameter is varied in the range 1–100 Td. An increase in the E/N parameter led to an increase in the number of "fast" electrons in the discharge and a decrease in electron density in the range of the emitter (E/N = 3–30 Td). The mean energy of discharge electrons (Figure 4.17) depended most

strongly on the parameter value E/N = 1–11 Td, while it increased linearly from 1.9 to 3.4 eV. In the range of the parameter E/N = 11–100 Td, mean electron energy also increased from 3.4 to 4.5 eV, but at a lower rate. The slower growth of mean electron energy in this range of the E/N parameter is due to the energy losses of the "fast" electrons upon excitation of the energy states of xenon and krypton atoms.

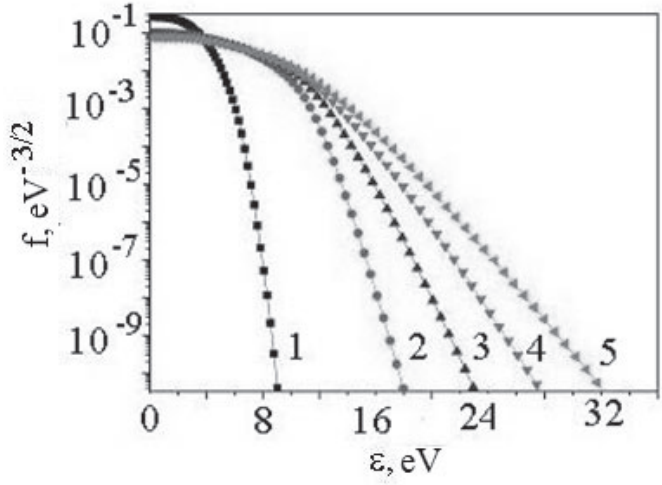

Figure 4.16. The electron energy distribution functions for the discharge in the mixture $HgBr_2$:Xe:Kr (0.28:7.98:91.74) % at a total pressure 100.3 kPa of the reduced electric field strength E/N: 1 (1), 25.8 (2), 50.5 (3), 75.3 (4), and 100 (5) [58].

The electron temperature increased from 52,432 K to 22,283.6 K with the change in the parameter E/N from 1 to 100 Td.

Electron mobility (Figure 4.18) decreased in the range $1.8 \cdot 10^{24} \cdot N$–$5.6 \cdot 10^{23} \cdot N$ (1/m/V/s) with an increase in the E/N parameter in the range 1–100 Td. This gives electron drift velocities of $1.3 \cdot 10^5$ m/s and $4.0 \cdot 10^4$ m/s, respectively, for a field strength acting on the plasma of $1.33 \cdot 10^6$ V/m for

the moment in time corresponding to the maximum voltage value (Figure 3.16, Chapter 3). The electron concentration was $2.74 \cdot 10^{16}$ m^{-3}–$9 \cdot 10^{16}$ m^{-3} at a current density 57 mA/cm^2 on the surface of the inner electrode of the radiation source (0.9 cm^2).

The distribution of specific power losses in the discharge acting on the main processes with a change in the value of the parameter E/N in the range 1–100 Td is shown in Figure 4.19.

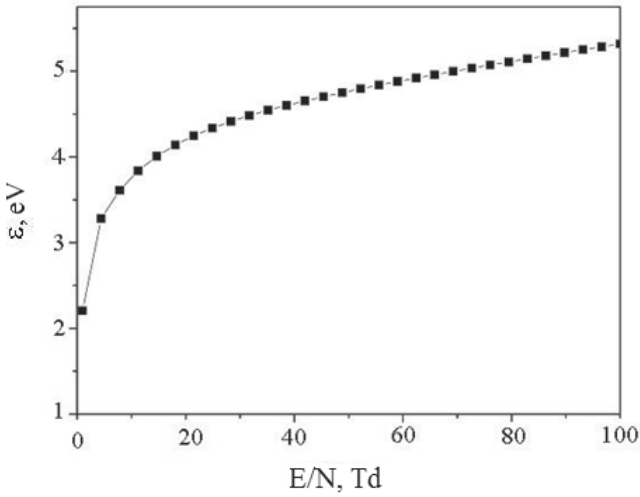

Figure 4.17. The dependency of mean electron energy on the parameter E/N for a mixture $HgBr_2$:Xe:Kr (0.28:7.98:91.74) % at a total pressure of 100.3 kPa [58].

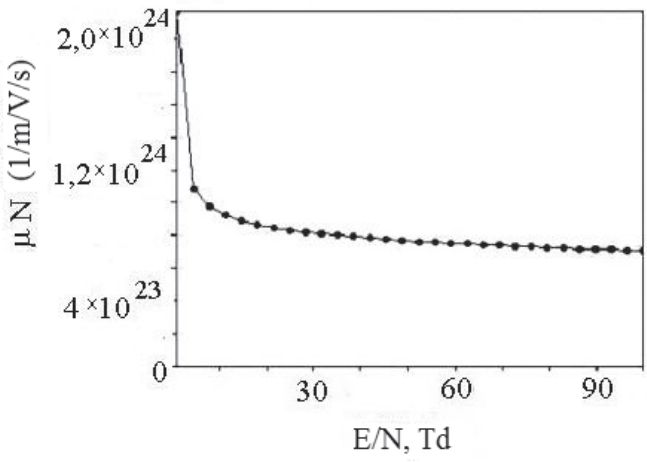

Figure 4.18. The dependency of reduced electron mobility on the value of the parameter E/N for a discharge in the mixture $HgBr_2$:Xe:Kr (0.28:7.98:91.74) % at a total mixture pressure of 100.3 kPa [58].

In the dissociative excitation of mercury monobromide molecules, the discharge power losses increased with increases in the parameter E/N. They reached maxima of 25 %, 12 %, and 53 % with E/N parameter values equal to 30 Td, 20 Td, and 10 Td for the electronic states of mercury dibromide molecules $HgBr_2(D)$ and the states $B^2\Sigma^+_{1/2}$ and $X^2\Sigma^+_{1/2}$ of mercury monobromide, respectively; with a further increase in the parameter E/N, they decreased. The rate of change in the discharge power losses in these processes, and its value, are related to the nature of the dependency of the effective excitation cross-sections of specific energy states; on the electron energy; on their absolute values; on the dependency of the electron energy distribution function for different values of the parameter E/N on the value of the threshold excitation energy of the electronic states of $HgBr_2(D)$ molecules; and the dissociative excitation of electronic states of mercury monobromide molecules. For the experimental value of the parameter E/N

= 54 Td, the discharge power losses were 18 %, 6 % and 11 % for the electronic states of mercury dibromide $HgBr_2(D)$ and mercury monobromide molecules in the states $B^2\Sigma^+_{1/2}$ and $X^2\Sigma^+_{1/2}$.

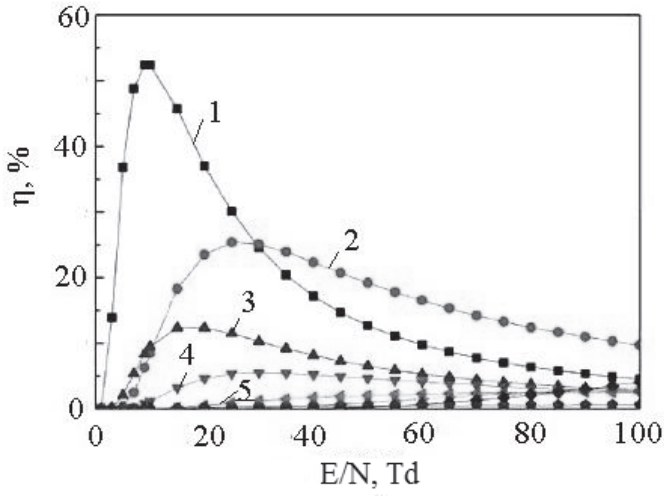

Figure 4.19. The dependency of specific power losses in the collisions of electrons with molecules of mercury dibromide, xenon and krypton atoms as a function of the E/N parameter in plasma in the mixture $HgBr_2$:Xe:Kr = (0.28:7.98:91.74) %: 1 - dissociative excitation of $X^2\Sigma^+_{1/2}$-state HgBr* molecules; 2 - excitation of the electronic state of mercury dibromide ($HgBr_2(D)$); 3 - dissociative excitation of $B^2\Sigma^+_{1/2}$-state HgBr* molecules; 4 - excitation of the electronic state of $1s^5$ xenon atoms; 5 – excitation of $5s[3/2]^0_2$-state krypton atoms [58].

Low losses of discharge power in the inelastic collisions of electrons with xenon and krypton atoms, as compared to losses in the inelastic collision of electrons with mercury dibromide molecules, were associated with lower absolute values of the effective cross-sections of these processes and the large value of their threshold energy.

Figure 4.20 shows the rate constants of electron collision processes with mercury dibromide molecules, and xenon and krypton atoms. The efficiency of electron collisions with mercury dibromide molecules is higher by more than one order of magnitude and three orders of magnitude in comparison to the efficiency of electron collision processes with xenon and krypton atoms, respectively—this is caused by higher absolute effective cross-sections and lower threshold excitation energies [30, 43, 73]. In the range of the parameter E/N = 1–100 Td, the rate constants of the electronic state of mercury dibromide $HgBr_2(D)$ and the ionization of mercury dibromide by electrons (curves 1 and 8, Figure 4.20) increased monotonically from $1 \cdot 10^{-15}$ to $3.4 \cdot 10^{-14}$ m^3/s and $8.4 \cdot 10^{-16}$ to $1.4 \cdot 10^{-15}$ m^3/s, respectively. The rate constants of the dissociative excitation of the $X^2\Sigma^+_{1/2}$ and $B^2\Sigma^+_{1/2}$ states of mercury monobromide molecules varied within the range $1.2 \cdot 10^{-15}$ m^3/s–$2.4 \cdot 10^{-14}$ m^3/s and $1.6 \cdot 10^{-17}$–$1.2 \cdot 10^{-14}$ m^3/s. With the parameter value E/N = 54 Td, at which the investigations were carried out, the excitation rate constant of exciplex HgBr* molecules was ~$9 \cdot 10^{-15}$ m^3/s.

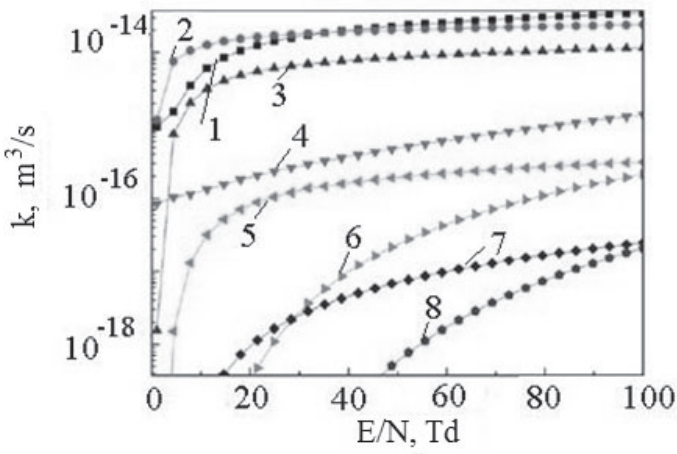

Figure 4.20. The dependencies of the rate constants of electron collisions with mercury dibromide molecules on the E/N parameter in plasma in the mixture $HgBr_2$:Xe:Kr = (0.28:7.98:91.74) % at total pressure 100.3 kPa: 1 - excitation of the energy state of mercury dibromide ($HgBr_2$(D)); 2 - dissociative excitation of $X^2\Sigma^+_{1/2}$-state HgBr* molecules; 3 - dissociative excitation of $B^2\Sigma^+_{1/2}$-state HgBr* molecules; 4 - ionization of $HgBr_2$ molecules; 5 - excitation of $1s^5$ energy state xenon atoms; 6 - ionization of xenon atoms; 7 - excitation of the electronic state $5s[3/2]^0_2$ in krypton atoms; 8 - ionization of krypton atoms [58].

4.1.6. Transport and energy characteristics of plasma in a mixture of mercury dibromide vapor, krypton and helium. The rate constants of electron collision processes with the components of the mixture

Figure 4.21 shows a characteristic form of the EEDF for different values of the parameter E/N in the range 1–100 Td. An increase in the parameter E/N led to an increase in the number of “fast” electrons in the discharge and a decrease in the electron density in the region of low values of the reduced strength electric field. The mean energy of the discharge

electrons (insert in Figure 4.21) depended most strongly on the E/N parameter in the range 1–8 Td, as it increased linearly from 0.6 to 3.9 eV. In the range of variation of the parameter E/N = 8–100 Td, mean electron energy also increased from 3.9 to 9.4 eV, but at a lower rate. The slower growth of mean electron energy in this region of E/N variation is due to the energy losses of "fast" electrons in the excitation of electronic energy states of mercury dibromide molecules, and krypton and helium atoms. The electron temperature increased from 6,960 K to 109,040 K as the parameter changed from 1 to 100 Td.

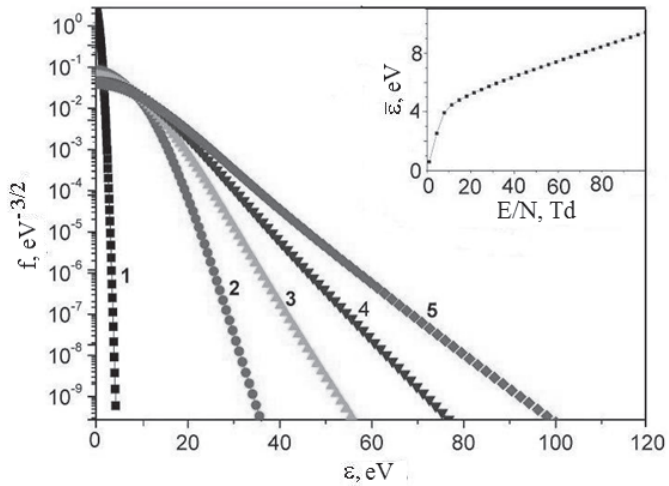

Figure 4.21. The electron energy distribution functions for the discharge in the $HgBr_2$:Kr:He mixture (0.0009:8.3999:91.5992) % at a total pressure of 120,001 Pa for the values of the reduced field strength E/N: 1 (1), 25.8 (2), 50.5 (3), 75.3 (4), and 100 (5) Td. The insert shows the dependency of mean electron energy on the parameter E/N for a discharge in the same mixture [61].

The reduced electron mobility in Figure 4.22 varies in the range $5.1 \cdot 10^{24} \cdot N$–$1.8 \cdot 10^{24} \cdot N$ (1/m/V/s) with an increase in the parameter E/N in

the range 1–100 Td. This led to electron drift velocity values of $5.3 \cdot 10^5$ m/s and $1.89 \cdot 10^5$ m/s, respectively, with an electric field strength acting on the plasma of $2.7 \cdot 10^6$ V/m. With an increase in the E/N parameter in the range 1–100 Td, electron concentration increased from $1.79 \cdot 10^{18}$ m^{-3} to $5 \cdot 10^{18}$ m^{-3} (with a current density of 15.2 A/cm^2 on the surface of the inner electrode of the radiation source). Mean electron energy at E/N = 100 Td was ~9.4 eV, which corresponded to an electron temperature of 109,040 K.

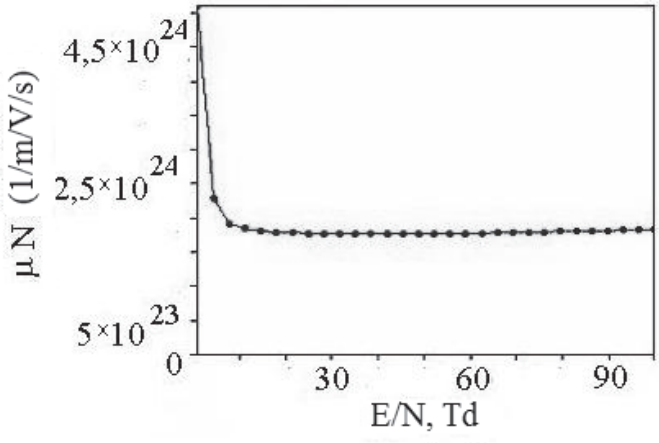

Figure 4.22. The dependency of the reduced mobility of electrons on the value of the parameter E/N for a discharge in the mixture $HgBr_2$:Kr:He (0.0009:8.3999:91.5992) % at a total pressure of 120,001 Pa [61].

The distribution of specific power losses of the discharge with the changing value of the parameter E/N in the range 1–100 Td is shown in Figure 4.23. In the dissociative excitation of mercury monobromide molecules, the discharge power losses increased with an increase in the parameter E/N. They reached maxima of 0.24 %, 0.47 %, and 0.69 % with the E/N parameter equal to 8 Td for electronic states of mercury

monobromide $B^2\Sigma^+_{1/2}$, mercury dibromide $HgBr_2$ (D), and mercury monobromide $X^2\Sigma^+_{1/2}$, respectively. With a further increase in the parameter E/N, they decreased. For the excitation of the $5s[3/2]^0_2$ electronic state krypton atom, discharge power losses increased from E/N = 5 Td, reached a 3.4 % saturation at E/N = 18 Td, and subsequently decreased monotonically to 1.4 % (at E/N = 100 Td). In the excitation of the electronic state 2^3S_1 helium atom, the power losses of the discharge monotonically increased from E/N = 18 Td and reached a maximum of 3.9 % at E/N = 100 Td.

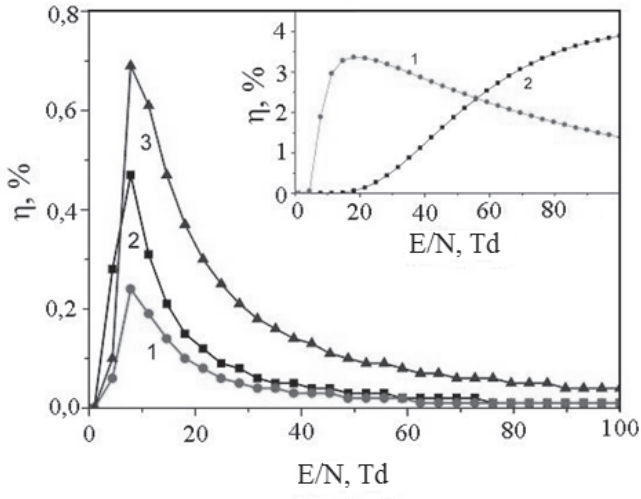

Figure 4.23. The dependency of specific power losses during the collision of electrons with mercury dibromide molecules, as a function of the E/N parameter in plasma in the mixture $HgBr_2$:Kr:He (0.0009:8.3999:91.5992) % at a total pressure of 120,001 Pa: 1, 2 - dissociative excitation of electronic states $B^2\Sigma^+_{1/2}$ and $X^2\Sigma^+_{1/2}$ of HgBr* molecules; 3 - excitation of the electronic state of mercury dibromide ($HgBr_2$(D)). On the insert: 1 - excitation of the electronic state $5s[3/2]^0_2$ krypton atoms; 2 - excitation of the electronic state of 2^3S_1 helium atoms [61].

The rates of growth and decrease in the discharge power losses in these processes and their values are related to the nature of the dependency of the effective excitation cross-sections of specific states; the electron energies; their absolute values; as well as the dependency of the electron distribution function for different values of the parameter E/N on the threshold energy of the dissociative excitation of electronic states $B^2\Sigma^+_{1/2}$ and $X^2\Sigma^+_{1/2}$ of mercury monobromide molecules; the excitation of electronic states of the mercury dibromide molecule $HgBr_2(D)$; and the excitation of the electronic states of $5s[3/2]^0_2$ krypton atoms and 2 $^3S_1$ helium atoms.

Low losses of discharge power in the inelastic collision of electrons with mercury dibromide molecules, as compared to losses in the inelastic collision of electrons with krypton and helium atoms, are associated with a fairly small concentration of mercury dibromide molecules ($2.4\cdot10^{14}$ cm^{-3}) in the mixture under study.

Figure 4.24 presents the rate constants of electron collision processes with molecules of mercury dibromide and krypton atoms. The efficiency of electron collision processes with mercury dibromide molecules is more than two and four orders of magnitude higher than that of electron collisions with krypton and helium atoms, respectively. This is due to the higher values of their absolute effective cross-sections, as well as lower excitation thresholds [30, 41–43, 73]. The values of the rate constants (k) of electron collisions with $HgBr_2$ molecules and krypton atoms increased in the range $1\cdot10^{-16}$ to $1\cdot10^{-13}$ m^3/s with an increase in the parameter E/N from 1 to 100 Td. In the range of the parameter E/N = 1–100 Td, the rate constants of the dissociative excitation of the electronic state of mercury dibromide $HgBr_2(D)$ and the ionization of the mercury dibromide by electrons (curves 1 and 2, Figure 4.25) increased from $4.4\cdot10^{-17}$ to $4.8\cdot10^{-14}$ m^3/s and $4.96\cdot10^{-16}$ to $1.1\cdot10^{-15}$ m^3/s, respectively. The rate constants of the vibrational excitation processes

of mercury dibromide molecule increased from $4.2 \cdot 10^{-17}$ m^3/s to $3.8 \cdot 10^{-14}$ m^3/s. The values of the rate constants of the dissociative excitation of $X^2\Sigma^+_{1/2}$ and $B^2\Sigma^+_{1/2}$ states of mercury monobromide molecules increased in the range of values $4.4 \cdot 10^{-16}$ m^3/s to $4.2 \cdot 10^{-14}$ m^3/s and $4.7 \cdot 10^{-29}$ to $2.1 \cdot 10^{-14}$ m^3/s. In the process of dissociative attachment of electrons to molecules of mercury dibromide, they grew from $3.4 \cdot 10^{-18}$ m^3/s, reached a saturation point of $2 \cdot 10^{-16}$ m^3/s at E/N = 6 Td, and then decreased to $8.5 \cdot 10^{-17}$ m^3/s (as

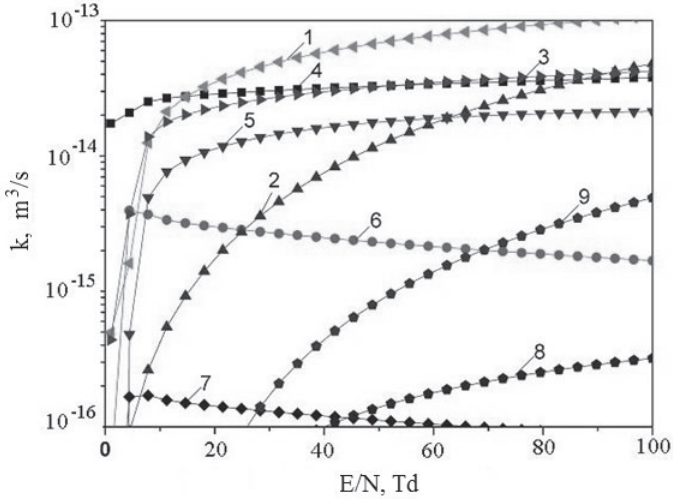

Figure 4.24. The dependencies of the rate constants of electron collisions with mercury dibromide molecules on the value of the E/N parameter in plasma in the mixture $HgBr_2$:Kr:He (0.0009:8.3999:91.5992) % at a total pressure of 120,001 Pa: 1 - excitation of the electronic state of mercury dibromide ($HgBr_2$(D); 2 - ionization of $HgBr_2$ molecules by electrons; 3 - dissociative excitation of $X^2\Sigma^+_{1/2}$-state HgBr* molecules; 4 - vibrational excitation of $HgBr_2$ molecules; 5 - dissociative excitation of $B^2\Sigma^+_{1/2}$-state HgBr* molecules; 6 - resonant vibrational excitation of $HgBr_2$ molecules; 7 - electron attachment to $HgBr_2$ molecule; 8 - excitation of electronic state $5s[3/2]^0_2$ krypton atoms; and 9 - ionization of krypton atoms [61].

the parameter E/N increased to 100 Td). In the range of the parameter values E/N = 100 Td, at which the studies were carried out, the excitation rate constant of exciplex HgBr* molecules was ≅ $2.1 \cdot 10^{-14}$ m^3/s.

Based on the numerical calculations, it may be concluded that it is possible to improve the output characteristics (radiation power and efficiency in the blue-green, λ = 502 nm, and ultraviolet, λ = 207 nm, spectral ranges of a multi-wavelength lamp in a mixture of mercury dibromide vapor, krypton and helium) by decreasing the parameter E/N to 8 Td and 18 Td. Possible ways to achieve such values of the parameter E/N include increasing the inter-electrode distance (d) and (or) increasing the concentration (N); this assumption still needs to be verified experimentally.

4.1.7. Transport and energy characteristics of plasma in a mixture of mercury dibromide vapor and argon. The rate constants of electron collision processes with the components of the mixture

Figure 4.25 presents the characteristic view of the EEDF when the E/N parameter varies in the range 1–100 Td [102]. An increase in the E/N parameter led to an increase in the number of "fast" electrons in the discharge. Mean energy of the discharge electrons increased sharply from 2.2 to 4.6 eV with an increase in the E/N parameter from 1 to 18 Td. With further growth of the reduced electric field, the rate of increase in the mean electron energy slowed down and reached 6.6 eV for E/N = 100 Td.

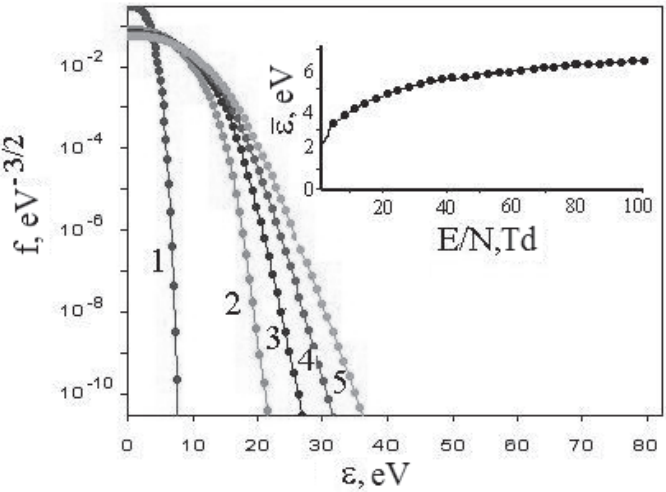

Figure 4.25. Electron energy distribution functions in the discharge for the mixture $HgBr_2$:Ar = 0.005:0.995 with total mixture pressure P = 115 kPa for the following values of the parameter E/N: 1 (1), 25.8 (2), 50.5 (3), 75.3 (4), and 100 (5) Td. The inset shows the dependency of mean electron energy on the parameter E/N [102].

The temperature of the electrons in the gas-discharge plasma of the radiator was determined by the formula [1]:

$$\varepsilon = 3/2 \cdot kT$$

where ε is the mean electron energy; k is the Boltzman constant; and T is the temperature in degrees Kelvin. The temperature increased from 25,520 to 76,560 K.

The product of the electron mobility by density, as follows from the numerical data, varies within the range $2.8 \cdot 10^{24} \cdot N – 6.8 \cdot 10^{23} \cdot N$ (1/m/V/s), when the parameter E/N changes in the range 1–100 Td, which gives electron drift velocity values of $5.7 \cdot 10^4$ m/s and $1.4\ 10^4$ m/s, respectively, and when the field intensity of the plasma was 376,900 V/m and the electron

concentration value was $8.6 \cdot 10^{18}$ m^{-3}–$3.5 \cdot 10^{19}$ m^{-3} at a current density equal to $7.85 \cdot 10^{4}$ A/m^2 on the surface of the internal electrode.

The dependencies of the ionization coefficients of mercury dibromide molecules and argon atoms on the value of the E/N parameter increased as the E/N parameter increased (Fig. 4.26). The attachment coefficient of electrons to mercury dibromide molecules also increased, reaching its maximum in the region E/N = 9 Td (exceeding the ionization coefficient). It reached the same values as the coefficient of total ionization for the parameter E/N = 30 Td: $\alpha = 0.775 \cdot 10^{-2}$ cm^{-1} $Torr^{-1}$. The regularity of this dependency shows that for the parameter value E/N = 30 Td, ionization compensates the attachment and the capture of electrons is controlled by

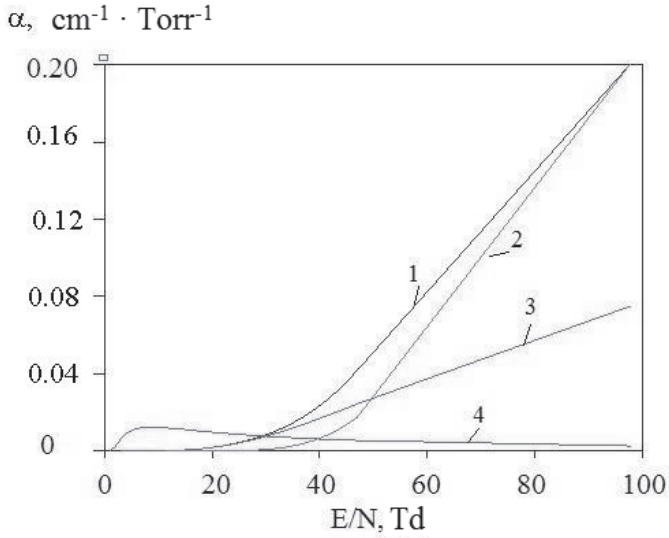

Figure 4.26. The dependency of the ionization and attachment coefficients of electrons for mercury dibromide molecules and argon atoms on the parameter E/N for the mixture $HgBr_2$:Ar = 0.005:0.995 and total pressure of the mixture P = 115 kPa: 1 - total ionization; 2 - ionization of argon atoms; 3 - ionization of mercury dibromide molecules; and 4 - attachment [102].

attachment. As the values of the E/N parameter exceeded 30 Td, the coefficient of electron attachment to mercury dibromide molecules sharply decreased according to a near hyperbolic law, and electron capture was controlled by other processes (diffusion and recombination) affecting the balance of the number of electrons.

The distribution of specific losses of discharge power in the main processes is shown in Fig. 4.27. The fraction of the discharge power spent on the dissociative excitation of mercury monobromide molecules increased with an increase in the parameter E/N. It reached maxima of 15 %, 51 % and 40 % with E/N parameter values equal to 30 Td, 13 Td and 46 Td for the electronic states of mercury monobromide $B^2\Sigma^+_{1./2}$, mercury monobromide $X^2\Sigma^+_{1/2}$ and mercury dibromide ($HgBr_2$(D)), respectively. With a further increase in the parameter E/N, it decreased. The rates of increase and decrease in the fraction of the discharge power spent on these processes and their magnitudes are related to the nature of the dependency of the effective cross-sections for the excitation of specific states; the electron energies; their absolute values; and the dependency of the electron distribution function for different values of the E/N parameter on the threshold energy of dissociative excitation of electronic states of the mercury monobromide molecule. The fraction of the discharge power spent on the vibrational resonant excitation of mercury dibromide molecules reached a maximum of 43 % for E/N = 4 Td; with an increase in the parameter values, this decreased sharply. The fractions of discharge power spent on the vibrational excitation of mercury dibromide molecules; the dissociative attachment of electrons to mercury dibromide molecules; and the elastic scattering of electrons by argon atoms were significant only at E/N<7 Td. When the E/N parameter increased to >7 Td, they decreasd dramatically. The fraction of the discharge power spent on ionization was

most significant in the ionization of argon atoms (dependency (7)). This is due to the large value of the effective ionization cross-section compared to that for mercury dibromide molecules. The fraction of the discharge power spent on the ionization of argon atoms began to increase dramatically with values of the parameter E/N>40 Td; for E/N = 100 Td it was 22 %. The fraction of the discharge power spent in inelastic processes for argon became noticeable for values of the parameter E/N>20 Td. Its value for the excitation of electronic states with an electron threshold energy of 11.273 eV (dependency 6, Fig. 4.27) and 11.623 (dependency 8, Fig. 4.27) was 23 % and 9.8 % with the value of the parameter E/N = 100 Td. Low fractions of the discharge power spent on the inelastic collision of electrons with argon atoms, as compared to the fraction spent on the inelastic collision of electrons with mercury dibromide molecules, were associated with lower absolute values of the effective cross-sections of these processes and large energies and thresholds [30, 31, 95].

Figure 4.28 presents the rate constants for the collision of electrons with mercury dibromide molecules, which are a quantitative measure of the efficiency of these processes [3]. The efficiency of these processes for mercury dibromide molecules is higher. The values of the rate constants (k) for mercury dibromide molecules are in the range $1.8 \cdot 10^{-16}$–$6.1 \cdot 10^{-14}$ m^3/s when the parameter E/N varies from 11 to 100 Td. This is caused by higher values of the absolute effective cross-sections of the corresponding processes compared to the data for argon atoms [30, 31, 95]. The rate constants of the excitation of mercury dibromide ($HgBr_2(D)$) states and ionization of mercury dibromide by electrons (dependencies 1 and 3, Fig. 4.28) sharply increased from $9.7 \cdot 10^{-16}$ to $3.9 \cdot 10^{-14}$ m^3/s and $8.6 \cdot 10^{-17}$ to $1.6 \cdot 10^{-15}$ m^3/s with changes in the parameter E/N from 1 to 42 Td, respectively.

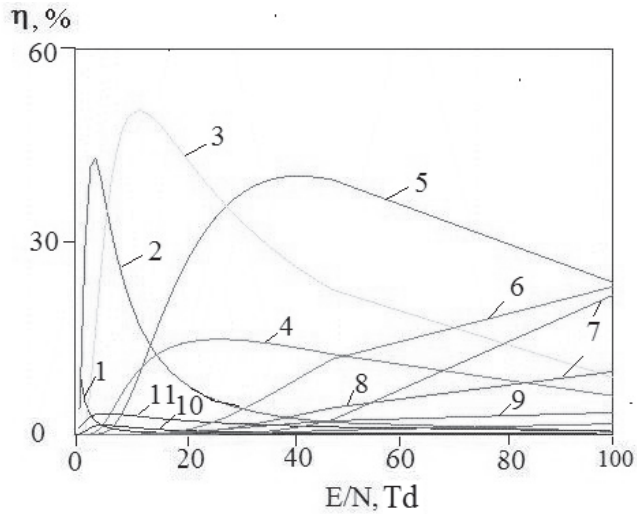

Figure 4.27. The dependency of specific power losses of the discharge during electron collisions with mercury dibromide molecules and argon atoms as a function of the parameter E/N for the $HgBr_2$:Ar = 0.005:0.995 mixture at a total mixture pressure of P = 115 kPa: vibrational excitation of mercury dibromide molecules (1); vibrational resonant excitation of mercury dibromide molecules (2); dissociative excitation of $X^2\Sigma^+_{1/2}$ (3) and $B^2\Sigma^+_{1/2}$ (4) electronic states of mercury monobromide molecules; excitation of the electronic state ($HgBr_2$(D)) (5) of mercury dibromide molecules; excitation of energy states of argon atoms with threshold 11.273 eV (6); ionization of argon atoms (7); excitation of energy states of argon atoms with the energy threshold 11.623 eV (8); ionization of mercury dibromide molecules (9); electron attachment to mercury dibromide molecules (10); elastic scattering of electrons on argon atoms (11) [102].

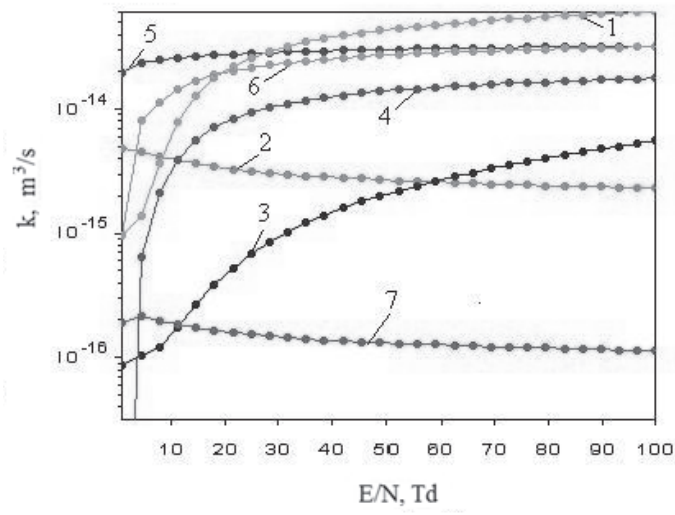

Figure 4.28. The rate constants of electron collisions with mercury dibromide molecules in a gas-discharge plasma in the mixture $HgBr_2$:Ar = 0.005:0.995 at a total mixture pressure of P = 100 kPa: 1 - excitation of the electronic state ($HgBr_2$(D)) of mercury dibromide molecules; 2 - resonant vibrational excitation of $HgBr_2$ molecules; 3 - ionization of $HgBr_2$ molecules by electrons; 4 - dissociative excitation of $B^2\Sigma^+_{1/2}$-state of HgBr* molecules; 5 - vibrational excitation of $HgBr_2$ molecules; 6 - dissociative excitation of $X^2\Sigma^+_{1/2}$-state of HgBr* molecules; and 7 - electron attachment to $HgBr_2$ molecules [102].

In the range E/N = 42–100 Td, the rate of increase slowed down. The maximum values of the rate constants for the excitation of mercury dibromide ($HgBr_2$(D)) states and the ionization of mercury dibromide by electrons $6.1 \cdot 10^{-14}$ and $5.6 \cdot 10^{-15}$ m^3/s were achieved for E/N = 100 Td. The rate constant of the process of vibrational excitation of mercury dibromide molecules increased from $2.0 \cdot 10^{-14}$ to $3.2 \cdot 10^{-14}$ m^3/s. The rate constants of the dissociative excitation of $X^2\Sigma^+_{1/2}$ and $B^2\Sigma^+_{1/2}$ states of mercury

monobromide molecules increased to values of $3.2 \cdot 10^{-14}$ m^3/s and $1.8 \cdot 10^{-14}$ m^3/s, respectively; for the processes of resonant vibrational excitation of molecules $HgBr_2$ and dissociative attachment of electrons to mercury dibromide molecules (curves 2 and 7, Fig. 4.28) they did not exceed $2.3 \cdot 10^{-15}$ and $1.1 \cdot 10^{-16}$ m^3/s, respectively.

The processes of excitation of argon atoms by electrons had smaller values of the rate constants compared to the data for mercury dibromide molecules. These increased from a value of $1.2 \cdot 10^{-26}$ to $2.5 \cdot 10^{-16}$ m^3/s. The rate constant of the ionization of argon atoms by electrons increased within the range $5.1 \cdot 10^{-33}$ to $1.3 \cdot 10^{-16}$ m^3/s. In the process of elastic scattering of electrons by argon atoms, the value of the rate constant was within the range $3.4 \cdot 10^{-14}$ –$1.9 \cdot 10^{-13}$ m^3/s.

4.1.8. Transport and energy characteristics of plasma in a mixture of mercury dibromide vapor and neon. The rate constants of electron collision processes with the components of the mixture

Figure 4.29 presents the characteristic form of the EEDF when the E/N parameter varies in the range 1–100 Td [103]. An increase in the E/N parameter led to an increase in the number of "fast" electrons in the discharge. The mean energy of the discharge electrons slowly increased from 1 to 2.7 eV as the E/N parameter increased from 1 to 20 Td. It grew most sharply (from 2.7 to 8 eV) in the range of the parameter E/N = 20–50 Td. With further growth in the reduced electric field, the rate of increase in the mean electron energy slowed down and reached 12.5 eV for E/N = 100 Td.

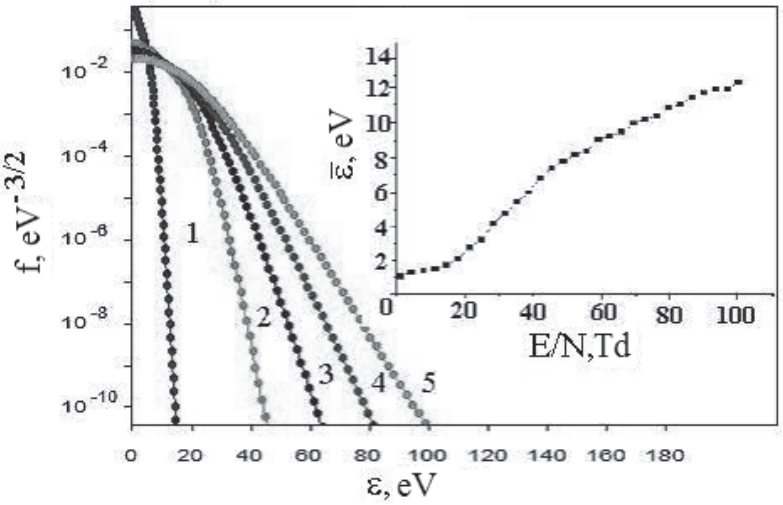

Figure 4.29. The electron energy distribution functions in the discharge for the mixture $HgBr_2$:Ne = 0.005:0.995 with a total mixture pressure of P = 100.8 kPa for the values of the parameter E/N: 1 (1), 25.8 (2), 50.5 (3) 75.3 (4), and 100 (5) Td. The inset presents the dependency of mean electron energy on the parameter E/N [103].

The temperature of electrons increased from 11,600 to 145,000 K as the parameter E/N changed from 1 to 100 Td.

The calculated electron mobility varied in the range $1.5 \cdot 10^{25} \cdot N$–$2.6 \cdot 10^{24} \cdot N$ (1/m/V/s), when the E/N parameter changed in the range 1–100 Td, giving electron drift velocities values of $17.5 \cdot 10^5$ m/s and $29.9 \cdot 10^4$ m/s, respectively, with a plasma field strength of $19.9 \cdot 10^5$ V/m and an electron concentration value of $0.68 \cdot 10^{17}$ m^{-3}–$3.9 \cdot 10^{17}$ m^{-3} at a current density of 19.1 A/cm^2.

The dependencies of the ionization coefficients of mercury dibromide molecules and neon atoms on the value of the parameter E/N increase as

E/N increases (Fig. 4.30). The coefficient for electron attachment to mercury dibromide molecules also increases, reaching a maximum in the E/N = 5 Td region (exceeding the ionization coefficient) and reaches the same values as the total ionization coefficient for the parameter E/N = 10 Td: $\alpha = 0.004$ cm^{-1} Torr^{-1}. The regularity of this dependency shows that for the values of the parameter E/N = 10 Td, ionization compensates the attachment—the capture of electrons is controlled by attachment. As the values of the E/N parameter exceed 10 Td, the coefficient of electron attachment to mercury dibromide molecules sharply decreases according to a near hyperbolic law, and electron capture is controlled by other processes (diffusion and recombination) affecting the balance of the number of electrons.

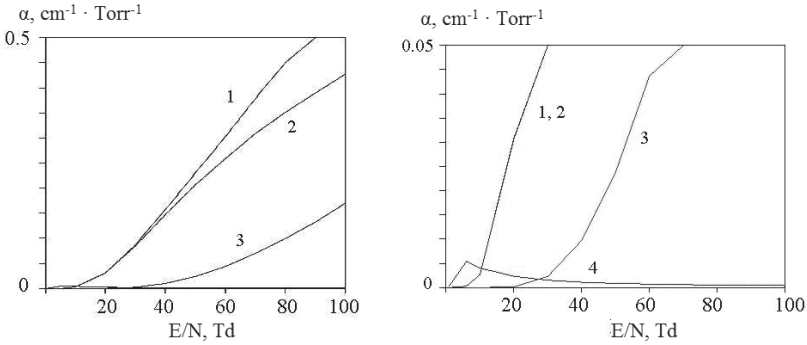

Figure 4.30. The dependency of the ionization and attachment coefficients of electrons for mercury dibromide molecules and neon atoms on the parameter E/N for the mixture $HgBr_2$:Ne = 0.005:0.995 with total mixture pressure P = 100.8 kPa: 1 - total ionization; 2 - ionization of neon atoms; 3 - ionization of mercury dibromide molecules; and 4 - attachment [103].

The distribution of specific power losses of the discharge in the main processes with a change in the value of the parameter E/N in the range of 1–100 Td is shown in Fig. 4.31.

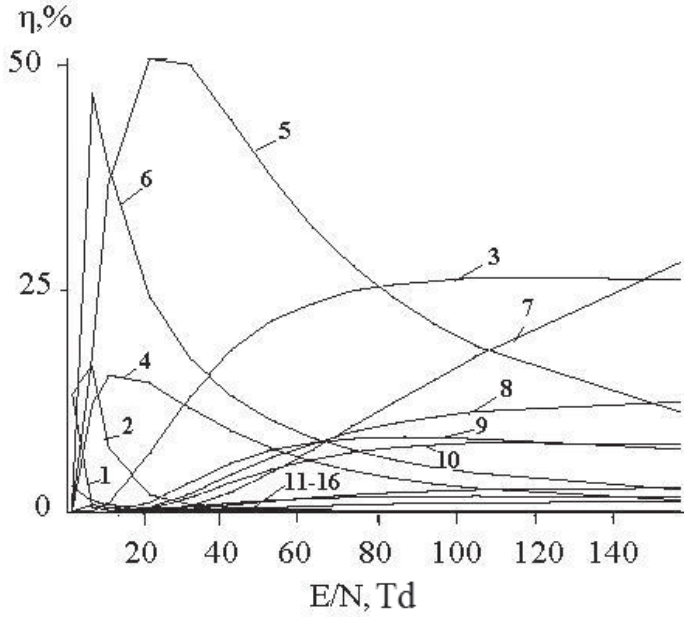

Figure 4.31. The dependency of the specific power losses of the discharge in the collision of electrons with mercury dibromide molecules and neon atoms as a function of the parameter E/N for the mixture $HgBr_2$:Ne = 0.005:0.995 at a total mixture pressure P = 100.8 kPa: vibrational excitation of mercury dibromide molecules (1); vibrational resonant excitation of mercury dibromide molecules (2); ionization of mercury dibromide molecules (3); dissociative excitation of the $B^2\Sigma^+_{1/2}$ electronic state of mercury monobromide molecules (4); excitation of the electronic state ($HgBr_2$(D)) of mercury dibromide molecules (5); dissociative excitation of the $X^2\Sigma^+_{1/2}$ electronic state of mercury monobromide molecules (6); ionization of neon atoms (7); excitation of the energy state of a neon atom 1s2 (8); excitation of the energy state of a neon atom with an energy threshold of 16.62 eV (9); excitation of the energy state of a neon atom 2p (10); elastic scattering of electrons on neon atoms

(11); excitation of the energy state of neon atom 1s4 (12); the excitation of the energy states of neon atoms (2s + 3d) with an energy of 20.00 eV (13); the excitation of the energy state of neon atom (4p) (14); the attachment of electrons to mercury dibromide (15); ionization of a metastable neon atom (threshold energy 4.9 eV) (16)) [103].

The fraction of the discharge power spent on the dissociative excitation of mercury monobromide molecules increased with an increase in the parameter E/N. It reached maxima of 15 %, 46 % and 52 % with values of the parameter E/N equal to 10 Td, 2 Td and 20 Td for the electronic states of $B^2\Sigma^+_{1/2}$, mercury monobromide $X^2\Sigma^+_{1/2}$ and mercury dibromide ($HgBr_2(D)$), respectively; with a further increase in the parameter E/N, it decreased. The rates of increase and decrease in the fraction of the discharge power spent on these processes and their magnitudes are related to the nature of the dependency of the effective cross-sections for the excitation of specific states; the electron energies; their absolute values; and the dependency of the electron distribution function for different values of the E/N parameter on the threshold energy of the dissociative excitation of electronic states of mercury monobromide molecules. The fraction of discharge power spent on the oscillatory resonant excitation of mercury dibromide molecules reached a maximum of 16 % at E/N = 6 Td; as the parameter values increased, it sharply decreased. The fractions of discharge power spent on the vibrational excitation of mercury dibromide molecules; the dissociative attachment of electrons to mercury dibromide molecules; and the elastic scattering of electrons by neon atoms were significant only at E/N<6 Td; with an increase of E/N>6 Td, they decreased dramatically. The fraction of the discharge power spent on ionization processes was most significant in the ionization of mercury dibromide molecules (dependency

(3)). This is due to the smaller value of their ionization potential compared to the ionization potential of neon atoms and the large value of the effective ionization cross section. The fraction of discharge power spent on the ionization of mercury dibromide molecules began to increase dramatically when the value of the parameter was E/N>10 Td; when E/N>30 Td became higher than the value (12.7 %) of the fraction of discharge power spent on the excitation of the $B^2\Sigma^+_{1/2}$ state of mercury monobromide. The fraction of the discharge power spent on inelastic processes with neon became noticeable for values of the parameter E/N>30 Td. Its value for the excitation of electronic states did not exceed 11 % with the value of the parameter E/N = 100 Td. Low fractions of discharge power spent on the inelastic collision of electrons with neon atoms, compared to fractions spent on the inelastic collision of electrons with mercury dibromide molecules, are associated with lower absolute values of the effective cross-sections of these processes and large energies, as well as their thresholds [30, 31, 95].

Figure 4.32 presents the rate constants for the processes of collision of electrons with mercury dibromide molecules, which are a quantitative measure of the efficiency of these processes [3]. The efficiency of these processes for mercury dihalide molecules is higher. The values of the rate constants (k) for them are in the range $1\cdot10^{-14}$–$1.6\cdot10^{-13}$ m^3/s when the E/N parameter changes from 10 to 100 Td, which is caused by higher values of the absolute effective cross-sections of the corresponding processes compared to the data for neon atoms [30, 31, 95]. In the region of the parameter E/N = 1–100 Td, the rate constant for the excitation of mercury dibromide ($HgBr_2(D)$) states and the ionization of mercury dibromide by electrons (dependencies 1 and 2, Fig. 4.32) increased monotonically from $0.6\cdot10^{-15}$ to $1.6\cdot10^{-13}$ m^3/s and $0.6\cdot10^{-16}$ to $1.2\cdot10^{-13}$ m^3/s, respectively. The rate constant of the process of vibrational excitation of mercury dibromide

molecules increased from $1.6 \cdot 10^{-14}$ to $4.4 \cdot 10^{-14}$ m^3/s. The rate constants of the dissociative excitation of $X^2\Sigma^+_{1/2}$ and $B^2\Sigma^+_{1/2}$ states of mercury monobromide molecules increased to values of $4 \cdot 10^{-14}$ m^3/s and $2.1 \cdot 10^{-14}$ m^3/s, respectively. For the processes of the resonant vibrational excitation of molecules $HgBr_2$ and dissociative attachment of electrons to mercury dibromide molecules, they do not exceed the value $1 \cdot 10^{-15}$ m^3/s.

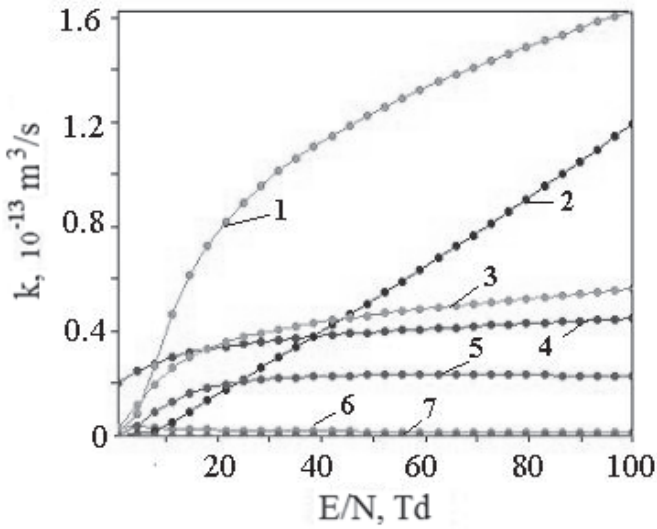

Figure 4.32. The rate constants of electron collisions with mercury dibromide molecules in a gas-discharge plasma in the mixture: $HgBr_2$:Ne = 0.005:0.995 with a total mixture pressure of P = 100 kPa: 1 - excitation of mercury dibromide ($HgBr_2$(D)) states; 2 - ionization of $HgBr_2$ molecules by electrons; 3 - dissociative excitation of $X^2\Sigma^+_{1/2}$ state of HgBr* molecules; 4 - vibrational excitation of $HgBr_2$ molecules; 5 - dissociative excitation of $B^2\Sigma^+_{1/2}$-state HgBr molecules; 6 - resonant vibrational excitation of $HgBr_2$ molecules; and 7 - electron attachment to $HgBr_2$ molecules[103].

The processes of excitation of neon atoms by electrons had smaller values for rate constants in comparison to the data for mercury dibromide

molecules. They increased from a value of $1 \cdot 10^{-22}$ to $3.2 \cdot 10^{-16}$ m^3/s in the range of changes in the parameter E/N = 1–100 Td. The rate constant of the process of ionization of neon atoms by electrons increased within the range $6.5 \cdot 10^{-30}$ to $3 \cdot 10^{-16}$ m^3/s in the same range of the parameter E/N (1–100 Td). For the elastic scattering of electrons by neon atoms, the value of the rate constant is within $9 \cdot 10^{-15}$–$5 \cdot 10^{-14}$ m^3/s in the range of the parameter E/N = 1–100 Td.

4.2. Conclusions to Chapter 4

1. The parameters were determined for barrier discharge plasma in mixtures of mercury dibromide vapor and the following gases: helium, argon, neon, krypton, xenon, nitrogen, and sulfur hexaflouride. With the increase of the parameter E/N from 1 to 100 Td for discharge in the following mixtures—$HgBr_2$:He; $HgBr_2$:Ar, $HgBr_2$:Ne; $HgBr_2$:N_2:He; $HgBr_2$:SF_6:He; $HgBr_2$:SF_6:N_2:He; $HgBr_2$:Xe:Kr; $HgBr_2$:Kr:He—respectively, mean electron energy; electron drift velocity; electron concentration; and electron temperature were in the ranges: (1–12) eV, ($74.4 \cdot 10^4$–$37.2 \cdot 10^4$) m/s, ($3.9 \cdot 10^{17}$–$7.8 \cdot 10^{17}$) m^{-3}, (11,600–139,200) K; (2.2–6.6) eB, ($5.7 \cdot 10^4$–$1.4\ 10^4$) m/s, ($8.6 \cdot 10^{18}$–$3.5 \cdot 10^{19}$) m^{-3}, (25,520–76,560) K; (1–12.5) eV, ($17.5 \cdot 10^5$–$29.9\ 10^4$) m/s, ($6.8 \cdot 10^{17}$–$3.9 \cdot 10^{17}$) m^{-3}, (11,600–145,000) K; (1.5–11) eV, ($92.3 \cdot 10^4$–$39.1 \cdot 10^4$) m/s, ($3.9 \cdot 10^{17}$–$9.1 \cdot 10^{17}$) m^{-3}, (5,800–127,600) K; (1.37–10.26) eV, ($53.4 \cdot 10^4$–$40.2 \cdot 10^4$) m/s, ($6.1 \cdot 10^{17}$–$8.1 \cdot 10^{17}$) m^{-3}, (15,892–119,016) K; (0.5–10.1) eV, ($105\ 10^4$–$37.5 \cdot 10^4$) m/s, ($2.9 \cdot 10^{16}$–$8 \cdot 10^{17}$) m^{-3}, (5,800–117,160) K; (1.9–4.5) eV, ($1.3\ 10^5$–$4\ 10^4$) m/s, ($2.74\ 10^{16}$–$9\ 10^{16}$) m^{-3}, (52,432–222,836) K; (0.6–9.4) eV, ($5.3\ 10^5$–$1.89\ 10^5$) m/s, ($1.79\ 10^{18}$–$5\ 10^{18}$) m^{-3}, (6,960–109,040) K.

2. The efficiency of elastic and inelastic electron scattering processes in the components of gas mixtures (helium, krypton, xenon, mercury dibromide molecules, nitrogen, and sulfur hexaflouride) was characterized by high values. The constants of their velocities were in the range ($2 \cdot 10^{-17}$–$1.2 \cdot 10^{-13}$) m^3/s when the parameter E/N varied from 1 to 100 Td. To excite the $B^2\Sigma^+_{1/2}$ state of mercury monobromide molecules, they reached $1 \cdot 10^{-14}$ m^3/s in plasma in the mixture $HgBr_2$:He, and gradually increased from $1 \cdot 10^{-15}$ to $1.5 \cdot 10^{-14}$ m^3/s in the discharge in the mixtures $HgBr_2$:N_2:He, $HgBr_2$:SF_6:He, $HgBr_2$:SF_6:N_2:He, $HgBr_2$:Xe:Kr, and in the plasma the mixture $HgBr_2$:Kr:He reached $2.1 \cdot 10^{-14}$ m^3/s in the range of values of the parameter E/N = 10–40 Td, 54 Td and 100 Td, at which the radiation source operated.

3. Specific losses of barrier discharge power in the excitation of electronic states $X^2\Sigma^+_{1/2}$ and $B^2\Sigma^+_{1./2}$ of mercury monobromide molecules and the excitation of the electronic state of mercury dibromide ($HgBr_2$(D)) reached maximum values of 35 %, 14 % and 49 % at E/N = 10, 30, 40 Td; 51 %,15 % and 40 % for E/N = 13 Td, 30 Td, and 46 Td; 46 %, 15 % and 52 % for E/N = 2 Td,10 Td and 20 Td; 18.9 %, 9.5 % and 35.7 % for E/N = 20 Td, 30 Td and 40 Td; 39.5 %, 13.7 % and 47.0 % for E/N = 11 Td, 23 Td and 37 Td; 52 %, 12 %, 25 % for E/N = 10 Td, 20 Td, 30 Td; 0.69 %, 0.24 %, 0.47 % for E/N = 8 Td in plasma in the following mixtures: $HgBr_2$:He; $HgBr_2$:Ar; $HgBr_2$:Ne; $HgBr_2$:N_2:He; $HgBr_2$:SF_6:He; $HgBr_2$:Xe:Kr; $HgBr_2$:Kr:He, respectively.

4. Total losses in discharge power in inelastic processes: the dissociative excitation of energy states of mercury monobromide molecules; the excitation of vibrational energy states of mercury dibromide molecules; the excitation of energy states of nitrogen molecules; the excitation of vibrational energy states of nitrogen molecules; and the excitation of

electron energy states of helium atoms increased in the values of the parameter E/N = 1Td, reached a maximum of 90 % at E/N = 20–30 Td, and then monotonically decreased to 50 % at E/N = 100 Td in the discharge in $HgBr_2$:He and $HgBr_2$:N_2:He mixtures.

5. Specific losses of discharge power in the inelastic processes for helium atoms were noticeable for the parameter E/N>30 Td; their values for the excitation of electronic states did not exceed 10 %; for ionization it was 20 % at the parameter E/N = 100 Td in plasma in the mixture $HgBr_2$:He.

6. Specific losses of the discharge power in the excitation of the electronic states of nitrogen molecules were significant only for $C^3\Pi_u$ states and the sum of singlet states above the threshold 13 eV. They were 5.8 % and 3.2 %, respectively, for the parameter value E/N = 50 Td. The losses of discharge power in inelastic processes associated with the helium atom became noticeable at E/N>30 Td; their value for the excited electronic states did not exceed 1 %; for ionization it was 0.8 % at E/N = 100 Td in plasma in the mixture $HgBr_2$:N_2:He.

7. Specific losses of discharge power in inelastic processes for sulfur hexafluoride molecules and the excitation of helium energy states became noticeable for E/N parameter values exceeding 25 Td; their values did not exceed 6.5 % for the parameter E/N = 100 Td in plasma in the mixture $HgBr_2$:SF_6:He.

CONCLUSION

1. Physicochemical regularities were revealed in terms of the spectral and integral characteristics of the radiation of a gas-discharge plasma in two-component and multicomponent mixtures of mercury dibromide vapor with gases: helium, argon, neon, nitrogen, and sulfur hexafluoride, in the range of the pump pulses:

-3,000–9,000 Hz of sub-microsecond pulse duration (0.2–0.7) μs,

- 10 Hz of nanosecond duration (30 ns) in a mixture of mercury dibromide vapor, krypton and helium,

- with sinusoidal pumping at a frequency of 120 kHz in a mixture of mercury dibromide vapor, krypton, xenon and helium.

In the visible range, a spectral band with maximum intensity at a wavelength of $\lambda = 502$ nm, corresponding to the $B^2\Sigma^+_{1/2} \rightarrow X^2\Sigma^+_{1/2}$ electron-vibrational transition of exciplex molecules of mercury monobromide, was significantly allocated. There was a physico-chemical regularity of increasing the average radiation power in this band to the maximum value, and further, with increasing partial pressure of the components of the mixture, a decrease.

The maximum average radiation power from a volume of 1 cm^3 was reached in the spectral band with a maximum at a wavelength of $\lambda = 502$ nm in the four-component mixture $HgBr_2$:SF_6:N_2:He, with 48.8 $mW/cm^3 \pm$ 2.9 mW/cm^3 at partial pressures of the components: 0.1 kPa to 70 Pa–4 kPa–117.2 kPa, respectively.

An increase in the partial pressure of mercury dibromide vapor to 0.8 kPa led to an increase in the average power for each mixture by an order of magnitude.

2. An increase in the radiation power by a factor of seven in the blue-green spectral range in plasma based on a multicomponent mixture of mercury dibromide vapor with helium, nitrogen, and sulfur hexafluoride was established; the mechanism for increasing the radiation power was the increase in the population of the energy state-$B^2\Sigma^+_{1/2}$-molecules of mercury monobromide due to the quenching of its overlying energy states $C^2\Pi_{1/2}$ and $D^2\Pi_{3/2}$ by sulfur hexafluoride and nitrogen molecules.

3. The efficiencies of the process of dissociative excitation of the $B^2\Sigma^+_{1/2}$ state of mercury monobromide molecules by electrons in collisions with molecules of mercury dibromide were determined. The values of the rate constants were in the range $2\cdot10^{-17}$–$1.6\cdot10^{-13}$ m^3/s when the reduced field strength (E/N) changed in the range 1–100 Td.

4. The rate constants of the quenching process of $B^2\Sigma^+_{1/2}$-state mercury monobromide by molecules of mercury dibromide, sulfur hexafluoride and nitrogen for three and four-component mixtures of mercury dibromide vapor with gases of sulfur hexafluoride and nitrogen were within the range $(0.04 \pm 0.01–71.1 \pm 14.2) \times10^{-16}$ m^3/s.

5. The emission of exciplex mercury monobromide and xenon bromide molecules in the visible ($\lambda_{max.}$ = 502 nm) and ultraviolet ($\lambda_{max.}$ = 281 nm) spectral ranges at the high-frequency sinusoidal pump mode of mercury dibromide vapor with krypton and xenon mixtures, as well as simultaneous emission of exciplex mercury monobromide and krypton bromide molecules in the visible ($\lambda_{max.}$ = 502 nm) and ultraviolet ($\lambda_{max.}$ = 207 nm) spectral ranges in a mixture with krypton and helium for pulsed periodic pumping of nanosecond duration were revealed. The formation of exciplex

krypton bromide molecules in a mixture of mercury dibromide vapor, krypton and helium involves the collision of krypton atoms in the metastable state $^3P_2$ with mercury dibromide molecules.

6. Parameters and characteristics of a gas-discharge plasma in multicomponent mixtures of mercury dibromide vapor with helium, argon, neon, krypton, xenon, nitrogen and sulfur hexafluoride for the component composition were determined, at which the maximum values of the radiation power in the blue-green spectral range were obtained. When the value of the reduced field strength (E/N) varied from 1 Td to 100 Td, mean energy and electron temperature increased from 0.5 eV to 12 eV and 5,800 K to 145,000 K, respectively.

Specific losses of discharge power in the dissociative excitation of mercury monobromide molecules by electrons for mixtures increase with an increase in reduced field strength. They reached maxima within the limits: 9.5 %–15 %, 18.9 %–52.7 %, 25 %–52 % at values of the reduced field strength in the range (10–40) Td for the electronic states of mercury monobromide $B^2\Sigma^+_{1/2}$, mercury monobromide $X^2\Sigma^+_{1/2}$, and mercury dibromide (D), respectively.

7. The construction of a gas discharge cuvette is proposed, with the help of which the efficiency of gas discharge excilamps acting on mixtures of mercury dibromide vapor with gases will increase by 40 %.

8. The results of the research are recommended for scientific and practical use in the development of high-efficiency sources of incoherent and coherent radiation in the blue-green and ultraviolet spectral ranges; expanding the database on the rate constants of the collision of electrons with molecules and atoms; the quenching of the $B^2\Sigma^+_{1/2}$-state of mercury monobromide molecules in a gas-discharge plasma in multicomponent mercury dibromide vapor mixtures with inert gases, nitrogen and sulfur

hexafluoride; and for the improvement of the theoretical models and calculations of converting electrical energy of external sources into the radiation of exciplex molecules.

BIBLIOGRAPHY

1. Raizer, Yu.P. 1991. *Gas Discharge Physics.* Berlin: Springer.

2. Rhodes, Ch.K. 1979. *Excimer lasers.* Berlin: Springer-Verlag.

3. McDaniel, E.W., and Nigan W.L. 1982. *Gas Lasers.* New York: Academic Press.

4. Sugii, M., and Sasaki K. 1986. "Improved perfor mance of the discharge pumped HgBr and HgCl lasers by adding SF_6." *Appl. Phys. Lett.* 48: 1633-35.

5. Schimitschek, E.J., and Celto, J.E. 1978. "Mercuric bromide dissociation laser in an electric discharge." *Optics letters* 2(3): 64-6.

6. Burnham R. 1978. "Discharge pumped mercuric halide dissociation lasers." *Appl. Phys.Lett.* 33(2): 152-56.

7. Bogachev, I.D., Zrodnikov, V.S., Klementov, A.D., Mitin, I.B., Molchanov, A.G., Podsosonnyi, A.S., and Timofeev, Y.T. 1981. "HgBr electronic-discharge laser." *Sov. Tech. Phys. Lett.* 7(2): 220-25.

8. Burhman R., and Schimitschek, E.J. 1981. "High-power blue-green lasers." *Laser Focus* 6: 54-61.

9. Schimitschek, E.J. 1981. "High power blue-green molecular lasers." Washington (USA): Proc. Conf. Lasers and Electroopt., 96-98.

10. Znotins, T.A., Fisher, C.H., De Hart, T.E., Mc Daniel, J.P, and Ewing, J.J. 1985. "High efficiency 3-J mercury bromide discharge laser." *Appl. Phys. Lett.* 46 (3): 228-30.

11. Petrukhin, E.A., and Podsosonnyi, A.S. 1990. "Electric-discharge ultraviolet-preionized HgBr laser with an active volume of 1 liter, an output

pulse energy of 1.4 J, and an efficiency of 0.7%." *Kvantovaya Elektronika* 17(5): 535–36.

12. Malinin, A.N., Shuaibov, A.K., and Shevera, V.S. 1980. "Excitation of a mixture of mercury vapor and halogen-containing molecules by a pulsed discharge through a dielectric." *Journal of Applied Spectroscopy* 32(4): 313-16.

13. Malinin, A.N., and Shimon, L.L. 1996. "Excitation of the $B^2\Sigma^+_{1./2}$ state of the HgBr* molecules in a gas-discharge plasma formed from a mixture of mercury dibromide and helium." *Kvantovaya Elektronika* 23(12):1077-80.

14. Malinin, A.N., Shimon, L.L., Guivan, N.N., and Polyak, A.V. 1999. "Optimization of energy characteristics in gas discharge plasma on working mixtures HgBr-laser." *Atmospheric and Oceanic Optics* 12(11): 1024-26.

15. Duley, W.W. 1983. *Laser processing and analysis of materials.* New York and London: Plenum Press.

16. Kogelschatz, U. 2003. "Dielectric barrier discharges: Their history, Discharge physics and industrial applications." *Plasma Procecessing* 23(1): 1-46.

17. Posudin, Yu.I. 1989. *Laser Photobiology*. Kiev: Vishchashkola.

18. Romanenko, V.D., Krot, Yu.G., Sirenko, L.A., and Solomatina, V.D. 1999. *Biotechnology of Hidrobion Cultivation.* Kiev: Institute of Hydrobiology, NAS Ukraine.

19. Sosnin, Edward A., Thomas, Oppenlander, and Tarasenko, Victor F. 2006. "Applications of capacitive and barrier discharge excilamps in photoscience." *Journal of Photochemistry and Photobiology C: Photochemistry Reviews* 7: 145-63.

20. Wieland, Von K. 1960. “Bandensysteme B($^2\Sigma^+$) → X($^2\Sigma^+$) und Dissosiationswerte der Rodikale HgJ und HgBr.” *Zeitchrifstfur Elektronale* 64: 761-69.

21. Pearse, R.W., and Gaydon, A.G. 1963. *The identification of molecular spectra/ Third edition.* L: Chopman Holl LTD.

22. Helvajian, H., and Witting C. 1981. “Vibration quenching of HgBr ($X^2\Sigma^+$).” *Appl. Phys. Lett.* 38(10): 731-33.

23. *Flygar*, W.H. 1978. *Molecular structure and dynamics.* New Jersey: *Prentice-Hall*.

24. Datsyuk, V.V., Izmailov, I.A. and Kochelap, V.A. 1998. “Vibrational relaxation of excimers.” *Physics Uspekhi* 41: 379-02.

25. Schimitschek, E.J., and Celto, J.E. 1980. “Oscillator and oscillator-amplifie experiments with HgBr /HgBr dissociation laser.” *Appl. phys. lett.* 36 (3): 176-78.

26. Malinin, A.N. 1997. “Excitation of Mercury Monohalides in the Plasma of Pulse-Periodic Discharge in Mixtures of Mercury Dihalides and Rare Gases.” *Laser Physics* 7(5): 1032-40.

27. Guivan, M.M. 1999. “Optimization of gas discharge plasma component composition of HgBr-excimer lamp.” *Scientific Bulletin of Uzhgorod National University. Series Physics* 4: 12-17.

28. Guivan, M.M., and Malinin, O.M. 2000. “Excitation of excimer molecules HgBr and HgCl in plasma of high-frequency discharge through dielectric.” *Scientific Bulletin of Uzhgorod National University. Series Physics* 7: 131-38.

29. Nighan, W.L. 1980. “Kinetic processes in the electronically excited mercuric-bromide dissociation laser.” *Appl. Phys. Lett.* 36(3): 173-75.

30. Nighan, W.L., and Brown, R.T. 1982. “Kinetic prosses in the HgBr(B →X) HgBr dissociation laser.” *J. Appl. Phys* 53(11): 7201-10.

31. Kushner, M.J., Pindrof, A.L., Fisher, C. H., and Znotins, T.A. 1985. "Muldimensional modelling of transverse avalanche laser discharges: application to the HgBr laser." *J. Appl. Phys.* 75: 2406-22.

32. Malinin, A.N. 1998. "The Main Characteristics of the Plasma of Pulse Glow Discharge in Mixtures of Mercury Dihalide and Rare Gases." *Laser Physics* 8(2): 395-06.

33. Eden, J.G., and Waynaut, J.G. 1979. "HgBr and HgJ B-state quenching rate constans." *Appl. Phys. Lett.* 34(5): 324-26.

34. Roxlo, C., and Mandl, A. 1980. "Quenching kinetics for the HgBr ($B^2\Sigma_{1/2}$) and HgJ ($B^2\Sigma_{1/2}$, $C^2\Pi_{1/2}$) states." *J. Chem. Phys.* 72(1): 541-43.

35. Malinin, A.N., Shuaibov, A.K., and Shevera V.S. 1981. "Determining the quenching constants for single halides of mercury in a discharge'. *Journal of Applied Spectroscopy* 34(4): 752-54.

36. Malinin, A.N. 1997. "The Efficiency of the Quenching of the $B^2\Sigma^+_{1/2}$-state in Mercury Monohalides by Halogen-Containing Molecules in Active Media of HgCl, HgBr, and HgI Excimer Lasers." *Laser Physics* 7(6): 1177-81.

37. Chang, R.S.T., and Burnham, R. 1980." Dissociative excitation of HgBr by rare gas metastable atoms and N_2 ($A\ ^3\Sigma_u^+$)." *Appl. Phys. Lett.* 36(6): 397-00.

38. Wadt, W.R. 1979. "The electronic structure of HgCl and HgBr." *Appl. Phys. Lett*. 34: 658-60.

39. Wadt, W.R. 1980. "The electronic structure of $HgCl_2$ and $HgBr_2$ and its relationship to photodissociation." *J.Chem. Phys.* 72(4): 2469-78.

40. Allison, J., and Zare, R.N. 1978. "Study of excited fragment emission from the electron impact dissosiation of volatile mercury II halides." *Chem. Phys.*35: 263-273.

41. Malinin, A.N., Shuaibov, A.K. and Shevera, V.S. 1983. "Dissociative excitation of the $B^2\Sigma^+_{1/2}$ states of mercury monohalides by electron impact." *Soviet Journal of Quantum Electronics* 13(7): 977.

42. Kushawaha, V., and Mahmood, M. 1987. "Electron impact dissociation of HgX_2 (X=Cl, Br, I)." *J. Appl. Phys.* 62(6): 2173-77.

43. Malinin, A.N. 1997. "Excitation of the $B^2\boldsymbol{\Sigma}^+_{1/2}$-state of mercury monohalides by electron impact." *Laser Physics* 7(6):1168-76.

44. Johanson, R., and Biondi, M.A. "Ion-molecule reactions of He^+, N^+, N_2^+, N_3^+ and N_4^+ ions with Hg atoms and $HgBr_2$ molecules at thermal energy." *J. Chem. Phys* 10: 5048-50.

45. Guivan, M.M., Malinin, A. N., and Shimon, L. L. 2002. "Optimization of the optical characteristics of the working mixtures HgBr and HgCl excilamps." *Journal of Physical Studies* 6(1): 74-77.

46. Guivan, M.M., and Malinin, A.N. 2002. "Investigation of the Process of Extitation of Mercury Monobromide and Monochloride Excimer Molecules in Dense Gas-Discharge Plasma" *Ukr. J. Phys.* 47(1): 24-27.

47. Furusawa, H., Okada, S., and Obara, M. "High-efficiency continuous operation HgBr excimer lamp excited by microwave discharge." *Appl. Phys. Lett.* 66: 1877-79.

48. Smith, K., and Thomson, R.M. 1978. *Computer Modeling of Gas Lasers.* New York: Plenum Press.

49. Boychenko, A.M., Lomaev, M.I., Panchenko, A.N., and others. 2011. *Ultraviolet and vacuum-ultraviolet excilamps: physics, technology and applications.* Tomsk: STT.

50. Sapozhnikov, R.A. 1977. *Theoretical photometry.* M.: Energia.

51. Efimov, A.E., L.P. Belorukova, L.P., Vasilkova, I.V., and Chechev, V.P. 1983. *Properties of inorganic compounds. Reference book.* L.: Chemistry.

52. Malinina, A.A., Guivan, N.N., and Shuaibov, A.K. 2009. "Optical characteristics and parameters of a gas discharge plasma based on a mixture of mercury dibromide vapor and helium." *Journal of Applied Spectroscopy* 76(5): 711-19.

53. Malinina, A.O., and Guivan, M.M. 2009. "Effectiveness of the process of excitation of the HgBr* exciplex in gas-discharge plasmas on the mixture of mercury dibromide vapor with helium." *Scientific Bulletin of Uzhgorod National University. Series Physics* 24: 115-20.

54. Malinina, A.O., Guivan, N.N., Shimon, L.L., and Shuaibov, A.K. 2010. "Optical characteristics and parameters of the plasma of a barrier discharge excited in a mixture of mercury dibromide vapor with nitrogen and helium." *Plasma Physics Reports* 36(9): 803-11.

55. Guivan, M. M., Malinina, A.A., and Brablec, A. 2010. "Multi-wavelength DBD-driven exciplex lamp operated with the mercury bromide/rare gases mixtures." Eindhoven (The Netherlands): Proc. of the 12 the Int. Symp. on the Science and Technology of Light Sources and the 3 Int.al Conf. on White LEDs and Solid State Lighting, 255-56.

56. Guivan, Mykola M., Malinina, Antonina A., and Guivan, Hanna M. 2010. "Multi-Wavelength Mode of Dielectric Barrier Discharge Operated with the Mercury Bromide/ Rare Gases Mixtures." Kúpeľná Dvorana, Trenčianske Teplice (Slovakia): Book of Contributed Papers of the 12th Intern. Symp. on High Pressure Low Temperature Plasma Chemistry (Hakone XII), 332-35.

57. Malinina, A.A., and Shuaibov, A.K. 2011). "Emission of Mercury Monobromide Exciplex in Gas-Discharge Plasma Based on Mixture of

Mercury Dibromide Vapor with Sulfur Hexafluoride and Helium." *Optics and Spectroscopy* 110: 218-227.

58. Guivan, M.M., Malinina, A.A., and Brablec, A. 2011." Experimental and theoretical characterization of the multi-wavelength DBD-driven exciplex lamp operated with the mercury bromide/rare gases mixtures." *J. Phys. D: Appl. Phys.* 44(22): 1-11.

59. Malinina, A.O. 2011. "Energy characteristics of low-temperature plasmas on mixtures of mercury dibromide vapor with gases." *Scientific Bulletin of Uzhgorod National University. Series Physics* 30: 225-233.

60. Malinina, A.A., and Shimon, L.L. 2012." Optical Characteristics and Plasma Parameters of a Blue-Green Exciplex Lamp." *Technical Physics* 57: 27-33.

61. Malinina, A.O. "Parameters of a gas discharge plasma of a barrier discharge on a mixture of mercury dibromide vapor, helium, and krypton." *Scientific Bulletin of Uzhgorod National University. Series Physics* 33:110-15.

62. Malinina, A.O., and Shimon, L.L. 2008." Rate constants of quenching the $B^2\Sigma^+_{1/2}$-state of the molecules HgBr* and HgI* by mercury dihalide vapor in the working mixture of exciplex radiator." *Scientific Bulletin of Uzhgorod National University. Series Physics* 23 91-9.

63. Malinina, A.O., and Guivan, M.M. 2009. "The efficiency of the process of excitation of the HgBr* exciplex in gas-discharge plasmas on the mixture of mercury dibromide vapor and helium." Uzhgorod: Book of abstracts international conference of young scientists and post-graduates, 137.

64. Malinina, A.A., and Shimon, L.L. 2009. "Exciplex miniature radiator." Tomsk (Russia): Book of Abstr. IX Int. Conf. "Atomic and Molecular Pulsed Lasers," 82.

65. Malinina, A.A. 2010.” Emission characteristics and parameters of a gas-discharge plasma on a mixture of mercury dibromide vapor, nitrogen and helium.” Volgograd: Book of abstracts Sixteenth All-Russian Scientific. Conf. of stud.-phys. and young scientists, 266-67.

66. Malinina, A.O. 2011. “Optical characteristics and parameters of low-temperature plasmas on mixtures of mercury dibromide vapor with gases.” Uzhgorod: Book of abstracts international conference of young scientists and post-graduates, 149.

67. Guivan, M.M., Malinina, A.A., and Shimon, L.L. 2011. “Exciplex gas discharge radiator of ultraviolet and visible spectral range.” Tomsk (Russia): Book of Abstr. X Intern. Conf. “Atomic and Molecular Pulsed Lasers,” 108.

68. Malinina, A.A., Starikovskaya, S.M., and Malinin, A.N. 2015. “Nanosecond Barrier Discharge in a Krypton/Helium Mixture Containing Mercury Dibromide: Optical Emission and Plasma Parameters.” *Optics and Spectroscopy* 118: 26-36.

69. Malinina, A.A., Guivan, M.M., and Shimon, L.L. 2012. “Optical characteristics and parameters of DBD plasma based on multicomponent mixtures of mercury dibromide vapor with gases.” Viana do Castelo, Portugal: Proceedings of the XXI Europhysics Conference on Atomic and Molecular Physics of Ionized Gases (ESCAMPIG), 10-14 July, 3.5.20.

70. Malinina, A.A. 2013.” Excitation of exciplex molecules krypton bromide and mercury monobromide in a barrier discharge on a mixture of mercury dibromide vapor with krypton and helium.” Uzhgorod: Book of abstracts international conference of young scientists and post-graduates IEP, 114-115.

71. Malinina, A.A., and Starikovskaya, S.M. 2013. “Emission characteristics of DBD plasma based on mixture of mercury dibromide

vapor, krypton and helium.” Balatonalmadi (Hungary): Book of Abstr. 5th Central European Symposium on Plasma Chemistry, MD11.

72. Malinina, A.A., and Starikovskaya, S.M. 2013. “Exciplex radiator of simultaneous UV and visible radiation.” Tomsk (Russia): Book of Abstr. XI Intern. Conf. “Atomic and Molecular Pulsed Lasers,” 106-107.

73. Malinina, A.O. Patent for utility model No. 64544 Ukraine, MPK H01S 3/097 (2006.01). Electrodischarge exciplex lamps with radiation in the blue-green spectral range; applicant and patent holder State Higher Educational Establishment “Uzhhorod National University” - No. u201104731; claimed. 18.04.2011; published on 10.11.2011, Bul.№21.

74. Malinina, A.O. Patent for invention No. 98262 Ukraine, MPK H01S 3/097 (2006.01). Electro discharge exciplex lamp with radiation in the blue-green area of the spectrum; applicant and Patent Holder State Higher Educational Establishment "Uzhgorod National University.”- № 2011 04731; stated. Apr 18, 2011; published April 25, 2012, Bul. №8.

75. Akishev, Yu.S., Dem’yanov, A.V., Karal’nik, V.B., Pan’kin, M. V., and Trushkin, N.I. 2001. “Pulsed Regime of the Diffusive Mode of a Barrier Discharge in Helium.” *Plasma Physics Reports* 27(2): 164-71.

76. Pearse, R.W., and Gaydon, A.G. 1963. *The identification of molecular spectra. Third edition.* L: Chopman Holl LTD.

77. Bates, D.R. 1962. *Atomic and molecular processes.* New York and London: Academic Press.

78. Malinin, A.N., and Shuaibov, A.K. 1982. “The quenching constants of the HgBr* state.” *Opt. and spectroscopy* 52 (3): 487-489.

79. Chantry, P.J. 1982. *Negative ion formation in gas lasers / in Gas Lasers (Eds McDaniel E.W., Nigan W.L) Appl. atom. collis. phys.* New York.: Academic Press.

80. Massey, Harrie. 1976. *Negative ions.* New York: Cambridge university press.

81. Christophorov, L.G. 1984. *Electron-Molecule Interactions and Their Applications.* New York: Academic Press.

82. Christophorov, L.G., and Stockdale, J.A. 1968. "Dissociative Electron Attachment to Molecules." *J. Chem. Phys.* 48 (5): 1956-60.

83. Nygaard, K.J., Brooks, H.L., and Hunters, S.R. 1979. "Negative ion production rates in rare gas-halide lasers." *IEEE Journal of Quantum Electronics* QE-15 (11): 1218-23.

84. Bazhulin, S. P., Basov, N. G., Bugrimov, S. N., Zuev, V. S., Kamrukov, A. S., Kashnikov, G. N., Kozlov, N. P., Ovchinnikov, P. A., Opekan, A. G., Orlov, V. K., and Protasov, Yu. S. 1986. "Blue-violet Hgl/Hgl2 laser with wide-band optical pumping by a linearly stabilized surface discharge." *Kvantovaya Elektronika* 13 (5): 1017-19.

85. Malinin, A.N., Polyak, A.V., Guivan, N.N., Zubrilin, N.G., and Shimon, L.L. 2002. "Coaxial HgI excimer lamps." *Kvantovaya Elektronika* 32(2): 155-59.

86. Malinin, A.N. 2005. "Optical characteristics of the gas-discharge plasma of working mixtures in an excimer HgBr/HgI radiation source." *Kvantovaya Elektronika* 35(3): 243-51.

87. Slovetsky, D.I., and Deryugin, A.A. 1987. *EEDF and the interaction of electrons with polyatomic fluorine-containing gases. In: Chemistry of Plasma.* Moscow: Energoatomizdat.

88. Bychkov, Yu.I., Gorchakov, S.L., and Yastremskii, A. G. 2000. "Homogeneity and stability of volume electrical discharges in gas mixtures based on SF_6." *Kvantovaya Elektronika* 30(8): 733–37.

89. Herzberg, G. 1949. *Spectra and structure of diatomic molecules.* Moscow: Publishing House of Foreign Literature.

90. Prokopiev, V.E., and Yatsenko, A.S. 1981. *Energy levels and radiative transitions of neutral atoms.* Novosibirsk: Preprint / IAE SB AS USSR, No. 161, 52p.

91. Zaydel, A.N., Prokofiev, V.K., Raysky, S.M., Slavny V.A., and Shreider, E.Ya. 1977. *Tables of spectral lines.* M.: Nauka.

92. Malinin, A. N., Guivan, N. N., Shimon, L. L., Polyak, A. V., Zubrilin, N. G., and Shchedrin, A. I. 2001. "Temporal characteristics of emission of working mixtures of a HgBr/HgCl excimer lamp." *Optics and Spectroscopy* 91(6): 864-68.

93. Kondratiev, V.N. 1974. *Kinetics and mechanism of gas-phase reactions.* M.: Science.

94. Mkrtchyan, M. M. and Platonenko, V. T. (1979). Kinetics of a gas-discharge XeF excimer laser, *Kvantovaya Elektronika* 6(8), 1639-1647.

95. http://www.siglo-kinema.com/

96. Bazhulin, S. P., Basov, N. G., Zuev, V. S., Leonov, Yu. S., and Stoilov, Yu. Yu. 1978." Stimulated emission at λ = 502 nm as a result of prolonged optical pumping of HgBr2 vapor." *Kvantovaya Elektronika* 5(3): 684-86.

97. Waynant, R.W., and Eden, J.G. 1978. "HgX(B) radiative lifetime by fas photolysis of HgX (X = Br, J)." *Appl. Phys. Lett.* 33(8): 708-10.

98. Mandl, A., Parks, J.J., and Roxlo, C. 1980. "Collisional quenching kinetics for the HgCl and HgBr (B) state." *J. Chem. Phys.* 72(1): 504-07.

99. Helvajian, H., and Witting, C. 1979." Quenching of HgBr ($B^2\Sigma^+_{1/2}$ $X\ ^2\Sigma^+_{1/2}$)." *Opt.Comm.* 30: 189.

100. Huddlestone, R.H., and Leonard, S.L. 1965. *Plasma diagnostic techniques.* NewYork-London: Academic Press.

101. Hagelaar, G. J. M., and Pitchford, L. C. 2005. “Solving the Boltzmann equation to obtain electron transport coefficients and rate coefficients for fluid models.” *Plasma Sources Sci. Techn.* 14: 722 –33.

102. Malinina, A.A., Malinin, A.N. 2015. “Optical characteristics and parameters of gas-discharge plasma in a mixture of mercury dibromide vapor with argon.” *Plasma Physics Reports.* 41(3): 281-89.

103. Malinina, A.A., Malinin, A.N. 2013. “Optical characteristics and parameters of gas-discharge plasma in a mixture of mercury dibromide vapor with neon.” *Plasma Physics Reports.* 39(12): 1035–42.